Arthritis and cholinergic transition of sympathetic nerve fibers

(Arthritis und die cholinerge Umwandlung sympathischer Nervenfasern)

DISSERTATION ZUR ERLANGUNG DES DOKTORGRADES DER

NATURWISSENSCHAFTEN (DR.RER.NAT)

DER FAKULTÄT CHEMIE UND PHARMAZIE

DER UNIVERSITÄT REGENSBURG

vorgelegt von

Hubert Werner Stangl aus

Regensburg

im Jahr 2015

Promotionsgesuch eingereicht am: 03.07.2015

Die Arbeit wurde angeleitet von: Prof. Jens Schlossmann (Lehrstuhl für Pharmakologie und Toxikologie, Universität Regensburg) in Kooperation mit Prof. Rainer H. Straub (Labor für experimentelle Rheumatologie und Neuroendokrinoimmunologie, Universitätsklinikum Regensburg)

Index

Abbreviations

ACh:	acetylcholine
AChE:	acetylcholine esterase, ACh degrading enzyme
AChR:	acetylcholine receptor
ACPA:	anti-citrullinated protein antibody
BGN:	biglycan
BMM:	bone marrow derived macrophage
catecholamine:	neurotransmitter with a catechol group
catecholaminergic:	signaling involving catecholamines as neurotransmitters
CCL:	chemokine (C-C motif) ligand
CCR:	chemokine receptor
CGRP:	calcitonin gene related peptide
ChAT:	choline acetyltransferase, ACh synthesizing enzyme
cholinergic:	signaling involving ACh and/or VIP as neurotransmitters
ChT:	high affinity choline transporter
CIA:	collagen type II-induced arthritis
CNS:	central nervous system
CNTF:	ciliary neurotrophic factor
CT-1:	cardiotrophin 1
CXCL:	chemokine (C-X-C motif) ligand
DBH:	dopamine beta hydroxylase, enzyme in catecholamine synthesis
DMARD:	disease modifying anti-rheumatic drug
DMMB:	1,9-dimethyl-methylene blue
ECM:	extracellular matrix
ELISA:	enzyme-linked immunosorbent assay
ERK:	extracellular signal-regulated kinase
FLS:	fibroblast like synoviocyte
gp130:	glycoprotein 130
HE:	hematoxylin-eosin
HLA:	human leukocyte antigen
IL:	interleukin

JAK:	janus kinase
LIF:	leukemia inhibitory factor
MAPK:	mitogen activated kinase
MCP-1:	monocyte chemoattractant protein-1
MCP-3:	monocyte chemoattractant protein-3
M-CSF:	macrophage colony stimulating factor
MIP-1a:	macrophage inflammatory protein-1a
MIP-2a:	macrophage inflammatory protein-2a
MMP:	matrix metalloproteinase
mRNA:	messenger ribonucleic acid
nAChR:	nicotinic acetylcholine receptor
NE:	norepinephrine
NFKb:	nuclear factor kappa b
NGF:	nerve growth factor
NPY:	neuropeptide Y
OA:	osteoarthritis
OCP:	osteoclast progenitor
OSF-2:	osteoblast specific factor
OSM:	oncostatin M
p.i.:	post immunization
parasympathetic:	belonging to the parasympathetic nervous system
Phox2a:	paired-like homeobox 2a
PNS:	peripheral nervous system
RA:	rheumatoid arthritis
RANK:	receptor activator of nuclear factor kappa b
RANKL:	receptor activator of nuclear factor kappa b ligand
RANTES:	regulated upon activation, normally T-cell expressed and presumably secreted
RF:	rheumatoid factor
RGDS:	arginine-glycine-aspartate-serine tetrapeptide
Satb2:	special AT-rich sequence binding protein 2
SDF-1:	stromal derived factor 1

SLC18A3:	solute carrier family member 18 member 3
SNS:	sympathetic nervous system
SP:	substance P
STAT:	signal transducer and activator of transcription
sympathetic:	belonging to the sympathetic nervous system
TH:	tyrosine hydroxylase, enzyme in catecholamine synthesis
TIMP-1:	tissue inhibitor of metalloproteinase 1
TNF:	tumor necrosis factor
V$GRE.02:	glucocorticoid receptor IR3 site
V$GREF:	glucocorticoid responsive and related elements
V$PRE.01:	progesterone receptor binding site
VAChT:	vesicular acetylcholine transporter
VIP:	vasoactive intestinal peptide
VMAT:	vesicular monoamine transporter
VPAC1:	vasoactive intestinal peptide receptor type 1
VPAC2:	vasoactive intestinal peptide receptor type 2
α7nAChR:	α7-subtype containing nicotinic acetylcholine receptor
αAR:	α-adrenoceptor
βAR:	β-adrenoceptor

1 Introduction

1.1 Rheumatoid arthritis

1.1.1 Prevalence and current models of pathology

Rheumatoid arthritis (RA) is a chronic inflammatory disease (CID) which mainly affects small interdigital, typically the proximal interphalangeal, metacarpophalangeal and wrist joints in hands, the metatarsophalangeal joints in the feet, and the knee joint (Aletaha *et al.*, 2010; McInnes & Schett, 2011). Worldwide, about 1% of the population is diagnosed with RA (Firestein, 2003). If left untreated, progression of RA leads to articular damage, typically expressed by symptoms like swelling and reoccurring pain at morning, and ultimately disability of affected joints, rendering this disease a socio-economical threat to patients and the whole population (Aletaha *et al.*, 2010; McInnes & O'Dell, 2010; McInnes & Schett, 2011). Moreover, due to the systemic and self-sustaining inflammatory nature of RA, the risk of developing secondary diseases related to the cardiovascular system, and insulin resistance, metabolic syndrome, osteoporosis, fatigue and depression increases, all possible reasons for an overall increased mortality observed in RA (Aletaha *et al.*, 2010; McInnes & Schett, 2011).

In the last few decades genetic association studies revealed that rheumatoid arthritis is in fact an autoimmune disease, based on the identification of many risk alleles which alone or in synergy with environmental triggers (especially smoking) increase susceptibility of developing autoimmune mechanisms and eventually disease outbreak (McInnes & Schett, 2011): An important discovery was that the presence of circulating autoantibodies, like rheumatoid factor (RF) and ACPA (anti-citrullinated protein antibody) which are diagnostic markers for RA, is not only highly associated with the human leukocyte antigen (HLA)-DRB1 gene but even more so with a certain amino acid sequence (QKRAA motif) within the HLA-DRB1 protein, a major histocompatibility complex class II (MHCII) molecule (Firestein, 2003; McInnes & O'Dell, 2010; McInnes & Schett, 2011). Further it was demonstrated that the conversion of arginine residues to citrulline residues in endogenous proteins by exogenous noxae like smoking or exposition to certain pathogens, is highly associated with antigen presentation to T cells via HLA-DRB1 and production of autoantibodies like RF or ACPA which are directed against these modified endogenous proteins (Firestein, 2003; McInnes & O'Dell, 2010; McInnes & Schett, 2011). These observations suggest that the adaptive immune system is a key player in the accrual of auto-reactivity of the immune system in RA (Firestein, 2003; McInnes & O'Dell, 2010; McInnes & Schett, 2011). However, it was found that this could not be the sole reason for the pathogenesis, since there are RA patients

who do not display expression of circulating antibodies like RF or ACPA, although disease severity is mostly more intense in RF- or ACPA-positive patients (McInnes & Schett, 2011). There is strong evidence that the innate immune system is as well involved in the pathogenesis of RA since antagonizing of certain cytokines like tumor necrosis factor (TNF) or interleukin (IL)-6, which are mainly produced by cells of the innate immune system like macrophages, has been proven to be highly effective in the therapy of many RA patients (Firestein, 2003; McInnes & O'Dell, 2010; McInnes & Schett, 2011; van Vollenhoven, 2009). In general, leukocytes, cells of both innate and adaptive immune system, are attracted to the inflamed joint by a chemotactic gradient and eventually migrate into the joint (Firestein, 2003; McInnes & Schett, 2011). Enhanced adhesion of these immune cells to the vessels near the joint then promotes accumulation and invasion into inflamed tissues adjacent to these vessels (Firestein, 2003; McInnes & Schett, 2011). The synovial membrane is a special connective tissue surrounding a joint and producing the synovial fluid, which has the purpose of lubrication and exchange of nutrients and metabolites in chondrocytes of articular cartilage (Haywood & Walsh, 2001; Levick, 1995). In RA, the synovial membrane typically displays signs of inflammation (synovitis) including proliferation, increased angiogenesis, altered lymphatic vessels and activation of the endothelium which facilitates the attraction and accumulation of circulating leukocytes (McInnes & Schett, 2011). This has been shown by the accumulation of macrophages, mast cells and natural killer (NK) cells, T and B-cell aggregates in the synovial membrane as well as neutrophil granulocytes in the synovial fluid (Firestein, 2003; McInnes & Schett, 2011). Together with activated fibroblast like synoviocytes (FLS), these immune cells generate a self-sustaining pro-inflammatory milieu by producing pro-inflammatory cytokines like TNF, IL-1b, IL-6 and IL-17, reactive oxygen and nitrogen species, and matrix degrading proteases like matrix metallo-proteinases (MMPs). Since anti-inflammatory and inhibitory mechanisms especially signaling of regulatory T (Treg) cells, endogenous tissue inhibitors of metalloproteinases (TIMPs) and inhibitory cytokines increasingly fail during pathogenesis of RA, this local inflammatory milieu prevails and ultimately leads to breakdown of articular cartilage by invasive FLS and activity of MMPs thereby forming typical aggressive, pannus like structures (Firestein, 2003; McInnes & Schett, 2011). In addition to the degradation of articular cartilage, also erosions of articular bone are typical features of active RA, which seem to occur already soon after diagnosis and are detected in most RA patients (McInnes & Schett, 2011). Erosions of bone are uniquely mediated by osteoclasts, a specialized multinucleated cell type, which arises from the monocyte /macrophage linage of cells and is present in circulating blood and in the bone marrow (Herman *et al.*, 2008a; Udagawa *et al.*, 1990). Under the influence of certain locally enhanced cytokines, especially M-CSF (macrophage colony stimulating

factor) and RANK (receptor activator of nuclear factor kappa B) ligand, and further augmented by TNF, IL-1, IL-6, IL-17, these cells fuse and ultimately differentiate into active multinucleated bone resorbing osteoclasts (Herman *et al.*, 2008a). Under physiological conditions, bone turnover is tightly balanced between bone resorption by osteoclasts and bone formation by osteoblasts (Herman *et al.*, 2008a). In RA however, this homeostasis is disturbed by local conditions, which favor generation and activity of osteoclasts and simultaneously inhibit activity of bone forming osteoblasts (Herman *et al.*, 2008a; McInnes & Schett, 2007; Schett, 2011). Continuous resorption of bone can lead to a direct contact between the normally mutually separated bone marrow and the synovial fluid which contains activated immune cells, invasive FLS and inflammatory cytokines, leading to inflammation of the bone marrow (osteitis) (McInnes & Schett, 2011). However, there is still debate whether synovitis or osteitis and subsequent bone resorption precede initial steps of RA pathogenesis (Kleyer & Schett, 2014; McQueen & Naredo, 2011; Schett & Firestein, 2010).

Eventually, erosions of articular bone, degradation of articular cartilage and an expanding, destructive inflamed hypertrophic synovial membrane including an aggressive pannus lead to a loss of joint integrity and function, pain and immobility (Firestein, 2003; McInnes & Schett, 2011). The high systemic inflammatory load in established active RA further increases the risk of developing secondary, especially cardiovascular diseases and ultimately increases mortality (McInnes & O'Dell, 2010; McInnes & Schett, 2011). Hence, a diagnosis as early as possible is of upmost importance, distinguishing joints typically affected by osteoarthritis (OA) from joints typically affected by RA and further differentiating RA subgroups, as this has an impact on the treatment and disease development (Aletaha *et al.*, 2010; McInnes & O'Dell, 2010; McInnes & Schett, 2011).

1.1.2 Diagnosis and current treatment of RA

The current RA classification criteria of the American College of Rheumatology (ACR, formerly American Rheumatism Association) and the European League Against Rheumatism (EULAR) emphasize the importance of early diagnosis in order to initiate also an early aggressive treatment, ideally achieving remission of disease in the shortest possible period of time (Aletaha *et al.*, 2010). Diagnosis first involves the definite recognition of swelling in joints caused by inflammation in the synovial membrane (synovitis) and possibly erosions in articular bone which occur early in RA (Aletaha *et al.*, 2010; McInnes & Schett, 2011). Detection of these alterations should be confirmed by x-ray radiography, ultrasound, or magnet resonance imaging (MRI) (Aletaha *et al.*, 2010). Definite synovitis and/or tenderness in at least one joint that can not be explained better otherwise renders a patient eligible for

diagnosis of RA (Aletaha *et al.*, 2010). To diagnose a possible RA status of such an individual patient, an objective scoring further involves the number of affected joints, detection of auto-antibodies RF and/or ACPA (see 1.1.1), abnormalities in erythrocyte sedimentation rates and levels of C-reactive protein (CRP), and duration of observed symptoms (Aletaha *et al.*, 2010). While these criteria include the latest knowledge for the best and most early diagnosis of RA, many other scoring systems for evaluating current RA disease activity in patients have evolved in order to compare different treatments and to monitor and ensure efficacy of treatment (McInnes & O'Dell, 2010). Some of these are relative scores, describing the percentage of improvement (e.g. ACR20, 20% improvement), which renders them valuable in clinical trials but unsuitable in clinical practice (McInnes & O'Dell, 2010). Others are of absolute nature and highly accurate (DAS, disease activity score) (McInnes & O'Dell, 2010). Therefore, and owing to the fact that disease activity should be monitored regularly to ensure appropriate treatment, several other means of disease activity assessment are being used in practice, which do not require special equipment and can be acquired in a fast and relatively easy manner (McInnes & O'Dell, 2010).

It has been widely accepted that upon diagnosis initial and first line treatment of RA should rapidly begin with a monotherapy using disease modifying anti-rheumatic drugs (DMARDs) which includes most importantly methotrexate (MTX), leflunomide, sulfasalazine, hydroxychloroquin and glucocorticoids (McInnes & O'Dell, 2010; van Vollenhoven, 2009). Methotrexate and leflunomide are regarded as anti-metabolites with MTX antagonizing purine synthesis and leflunomide antagonizing pyrimidine synthesis, which is considered especially effective in lymphocytes (van Vollenhoven, 2009). The anti-inflammatory action of MTX is at least in part thought to be mediated by signaling via adenosine (van Vollenhoven, 2009). Although both drugs, MTX and leflunomide, display similar efficacy to safety ratios, MTX became the most widely used DMARD, probably also due to better compliance and lower costs (van Vollenhoven, 2009). Breakthrough in therapy for DMARDs was also due to the fact that DMARDs can be combined in therapy if needed, and that certain combinations are superior to MTX monotherapy (van Vollenhoven, 2009). According to current guidelines and several studies, initial therapy should start off early with administration of MTX only or MTX combined with low dose glucocorticoids (Aletaha *et al.*, 2010; McInnes & O'Dell, 2010), rendering MTX as the ‘anchor drug’ in mono- and combinational therapy (Aletaha *et al.*, 2010; Pincus *et al.*, 2003). In cases in which RA patients do not respond to MTX or adverse side effects are observed, alternatives like leflunomide or sulfasalazine, an anti-inflammatory drug should be tried in monotherapy, before a step up to certain combina-

tions of DMARDs is required (McInnes & O'Dell, 2010; van Vollenhoven, 2009). Other DMARDs like gold containing drugs, ciclosporin A (an immunosuppressive agent), certain antibiotics, and azathioprine (a cytostatic drug) are still used in certain cases but due to a higher risk of adverse side effects they are not considered first line medications (McInnes & O'Dell, 2010; van Vollenhoven, 2009). The anti-malaria drug hydroxychloroquine, which seems to interfere with antigen presentation, was shown to be effective especially in combination with MTX or sulfasalazine, and to decrease the risk of developing diabetes, while displaying only relatively mild adverse effects (McInnes & O'Dell, 2010; van Vollenhoven, 2009). The use of glucocorticoids has experienced a renaissance as a first line DMARD since it was found that administration of low doses during initial treatment is effective in limiting joint damage in RA and has the advantage of a relatively fast response, in contrast to most other DMARDs (McInnes & O'Dell, 2010; van Vollenhoven, 2009). However, it is still controversial whether or how fast administration of glucocorticoids in combination with MTX or alternative DMARDs should be tapered off in order to avoid adverse effects of glucocorticoids or be kept up to achieve remission of RA in the long run, also paying respect to the inadequate release of endogenous glucocorticoids (cortisol in humans, corticosteron in rodents) in arthritis (McInnes & O'Dell, 2010; Straub *et al.*, 2013; van Vollenhoven, 2009).

With gaining knowledge about the cellular and molecular signaling pathways in RA in recent decades, new classes of substances were developed and approved for treating RA. The need for new substances emerged due to a growing number of patients who were not responding to mono or combinational therapy at all, experienced adverse effects, or response to a combination of several DMARDs was inadequate (McInnes & O'Dell, 2010; van Vollenhoven, 2009). The relatively new class of substances, currently simply referred to as ‘biologicals’ due to their antibody or protein related molecular structure and (micro-)biological way of production (van Vollenhoven, 2009), mainly exploits its efficacy by interference with cytokine signaling pathways which play a major role in activation of leukocytes, synovial fibroblasts and osteoclasts (McInnes & Schett, 2011). Since TNF plays a central role in activating many cells and inflammatory pathways relevant to RA (Firestein, 2003; McInnes & Schett, 2007; McInnes & Schett, 2011; Schett *et al.*, 2013) several antibodies to TNF (adalimumab, certolizumab, golimumab, infliximab) and a fusion receptor (etanercept) have been approved for treatment of RA (McInnes & O'Dell, 2010; van Vollenhoven, 2009) and have shown efficacy even in other chronic inflammatory disorders (Schett *et al.*, 2013). Interestingly, all TNF inhibitors display similar efficacy to risk ratios (McInnes & O'Dell, 2010). The broad success and the high efficacy highlight the crucial

roles of TNF in these cytokine networks and led to development of further molecules targeting the IL-6 pathway (tocilizumab, an anti-IL-6 receptor antibody) and IL-1 pathway (anakinra, an IL-1 receptor antagonist), due to both cytokines being important in signaling of leukocytes, synovial fibroblasts, and also osteoclasts (McInnes & Schett, 2007; Schett, 2011). Yet, anakinra proved only modest efficacy in the treatment of RA but seems to be more efficient in treating other inflammatory diseases like juvenile idiopathic arthritis and gout (McInnes & Schett, 2007; Schett *et al.*, 2013; van Vollenhoven, 2009).

Moreover, also specific inhibition of B-cells with the help of a monoclonal antibody directed against CD20 (rituximab), which is believed to decrease production of auto-antibodies like RF and ACPA, and, hence, is especially useful in respective serum positive patients, has been approved (McInnes & Schett, 2007; McInnes & O'Dell, 2010; van Vollenhoven, 2009). Also specific inhibition of T-cell co-stimulation, a critical step of T-cell activation, by the CTLA-4 ligand abatacept has shown efficacy, e.g. in patients resistant to anti-TNF therapy (McInnes & Schett, 2007; McInnes & O'Dell, 2010; van Vollenhoven, 2009).

Existing general guidelines and the treat-to-target of remission principle suggest a step up, escalating therapy regime in which after failure of mono or combination therapy with DMARDs, first TNF inhibiting biologicals should be used or added, followed by more specialized agents like tocilizumab, rituximab and abatacept if needed or anti-TNF therapy fails (McInnes & O'Dell, 2010; van Vollenhoven, 2009). Effective and safe therapy has to be routinely monitored and adjusted if needed depending on each patient's individual medical records, which includes presence and treatment of co-morbidities, presence of serum auto-antibodies like RF or ACPA, efficacy or failure of DMARD mono or combination therapy, and step-up therapy with biologicals including possible adverse effects (McInnes & O'Dell, 2010; van Vollenhoven, 2009).

Recent research focused on intracellular signal transduction pathways, especially, on targets like Janus kinases (JAKs) and tyrosine kinases, which belong to cell surface receptors that trigger such intracellular signaling cascades often involved in activating expression of pro-inflammatory mediators (McInnes & Schett, 2011). This led to the recent approval of tofacitinib, a molecule which is thought to inhibit JAK1 and subsequent STAT (signal transducer and activator of transcription) 1 and 3 signaling, and was shown to decrease gene expression of MMPs and chemokines in synovial fibroblasts of RA patients (Boyle *et al.*, 2014). Despite promising preclinical results, p38-mitogen activated protein kinase (MAPK) inhibitors, and the phosphodiesterase (PDE)-4 inhibitor apremilast, which inhibits the degradation of the intracellular signaling molecule cyclic adenosine-mono-phosphate (cAMP) and,

thus, TNF production, displayed disappointing results in clinical studies with RA patients (McInnes & Schett, 2011; Genovese *et al.*, 2015; McCann *et al.*, 2010; McInnes & O'Dell, 2010). Further, two disadvantages of biologicals especially regarding TNF inhibitors remain: Compared to DMARDs they are costly and adverse effects include serious, potentially fatal infections and an increased risk of developing lymphoma and other malignancies (McInnes & Schett, 2007; McInnes & O'Dell, 2010; van Vollenhoven, 2009). Other potential drug targets still under trial include B-cell activating factors, the pro-inflammatory interleukin 17, RANK ligand, and other kinases (McInnes & Schett, 2011).

Due to developing therapy resistance after a certain time or adverse effects seen in some patients under treatment with DMARDs and biologicals, there still remains need for exploiting further pathways involved in RA pathogenesis (Lipsky, 2009; McInnes & O'Dell, 2010; van Vollenhoven, 2009). Such attempts also include targeting the peripheral nervous system (PNS), particularly since activation of certain (α7 subunit containing) nicotinic acetylcholine receptors (α7nAChR) in the periphery was suggested to elicit anti-inflammatory pathways (Waldburger *et al.*, 2008; Wang *et al.*, 2003) and these receptors were discovered on the surface of macrophages in the spleen (Rosas-Ballina *et al.*, 2011) and on fibroblasts and macrophages in the synovium (Forsgren, 2012; van Maanen *et al.*, 2009b; Waldburger *et al.*, 2008; Westman *et al.*, 2009). Exact mechanisms of observed effects are still unclear as proposed models have changed several times (reviewed in (Martelli *et al.*, 2014a)) and hence are subject of debate (Martelli *et al.*, 2014a; Martelli *et al.*, 2014b; Nance & Sanders, 2007; Pongratz & Straub, 2013; Straub *et al.*, 2013). However, pharmacological stimulation of α7nAChR and electrical stimulation of the vagus nerve, the anatomically biggest nerve of the cholinergic PNS, has shown promising results in experimental arthritis (Levine *et al.*, 2014; van Maanen *et al.*, 2009a) and it was suggested that exploiting these pathways might be a therapy option in treatment of RA (Koopman *et al.*, 2011; Koopman *et al.*, 2014; Levine *et al.*, 2014; van Maanen *et al.*, 2009c).

1.2 The peripheral nervous system in RA

Apart from a disturbed signaling of the CNS and the endocrine system with inadequate composition of sex hormones and inadequate provision of endogenous glucocorticoids during arthritis (Straub *et al.*, 2013; Del Rey *et al.*, 2010; Wolff *et al.*, 2014; Straub, 2014), it has been long established that the peripheral nervous system (PNS) locally modulates outbreak and progression of RA (Levine *et al.*, 1987; Pongratz & Straub, 2013). RA typically displays a symmetrical involvement of arthritic joints in the extremities, meaning that with increasing number of affected joints over time mostly also bilateral affection of extremities is observed (Aletaha *et al.*, 2010; Firestein, 2003). The most striking proof of an

involvement of the PNS in RA is the observation that patients who suffer from hemiplegia display RA mostly in the non-paralyzed hand, whereas the hemiplegic hand is typically spared from RA (Keyszer *et al.*, 2004). To verify this clinical observation, sciatic and femoral nerves were severed in an animal model of experimental arthritis and indeed, denervated limbs were protected from developing arthritis (Stangenberg *et al.*, 2014). Yet, the exact mechanisms like an involvement of the microvasculature and the immune system, as suggested by the interesting findings of Stangenberg et al., and how they are controlled by the PNS still remain to be further elucidated (Rabquer & Koch, 2014; Schaible & Straub, 2014).

However, drawing more specific conclusions from these observations can be potentially misleading because hemiplegia and experimental transection of limb nerves most likely affects all different kinds of nerves since the PNS is divided into different parts according to its function: The **sensory nervous system** which mainly transmits pain, inflammatory related stimuli and danger signals from the periphery to the brain (afferent function), the **parasympathetic nervous system,** which is often referred as 'rest and digest' promoting nervous system, but the role of which in arthritis is still relatively unclear, and its counterpart the **sympathetic nervous system**, which in regards to arthritis was shown to influence blood flow, vascular permeability and local immune processes (reviewed in (Pongratz & Straub, 2013; Schaible & Straub, 2014)). The sympathetic nervous system can be further subdivided into an (nor)-adrenergic catecholaminergic and a cholinergic branch, based on which neurotransmitters convey the signals in the post-ganglionic part of the connection between CNS and periphery (Ernsberger & Rohrer, 1999). The main neurotransmitters present in the sensory nervous system and important for the efferent function of sensory nerves are substance P (SP) and calcitonin gene related peptide (CGRP) (Pongratz & Straub, 2013), and detection of SP is commonly used to identify sensory nerve fibers. Important neurotransmitters of the (nor)-adrenergic part of the sympathetic PNS are norepinephrine (NE, also known as noradrenaline) and its co-transmitters neuropeptide Y (NPY) and adenosine (Pongratz & Straub, 2013; Straub, 2012). Detection of sympathetic nerve fibers containing these neurotransmitters is commonly accomplished by staining tyrosine hydroxylase (TH) or dopamine beta hydroxylase (DBH), as these two proteins are key enzymes in the biosynthesis of the catecholamines dopamine and NE, and hence are expressed in sympathetic nerves of CNS and PNS (Tekin *et al.*, 2014). Cholinergic parts of the PNS convey signals via the main cholinergic and eponymous neurotransmitter acetylcholine (ACh) and vasoactive intestinal peptide (VIP), a typical co-transmitter of cholinergic nerve endings (Ernsberger & Rohrer, 1999). These nerves are commonly detected by

staining the ACh synthesizing enzyme choline acetyltransferase (ChAT), the vesicular acetylcholine transporter (VAChT) or VIP protein (Duong *et al.*, 2002; Eiden *et al.*, 2004; Erickson *et al.*, 1994; Ernsberger & Rohrer, 1999; Guidry & Landis, 1998; Schafer *et al.*, 1998).

Interestingly, all of these systems including the respective neurotransmitters and their receptors are present in bone (**Figure 1**) and take part in the control of physiological bone turnover differently influencing bone formation by osteoblasts and bone resorption by osteoclasts (Aitken *et al.*, 2009; Bjurholm *et al.*, 1988; Eimar *et al.*, 2013; Elefteriou, 2005; Hill & Elde, 1991; Hohmann *et al.*, 1986; Imai & Matsusue, 2002; Lerner & Persson, 2008; Persson & Lerner, 2011; Suzuki *et al.*, 1998).

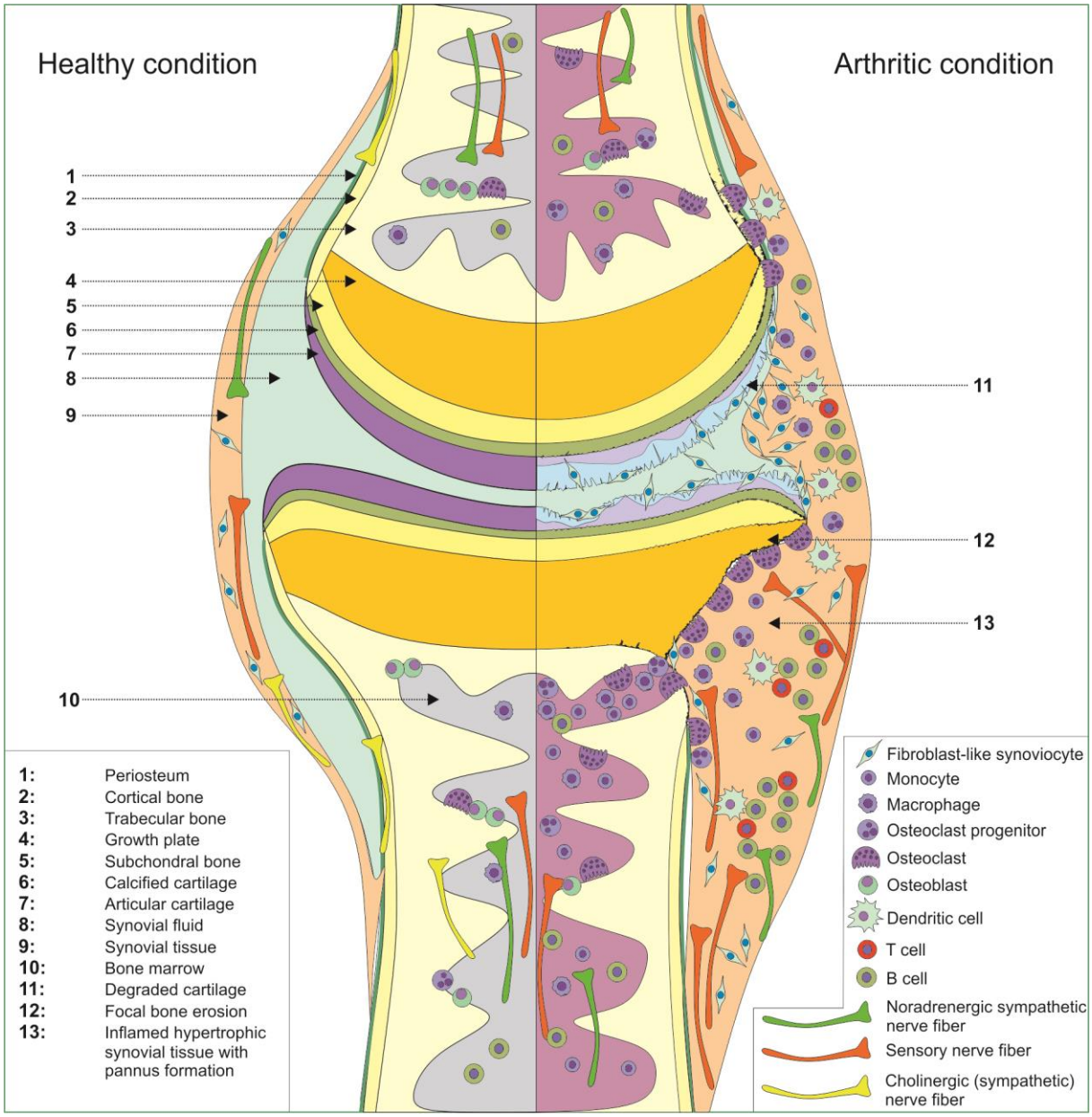

Figure 1. Schematic drawing of a joint in physiological, healthy condition (left) and during arthritis (right). Involved cells and the different parts of the peripheral nervous system are highlighted.

In RA however, this neuronal control is disturbed, and activity of osteoclasts is enhanced also due to inflammatory cytokines, leading to characteristic focal bony erosions (Braun & Zwerina, 2011; McInnes & Schett, 2007; Schett, 2011). Further, presence of sympathetic noradrenergic nerve fibers and sensory nerve fibers has been also demonstrated in the synovial tissue of humans and mice (reviewed in (Pongratz & Straub, 2013)). However, so far not much is known about a possible direct innervation by cholinergic nerve fibers in joints, although expression of VAChT-positive nerve fibers was recently shown in femora from mice (Bajayo *et al.*, 2012) and rats (Lips *et al.*, 2014) in addition to VIP containing nerve fibers in bone (Asmus *et al.*, 2000; Bjurholm *et al.*, 1988; Hill & Elde, 1991; Hohmann *et al.*, 1986; Sisask *et al.*, 1996) and synovial tissue of the rat (Bjurholm *et al.*, 1990). Moreover, in addition to the α7nAChR protein, mRNA transcripts of several parts of the cholinergic machinery like ChAT or the high affinity choline transporter (ChT), were shown to be expressed in the synovial tissue of arthritis patients (Beckmann *et al.*, 2015; Forsgren, 2012). However, no direct innervation by the PNS was shown, and the authors concluded that in the joint a local cell based, non-neuronal cholinergic system (NNCS) might be present (Beckmann & Lips, 2013), similar to such a system, which was shown by Kawashima and coworkers to exist in leukocytes (Kawashima & Fujii, 2004; Kawashima *et al.*, 2012). Further and in contrast to noradrenergic sympathetic innervation, nothing is known about a possible cholinergic innervation of joints in mice and humans during the course of arthritis.

Importantly, innervation by peripheral nerves is not static *per se* but under certain circumstances shows neuroplasticity (Pongratz & Straub, 2013). This phenomenon has been demonstrated in the joints of arthritic mice and RA patients, which during arthritis display a loss of sympathetic nerve fibers while sensory innervation increases (Pongratz & Straub, 2013). These observations have been mainly addressed to the action of elevated levels of the unspecific nerve growth factor NGF and semaphorins 3C and F, which are nerve repellent factors specific for noradrenergic sympathetic nerve fibers (Aloe *et al.*, 1993; Fassold *et al.*, 2009; Miller *et al.*, 2004). Interestingly, a local loss of sympathetic noradrenergic nerve fibers is not exclusive to arthritic joints but has been shown also in other inflammatory settings like in the colon wall of Crohn's disease patients (Straub *et al.*, 2008a), in chronic Charcot foot in diabetes (Koeck *et al.*, 2009), in the myocardium after heart failure (Parrish *et al.*, 2010), in inflamed pancreatic islands of diabetic rats (Mei *et al.*, 2002), and in secondary lymphoid organs of arthritic rats and mice (Lorton *et al.*, 2005; Lorton *et al.*, 2009; Straub *et al.*, 2008b).

Regarding the relationship between inflammation and the PNS during arthritis, a time-dependent, bimodal action was demonstrated for the noradrenergic sympathetic PNS as it acts pro-inflammatory in

early stage experimental arthritis and anti-inflammatory in later stages of arthritis (Harle *et al.*, 2005; Harle *et al.*, 2008). In contrast to this early pro-inflammatory effect, which was attributed to enhanced cell mobilization, action of certain pro-inflammatory T-cells and antibody production by B-cells, it is still relatively unclear how this late anti-inflammatory effect might be conveyed since noradrenergic sympathetic nerve fibers are seemingly lost (Pongratz & Straub, 2013). This has the consequence that, due to lower concentrations of NE and higher receptor affinity of NE towards α-AR (adrenoceptors), also receptor signaling changes from a predominantly β-AR based signaling, which may act pro- and anti-inflammatory, to a predominantly α-AR based signaling, thought to elicit mainly pro-inflammatory effects (Pongratz & Straub, 2013). It was suggested that this late anti-inflammatory effect at least in part might be due to locally emerging catecholamine-producing cells, which partially substitute input from sympathetic nerve endings (Jenei-Lanzl *et al.*, 2015; Capellino *et al.*, 2012; Miller *et al.*, 2000; Miller *et al.*, 2002), and an elevated production of the anti-inflammatory cytokine interleukin 10 in B-cells (Pongratz *et al.*, 2012; Pongratz & Straub, 2013).

Efferent signaling of sensory nerve fibers and its main neurotransmitters SP and CGRP is generally regarded as pro-inflammatory in arthritis (Lorton *et al.*, 2000; Uematsu *et al.*, 2011) as they induce general inflammatory symptoms like vasodilatation, reddening and edema (Pongratz & Straub, 2013), proliferation of T and B cells (Laurenzi *et al.*, 1989; Payan *et al.*, 1983) and in the case for SP stimulates osteoclast formation and activity (Kojima *et al.*, 2006; Lerner & Persson, 2008; Wang *et al.*, 2009).

Anti-inflammatory effects of cholinergic signaling have been described for the activation of nicotinic acetylcholine receptors, especially by activation of the α7nAChR on immune cells and synoviocytes (Kawashima *et al.*, 2012; van Maanen *et al.*, 2009a; van Maanen *et al.*, 2010; Waldburger *et al.*, 2008; Wang *et al.*, 2003; Yoshikawa *et al.*, 2006), but signaling of ACh via certain muscarinic receptors can also elicit pro-inflammatory pathways (Eglen, 2006; Fujii *et al.*, 2003; Fujii *et al.*, 2008; Kawashima *et al.*, 2012). Further, anti-inflammatory effects have been reported for VIP (Delgado *et al.*, 2001; Delgado *et al.*, 2003; Delgado & Ganea, 2008; Gonzalez-Rey *et al.*, 2006; Gonzalez-Rey & Delgado, 2008). Since presence of these systems has been identified in arthritis (Delgado *et al.*, 2008a; van Maanen *et al.*, 2009b; Waldburger *et al.*, 2008; Westman *et al.*, 2009), consequently it was suggested not to enhance general cholinergic signaling via ACh, but to specifically target the α7nAChR and VIP receptors to exploit their anti-inflammatory potential (Bencherif *et al.*, 2011; Delgado *et al.*, 2002;

Delgado *et al.*, 2008b; Delgado & Ganea, 2008; Gonzalez-Rey *et al.*, 2007; Koopman *et al.*, 2011; van Maanen *et al.*, 2009c).

In general however, whether signaling of different parts of the PNS results in activation of pro- or anti-inflammatory pathways, critically depends on local neurotransmitter concentration provided by the respective nerve endings and the locally present different neurotransmitter receptors (Pongratz & Straub, 2013), both of which themselves may change during developmental stages (Sisask *et al.*, 1996) and diseases such as RA (Pongratz & Straub, 2013).

1.3 Cholinergic transition of sympathetic nerve fibers

Under certain circumstances noradrenergic sympathetic nerve fibers are able to change towards a cholinergic phenotype of sympathetic nerve fibers (see **Figure 2**), the process of which is mostly referred to as sympathetic transition or cholinergic transition / differentiation of sympathetic nerve fibers and neurons (reviewed in (Ernsberger & Rohrer, 1999)).

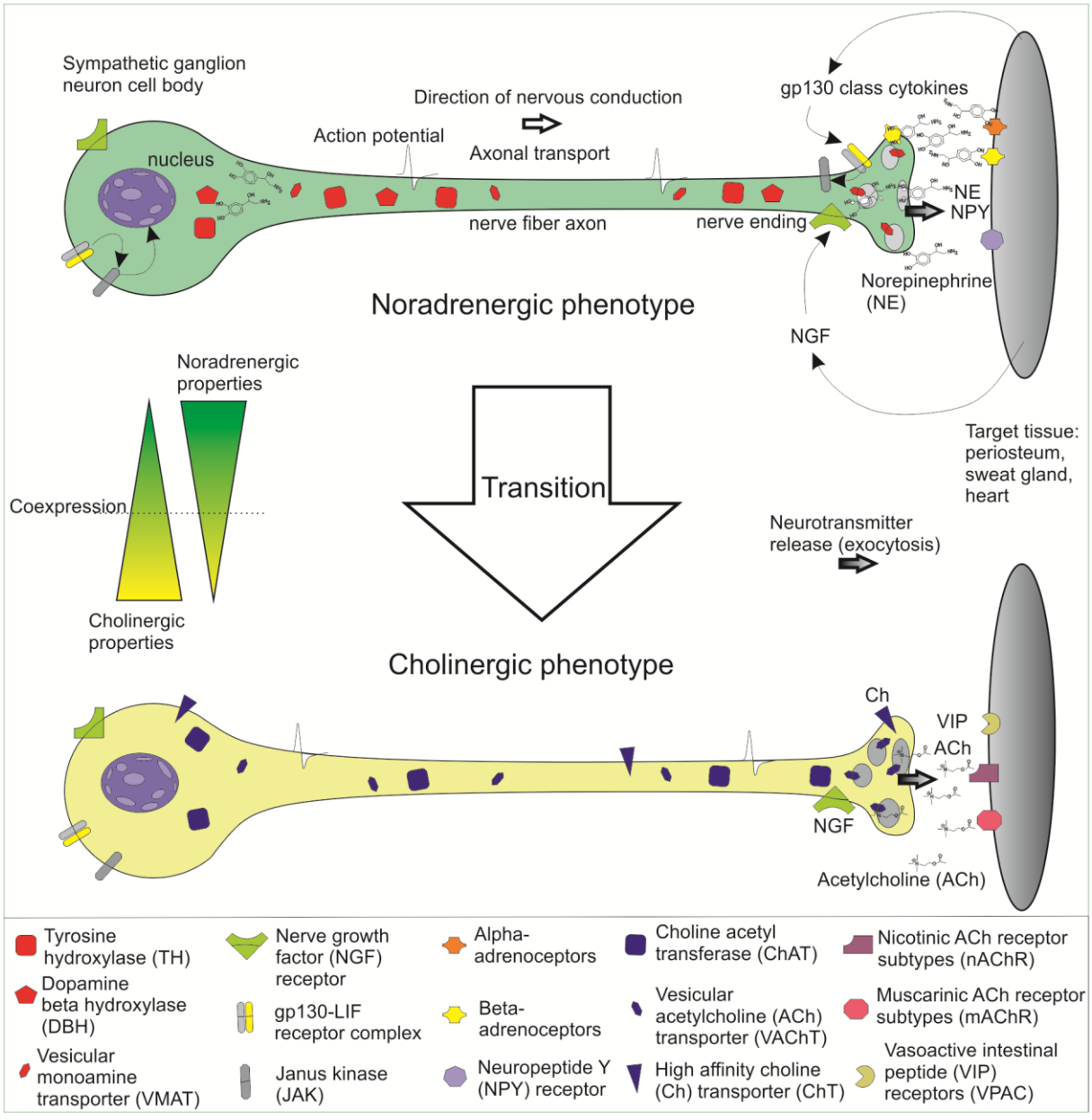

Figure 2. Scheme of catecholaminergic-to-cholinergic transition of sympathetic nerve fibers.

This phenomenon was first described by Landis and co-workers, who were investigating the innervation of developing sweat glands (Landis & Keefe, 1983; Landis *et al.*, 1988), and was later also found in the periosteum (Asmus *et al.*, 2000; Asmus *et al.*, 2001), and in the myocardium (Kanazawa *et al.*,

2010; Parrish *et al.*, 2010; Yamamori *et al.*, 1989) (reviewed in (Kimura *et al.*, 2012). Molecular mechanisms of these phenomena are highly complex and several pathways involved in these processes have been studied: Generally, there seem to be target-independent (initial induction of cholinergic properties) and target-dependent (later trans-differentiation after target contact) pathways which can drive the acquisition of cholinergic properties in sympathetic neurons (Apostolova & Dechant, 2009; Stanke *et al.*, 2006). Regarding sweat glands, there are studies supporting both, a target-dependent pathway, in which sympathetic neurons show cholinergic properties only after target contact (Guidry & Landis, 1998), or an early target-independent pathway, suggesting a neuronal co-expression of both noradrenergic and cholinergic properties before reaching the sweat glands (Schütz *et al.*, 2008).

While in the heart leukemia inhibitory factor (LIF) was identified as the responsible factor driving this transition (Yamamori *et al.*, 1989), the exact nature of the sweat gland specific transition factor still remains to be determined as several promising candidate cytokines belonging to the glycoprotein-130 (gp130) family of cytokines like LIF, ciliary neurotrophic factor (CNTF) and cardiotrophin-1 (CT-1) have already been ruled out. This was demonstrated *in vivo* by anti-cytokine treatment or mice lacking genetic information for one or more candidate cytokines. Both approaches did not inhibit the sympathetic transition in sweat glands, which is a hint for the existence of a further yet undiscovered cytokine (Francis *et al.*, 1997; Habecker *et al.*, 1995; Francis & Landis, 1999; Rao & Landis, 1990; Rao *et al.*, 1993). Still, the molecule that induces sympathetic transition in sweat glands seems to act via the gp130/ LIF-receptor-β receptor complex and, thus, could be a novel member of the gp130 cytokine class (Habecker *et al.*, 1997; Apostolova & Dechant, 2009). While it was established that signaling via the gp130/LIF-receptor-β and following activation of the JAK/STAT3 (Janus Kinase, signal transducer and activator of transcription) pathway plays a central role for the transition (Bamber *et al.*, 1994; Geissen *et al.*, 1998; Habecker *et al.*, 1997), there are also studies reporting secretory responsiveness in gp130 deficient mice and cholinergic reactivity in sympathetic neurons not induced by the LIF-receptor β. This raised the question whether secretory response is solely mediated via cholinergic signaling or if possible remnants of catecholaminergic signaling still can elicit a response (Stanke *et al.*, 2000; Stanke *et al.*, 2006).

Other pathways than the classical LIF-receptor-β/STAT activation influencing cholinergic development have been discovered: Loy et al. and Apostolova et al. demonstrated that the p38-mitogen activated kinases (p38-MAPK) subtypes α and β independently from the JAK/STAT pathway promote cholinergic properties by activating the nuclear matrix protein Satb2. Upon activation, Satb2 binds to the choliner-

gic gene locus and up-regulates expression of cholinergic markers while at the same time down-regulating expression of catecholaminergic properties (Apostolova *et al.*, 2010; Loy *et al.*, 2011). To add further complexity, it was also shown that in most sympathetic cholinergic neurons, which are positive for VIP, the GDNF (glial cell-line derived neurotrophic factor) family receptor GFR-alpha2 is co-expressed. In their respective target tissues, namely sweat glands and periosteum, gene expression of NRTN (neurturin), a ligand for GFR-alpha2 was detected. In GFR-alpha2 knock-out mice, innervation of sweat glands as such was unchanged but the density of cholinergic fibers was drastically reduced and even completely absent in the periosteum (Hiltunen & Airaksinen, 2004). Therefore, NRTN signaling via GFR-alpha2 also seems to play an important role in the acquisition and maintenance of cholinergic innervation in sweat glands. Additionally, the growth factors NGF (nerve growth factor) and NT-3 (neurotrophin-3), which are typically released by the target tissues critically influence induction, regulation and survival of a sympathetic catecholaminergic phenotype (Francis *et al.*, 1999; Francis & Landis, 1999). NT-3 signaling additionally seems to be influenced by the $p75^{NTR}$ receptor (Brennan *et al.*, 1999). Even for neurotransmitter molecules, such as catecholamines, an involvement in sympathetic transition of sweat glands was shown: While a direct activation of adenylyl cyclase (AC), an important signaling component after G-protein coupled receptor (GPCR) activation, by forskolin supports the process of the sympathetic transition to a cholinergic phenotype, a blockade of alpha and beta adrenoceptors inhibits the latter. Seemingly, the sympathetic axons release NE, triggering the up-regulation and release of the transition factor from the sweat glands, which in turn elicits the neuron to transform itself into a neuron with a cholinergic phenotype. In the same study, the sweat gland derived transition factor activity was absent in sympathectomized mice compared to control mice (Habecker & Landis, 1994). In a further study, TH deficient mice were treated with L-DOPA (the progenitor of dopamine in catecholamine synthesis), which increased the number of active sweat glands in these mice (Tian *et al.*, 2000). The role of acetylcholine has as well been investigated: Treatment of young rats with atropine, a nonselective ACh antagonist or with a selective antagonist against the muscarinic (gland) subtype of ACh receptors delayed the development of secretory responsiveness and hence also sympathetic transition to a cholinergic phenotype. Treatment of adult rats with atropine resulted in a complete loss of function. When rats were selectively denervated, the following loss of secretory responsiveness could be rescued by pilocarpine, a muscarinic ACh receptor agonist (Grant *et al.*, 1995).

1.4 Hypothesis and study aim

This study's aim was to elucidate such a possible transition of sympathetic nerve fibers to nerve fibers with cholinergic properties in highly inflamed tissues of arthritic mice and in synovial tissue from patients with arthritis, based on following hypothesis: The observed loss of TH in sympathetic catecholaminergic nerve fibers during arthritis is in fact not due to a loss of the entire sympathetic nerve fiber, but instead due to a sympathetic transition of the latter to a cholinergic phenotype.

The rationale for this thesis is founded on the well described loss of sympathetic nerve fibers in arthritis (see 1.2.) and the fact that such a loss of sympathetic nerve fibers is also being observed in tissues like developing sweat glands and the periosteum that show the phenomenon of sympathetic transition (Asmus *et al.*, 2000; Asmus *et al.*, 2001; Landis *et al.*, 1988; Landis, 1996). Furthermore, the presence of cytokines capable of inducing this transition, like LIF (see above) and oncostatin M (OSM) (Rao *et al.*, 1992), has been demonstrated in the synovium of RA patients ((Hui *et al.*, 1997; Lotz *et al.*, 1992) reviewed in (Richards, 2013).

This possible transition mediated by cytokines like LIF might resemble another part in the concept of an "anti-inflammatory cholinergic pathway" (Wang *et al.*, 2003), which is also being proposed for treatment of arthritis (see 1.2). The exact mechanisms of this pathway(s), however, especially the involvement and connection between noradrenergic sympathetic nerves in secondary lymphoid organs like the spleen, the cholinergic vagus nerve (Borovikova *et al.*, 2000; Koopman *et al.*, 2014; Rosas-Ballina *et al.*, 2011; Wang *et al.*, 2003), and the anti-inflammatory mechanisms of α7nAChR activation still remain controversial (reviewed in (Martelli *et al.*, 2014a; Martelli *et al.*, 2014b; Pongratz & Straub, 2013)).

2 Patients, materials and methods

2.1 Overview of chemicals and labware

An overview of the devices, chemicals and antibodies in use for this study is given in **table 1**, **table 2** and **table 3**, respectively. Details of the patients under study and of ELISA kits for proteome analysis are given in separate tables (**tables 4**, **5**, and **6**, respectively).

Table 1. Devices in use for this study.

Device	Company	Details	Purpose
iMark Microplate reader, Microplate reader imaging software	Bio-Rad, USA	Microplate manager software version 6.2	ELISA measurement and analysis
Fluorescence microscope, Visiview imaging software	Leica, Germany Visitron GmbH, Germany	-	Immunofluorescence microscopy, bright field microscopy
Axiovision fluorescence microscope, Axiovision imaging software	Zeiss, Germany	Axiovision software version 4.8	Immunofluorescence microscopy, bright field microscopy
STEMI, stereo microscope	Zeiss, Germany	-	Dissection, ganglia preparation
Nanodrop 2000 spectrophotometer	Thermo scientific, USA	Software version 1.4.2	Cell culture, BMM, RNA quantification
Bioanalyzer 2100 series	Agilent Technologies, USA	B.02.08.SI648 (SR2)	Cell culture BMM, RNA quality analysis
ChemiDoc Imager, ChemiDoc Imager software Image Lab	Bio-Rad, USA	Image Lab version 4.01	Cytokine profiling, imaging, image analysis
Cryotome	Leica biosystems, Germany	-	Histology
Ultra turrax dispersant	Ika, Germany	T-10	Immunization
Image J	Wayne Rasband, National Institutes of Health, USA	Image J version 1.46	Immunofluorescence microscopy, image analysis

Table 2. Chemicals in use for this study.

Chemical / Kit	**Company**	**Cat.no.**	**Purpose**
Erythrocyte lysis buffer	Qiagen, Germany	79217	Cell culture of BMM
Macrophage colony stimulating factor (M-CSF)	Peprotech, USA	315-02	Cell culture of BMM
Culture dish, 35mm	Corning, USA	430166	Cell culture of BMM
Cell lifter	Corning, USA	3008	Cell culture of BMM
RANK ligand	R&D systems, Germany	462-TEC-010	Cell culture of BMM
Acid phosphatase, leukocyte TRAP kit	Sigma Aldrich, USA	387A	Cell culture of BMM
Dispase II, neutral protease grade II	Roche Diagnostics, Germany	04942078001	Cell culture of ganglia
Nerve growth factor	Sigma Aldrich, USA	N0513	Cell culture of ganglia
8well µslide	Ibidi, Germany	80826	Cell culture of ganglia
Poly-D-lysine solution	Sigma Aldrich, USA	6407	Cell culture of ganglia
Leukemia inhibitor factor (LIF)	Applichem, Germany	A8831	Cell culture of ganglia
Progesterone	Sigma Aldrich, USA	P8783	Cell culture of ganglia
Tissue inhibitor of metalloproteinase 1 (TIMP-1)	R&D Systems, Germany	980-MT	Cell culture of ganglia
Culture inserts	Ibidi, Germany	80209	Cell culture of ganglia, co-culture
6well culture plate	Corning, USA	3516	Cell culture, BMM
Trypan blue	Sigma Aldrich, USA	T8154	Cell culture, BMM
Minimum essential medium eagle	Sigma Aldrich	M4526	Cell culture, BMM
Gene Chip® Mouse Gene 2.0 ST	Affymetrix, USA	902118	Cell culture, BMM, gene expression analysis
Cytokine profiler	R&D Systems, Germany	ARY006	Cell culture, BMM, proteome analysis
RNeasy mini kit	Qiagen, Germany	74104	Cell culture, BMM, RNA isolation
Arginine-glycine-aspartate-serine tetrapeptide (RGDS)	Cayman Chemical, USA	15359	Cell culture, ganglia

Biglycan	R&D Systems, Germany	8128-CM	Cell culture, ganglia
F12 Nut mix + Glutamax medium	Gibco/Life technologies, USA	31765-027	Cell culture, ganglia
RPMI 1640 medium	Sigma Aldrich, USA	R8758	Cell culture, lymph node cells
Hematoxylin solution	Merck-Millipore, USA	1.09249	Histology, staining
Eosin solution	Merck-Millipore, USA	1.09844	Histology, staining
1,9-dimethyl-methylene blue (DMMB)	Sigma Aldrich, USA	341088	Histology, staining
Ethylenediaminetetraacetic acid	Sigma Aldrich, USA	ED-1kg	Histology, tissue decalcification
Rapid decalcifying solution (RDO)	Apex Engineering, USA	-	Histology, tissue decalcification
Tissue Tek	Sakura Finetek, Netherlands	4583	Histology, tissue embedding
Formalin	Merck-Millipore, USA	1039991000	Histology, Tissue fixation
Chicken collagen type II	Sigma Aldrich, USA	C9301	Immunization
Mycobacterium tuberculosis H37Ra, heat inactivated	Difco Laboratories, USA	231141 (3114-33)	Immunization
Freund adjuvant, incomplete	Sigma Aldrich, USA	F5506	Immunization
Freund adjuvant, complete	Sigma Aldrich, USA	F5881	Immunization
Bovine collagen type II	MD Bioproducts, Switzerland	804001-sol	Immunization
Fluorescent mounting medium	Dako, Denmark	S3023	Immunofluorescence microscopy
Triton X-100	Sigma Aldrich, USA	X-100	Immunofluorescence microscopy
4',6-Diamidino-2-phenylindol	Sigma Aldrich, USA	D9542	Immunofluorescence microscopy, cell nuclei staining
Bovine serum albumin	Sigma Aldrich, USA	A7906	Immunofluorescence microscopy, staining
Fetal calf serum	Sigma Aldrich, USA	F0804	Immunofluorescence microscopy, staining
Donkey serum, donor herd	Equitech-BIO Inc., USA	SD-0100HI	Immunofluorescence microscopy, staining

Goat serum, donor herd	Sigma Aldrich, USA	G6767	Immunofluorescence microscopy, staining
3,3' diaminobenzidine (DAB)	Vector Labs, USA	SK4105	Immunohistochemistry

Table 3. Antibodies in use for this study.

Antibody	**Company**	**Cat.no.**	**Purpose**
Anti-VAChT, rabbit polyclonal	Synaptic Systems, Germany	139103	Immunofluorescence microscopy
Anti-TH, guinea pig polyclonal	Synaptic Systems, Germany	213004	Immunofluorescence microscopy
Anti-TH, rabbit polyclonal	Chemicon/Millipore, USA	AB152	Immunofluorescence microscopy
Anti-VIP, rabbit polyclonal	Abcam, UK	22736	Immunofluorescence microscopy
Anti-α7nAChR , rabbit polyclonal	Abcam, UK	10096	Immunohistochemistry
Alexa Fluor 546 labeled goat anti-rabbit antibody	Life Technologies, USA	A-11010	Immunofluorescence microscopy
Alexa Fluor 594 labeled donkey anti-rabbit antibody	Life Technologies, USA	A-21207	Immunofluorescence microscopy
Alexa Fluor 488 labeled goat anti-guinea pig antibody	Life Technologies, USA	A-11073	Immunofluorescence microscopy
Control immunoglobulin fraction, rabbit	Dako, Denmark	X0903	Immunohistochemistry
Goat anti-rabbit HRP conjugated antibody	Pierce/Thermo Scientific, USA	32260	Immunohistochemistry

2.2 Patients and tissue samples

Patients were informed about the studies and gave written consent. The Ethics Committee of the University of Regensburg approved the studies (Official reference numbers 13-101-0135 and 13-101-0031). Synovial tissue was obtained from patients with OA and RA, who underwent knee joint replacement surgery. Samples from distal or proximal interphalangeal finger joints including bone, cartilage, and connective tissue like synovial tissue but not dermal skin were obtained from patients with OA and RA who received finger joint arthrodesis surgery. Diagnosis of RA was based on the established criteria according to the American College of Rheumatology (formerly, the American Rheumatism Association) (Arnett *et al.*, 1988). Patients who received finger joint arthrodesis surgery are characterized in **table 4**. Patients who received total knee replacement surgery are described in **table 5**.

Table 4. Characteristics of patients under study for cholinergic markers VAChT and VIP in finger joints. *One patient was investigated on the left and right side. Data are given as means ± SEM, percentages in parentheses, and ranges in brackets.

	Osteoarthritis of finger joints	**Rheumatoid arthritis of finger joints**
Number	6	4
Age, yr	64.2 ± 11.4 [50-79]	63.8 ± 4.9 [59-70]
Gender male / female	1 / 5 (17/83)	1 / 3 (25/75)
Indication for surgery	6, finger joint arthrodesis	4, finger joint arthrodesis
Affected joint, proximal / distal	5 / 1	3 / 1
Affected side, right / left	5 / 2*	1 / 3

Table 5. Characteristics of patients under study for cholinergic markers VAChT and VIP in synovial tissue of the knee. Data are given as means ± SEM, percentages in parentheses, and ranges in brackets.

	Osteoarthritis of the knee	**Rheumatoid arthritis of the knee**
Number	44	24
Age, yr	67.7 ± 8.9 [51-86]	65.9 ± 9.4 [50-84]
Gender male / female	20 / 24 (45/55)	6 / 18 (25/75)
Indication for surgery	44, total knee arthroplasty	24, total knee arthroplasty
Affected side, right / left	23 / 21	13 /11
C-reactive protein, mg/L	2.5 ± 2.1 [0.1-7.2]	9.5 ± 12.4 [0.5-45.0]

Directly after surgery, samples of knee synovial tissue and finger joint samples were fixed in 3.7% formalin (Merck-Millipore, Billerica, Massachusetts) for 24 hr. Finger joint samples which partially contained bone tissue were decalcified for 7 – 14 d in a solution containing 20% EDTA (Ethylenediaminetetraacetic acid, Sigma Aldrich) buffered to a pH of 7.2. Both, samples of knee synovial tissue and samples from finger joints were dehydrated for 24 hr in phosphate buffered saline (PBS) containing 20% sucrose. After dehydratation, samples were then transferred into a cylinder made of aluminum foil containing Tissue Tek (Tissue Tek, Sakura Finetek, Zoeterwoude, The Netherlands) and quick frozen floating on liquid nitrogen. The Tissue Tek blocks containing the embedded samples were then stored at -20°C.

2.3 Animals, arthritis induction and sample collection

Male mice (8-10 weeks) were housed in cages, 5 animals per cage, were fed standard laboratory chow and water *ad libitum*, and exposed to a daily 12 hr light / 12 hr dark cycle (Elevage Janvier, Le Genest St. Isle, France). Male animals were chosen to exclude possible interference of the hormonal cycle in female mice with the outcome of the experiments. C57Bl/6J mice were immunized according to a published protocol (Inglis *et al.*, 2008) (see also below, 2.4, 2.5). Briefly, heat inactivated mycobacterium tuberculosis H37Ra (Difco Laboratories, Detroit, Michigan) was given to incomplete Freund adjuvant (Sigma Aldrich, St. Louis, USA) at a concentration of 3.3mg/mL (solution A). Chicken collagen type II (Sigma Aldrich, St. Louis, USA) was dissolved overnight in 0.1M acetic acid to obtain a solution of 4mg/mL (solution B). Equal amounts of solution A and B were emulsified with the help of a dispersing instrument (T10 Ultraturrax, Ika Werke, Staufen, Germany), and a total of 100µL of this emulsion was intradermally injected into the tail base of each mouse. Analogously, arthritis was also induced in male DBA1/J mice (8-10 weeks of age, Elevage Janvier, Le Genest St. Isle, France) with bovine collagen type II (MD Bioproducts, Egg b. Zurich, Switzerland) emulsified in an equal amount of complete Freund adjuvant (Sigma Aldrich).

All experiments with mice were conducted according to local institutional and governmental regulations for animal use (Government of the Oberpfalz, Az. 54-2532.1-25/13 and Az. 54-2532.1-04/13).

Progression of collagen type II-induced arthritis (CIA) was continuously monitored by evaluating clinical signs. At days 14, 21, 25, 28, 35, 40, and 55 after immunization, C57Bl/6J mice were killed and limbs were collected. After fixation for 24 hr with 3.7% formalin (Merck-Millipore, Billerica, Massachusetts), samples were decalcified with rapid decalcifying solution (RDO, Apex Engineering, Illinois). After 24 hr in PBS containing 20% sucrose, samples were embedded in Tissue Tek (Tissue Tek, Sa-

kura Finetek, Zoeterwoude, The Netherlands), quick frozen floating on liquid nitrogen, and stored at -20°C.

2.4 Histology and immunofluorescence staining

For investigation of neuronal innervation, 10 -12 µm thick cryo-sections were taken with the help of a cryostat (Leica biosystems, Wetzlar, Germany). After air-drying, the sections were rehydrated in PBS for 20 min. Hematoxylin-eosin (HE) staining was performed to evaluate overall structure and, particularly, bony erosions in the joints of arthritic mice. Histological scoring of arthritic mouse joints included evaluation of erosions in bone, degradation of cartilage, inflammation of synovial and joint surrounding tissue, and infiltration of immune cells into the joint cavity. In addition, in human finger joint samples, staining with a 0.1% aqueous solution of 1,9-dimethyl-methylene blue (DMMB) was performed to evaluate possible loss of cartilage.

Sections from mice and patients were blocked for 45 min (bovine serum albumin, fetal calf serum, goat serum and 0.3% Triton X-100). After washing with PBS, both sections were incubated for 3-12 hr with a primary antibody against VAChT (cholinergic marker, 1:750, cat.no. 139103, Synaptic Systems GmbH, Göttingen, Germany). In mice, limb sections were incubated with a primary antibody against TH in a separate staining process of neighboring tissue sections (1:500, cat.no. AB152, Chemicon, Temecula, California). In human samples, finger joint and knee synovial sections were incubated with a primary antibody against vasoactive intestinal peptide (VIP) in a separate staining process (1:500, cat.no. 22736, abcam, Cambridge, UK). In human finger joint samples, neighboring sections were also stained for TH in a separate staining process (cat.no. AB152, Chemicon).

After washing, sections were incubated with an Alexa Fluor 546 conjugated secondary antibody (1:500, cat.no. A-11010, goat anti rabbit IgG, Molecular Probes) to achieve immunofluorescent staining of cholinergic (VAChT+ or VIP+) and sympathetic catecholaminergic (TH+) nerve fibers. After an incubation time of 90 min, sections were washed, and slides were subsequently mounted with fluorescent mounting medium (Dako, Glostrup, Denmark).

The numbers of TH+ sympathetic catecholaminergic, VAChT+ cholinergic, and VIP+ cholinergic nerve fibers per square millimeter were determined by averaging the number of stained nerve fibers in 17 randomly selected high power fields of view (typical bead chain structure with at least four separated beads along the axon, minimum length 50 µm, determined by a micrometer eyepiece). Positive nerve fiber staining was controlled by incubating tissue without primary antibodies or with immunoglobulin-

matched control antibodies, which always yielded a negative result. General performance of anti-VAChT and anti-TH antibody was checked by pre-incubation with the respective blocking peptide.

Possible presence of the α7-subtype-containing nicotinic acetylcholine receptor (α7nAChR) in fibroblast like synoviocytes (FLS) from knee synovial tissue obtained from OA patients was tested by staining formalin fixed FLS with an rabbit polyclonal antibody raised against a peptide containing the amino acids 22-71 from human α7nAChR (cat.no. ab10096, abcam). FLS were first blocked for 45 min (bovine serum albumin, fetal calf serum, goat serum and 0.3% Triton X-100) and then treated with a 3% solution of hydrogen peroxide for 10 min. The stock solution (1mg/mL) of the antibody and a control immunoglobulin fraction from rabbit (cat.no. X0903, Dako, 20mg/mL) were diluted 1:500 and 1:10,000 respectively. FLS were stained overnight at 4° Celsius. After washing with PBS and 0.3% Triton X-100, FLS were incubated in a 1:500 dilution of a secondary goat anti rabbit antibody conjugated with horseradish peroxidase (HRP) for one hour (cat.no. 32260, Pierce/Thermo Scientific). After washing, cells were then incubated with a solution of 3,3' diaminobenzidine (DAB) according to the manufacturer's protocol (cat.no. SK4105, Vector Labs).

2.5 Generation of osteoclast progenitor cells

Generation of osteoclast progenitor (OCP) cells from bone marrow-derived macrophages (BMM) has been described (Takeshita *et al.*, 2000). After sacrifice, femoral and tibial bone marrow was aseptically removed from healthy and arthritic male C57Bl/6J mice, subjected to lysis of erythrocytes (Buffer EL, Qiagen GmbH, Duesseldorf, Germany), and cells were cultured with 20ng/ml murine M-CSF (cat.no. 315-02, Peprotech Inc., Rocky Hill, New Jersey) in a 35mm culture dish (cat.no. 430166, Corning Incorporated, NY, USA). After 2 d, non-adherent cells were washed off with PBS, adherent cells were removed with a cell lifter (cat.no. 3008, Corning Incorporated), and cells were re-suspended in medium with 20ng/ml M-CSF and 5ng/ml receptor activator of nuclear factor Kappa-B ligand (RANK ligand, cat.no. 462-TEC-010, R&D Systems, Wiesbaden, Germany). Viability and number of cells were determined using the trypan blue exclusion method. In co-culture experiments with sympathetic ganglia 20,000 BMM cells were seeded into each of the second compartment of the insert-equipped 8 well chamber slides (see 2.5 below). For the generation of whole RNA and cell culture supernatants 150,000 cells were seeded into each well of a 6-well culture plate (see also 2.7 and 2.8). Polynucleated (nuclei n≥3) and tartrate resistant acidic phosphate-positive cells appeared after 2 - 5 days after seeding and rated as OCP cells (Acid Phosphatase, Leukocyte TRAP Kit, cat.no. 387A, Sigma) (**Figure 3**).

In a separate set of experiments, OCPs were also obtained from healthy and arthritic DBA1/J mice to check a possible strain specificity of the co-culture experiments of sympathetic ganglia and OCP cells.

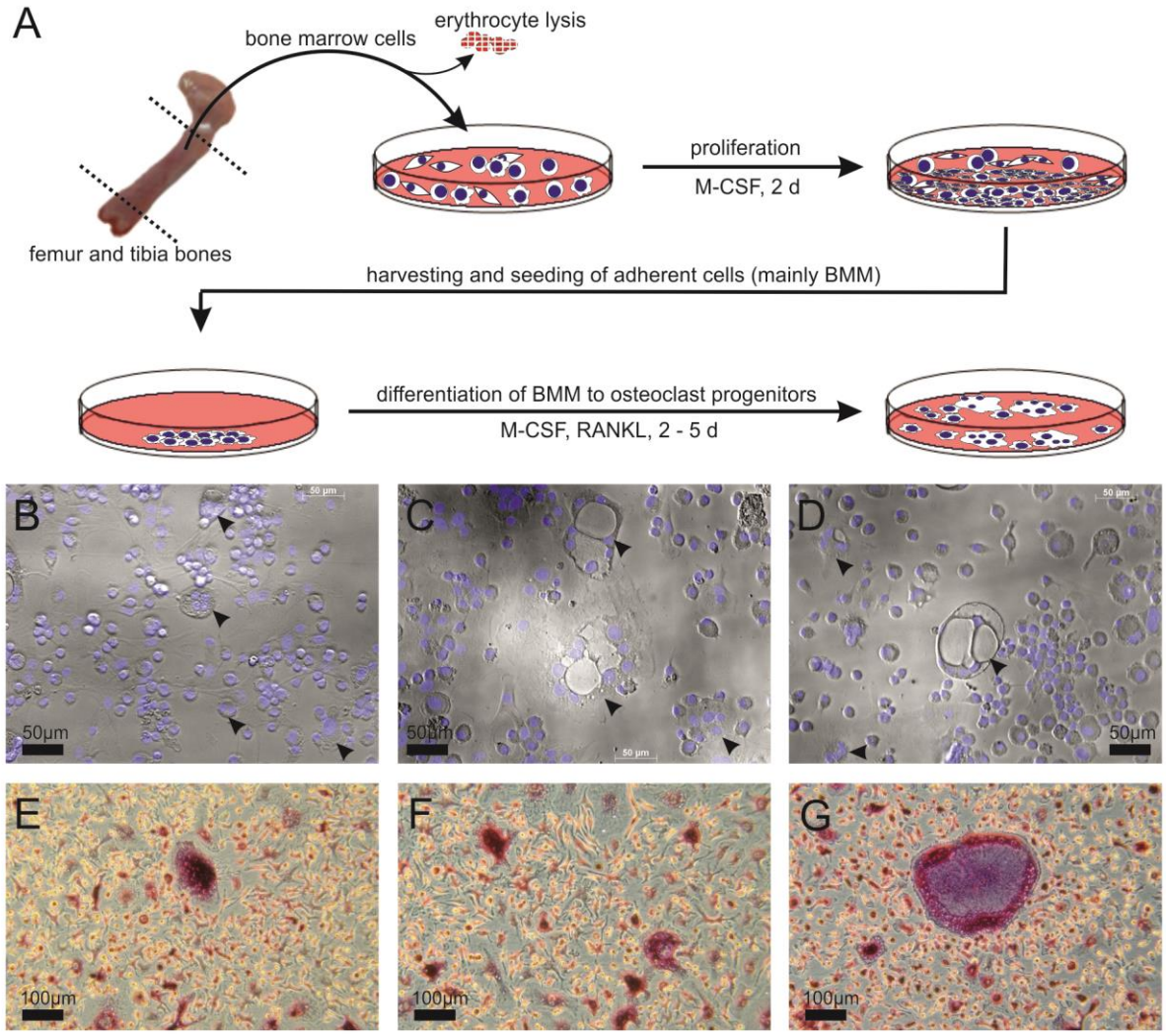

Figure 3. Generation of osteoclast progenitor cells from bone marrow derived macrophages. A) Diagram delineating the process of obtaining osteoclast progenitors from BMM. B,C,D) Examples of multinucleated (cell nuclei in blue, DAPI stain) osteoclast progenitor cells (arrow heads) after 2 d differentiation with M-CSF and RANKL, magnification x200. E,F,G) Examples of TRAP-positive (dark red/purple) osteoclast progenitor cells after 2 d differentiation with M-CSF and RANKL, magnification x100. Abbreviations: BMM, bone marrow derived macrophages; M-CSF, macrophage colony stimulating factor; RANKL, receptor activator of nuclear factor Kappa-B ligand; DAPI, 4',6-diamidino-2-phenylindole; TRAP, tartrate resistant acid phosphatase (osteoclast marker).

During the course of generating OCP cells from BMM for gene expression analysis and proteome profiling, two mentionable characteristics were observed: Firstly, the total amount of adherent BMM per animal which was harvested from the bone marrow of two tibiae and two femora and proliferated for two days with the help of M-CSF, was significantly higher in the group of arthritic animals compared to the group of healthy control mice (**Figure 4A**). Secondly, when BMM were differentiated for five consecutive days compared to 2 d, the size and number of giant multinucleated, TRAP-positive OCP

cells increased (**Figure 4B**). Yet, also more apoptotic events were observed, which were typically characterized by gaps and cell debris in the cell monolayer (**Figure 4C**), which had about the size of the giant OCPs as observed in (**Figure 4B**).

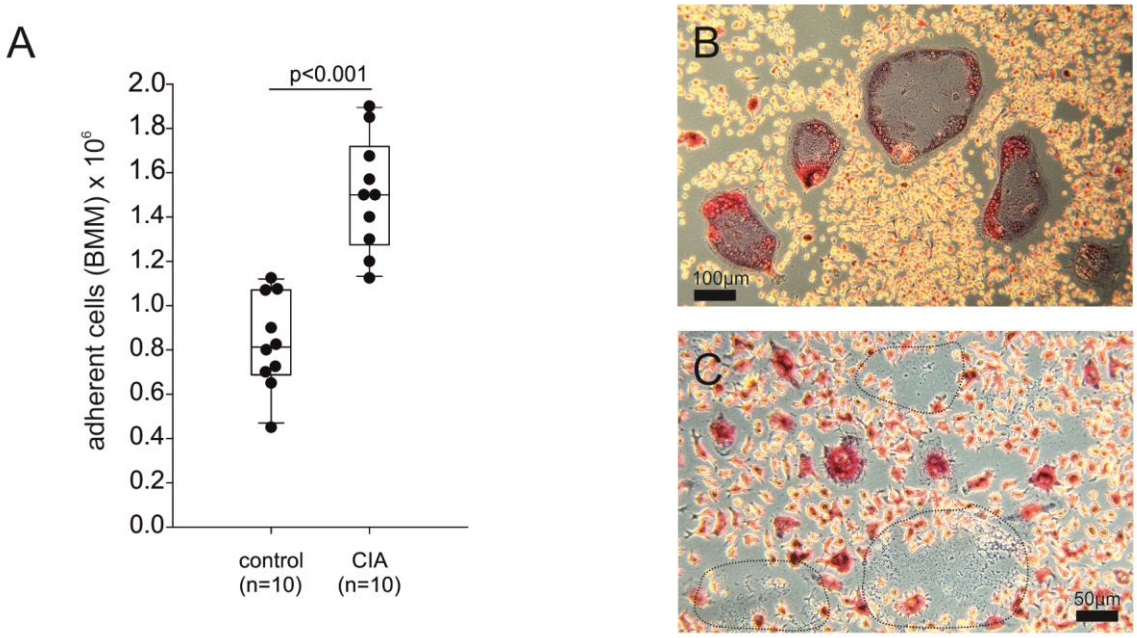

Figure 4. Characteristics of bone marrow derived macrophages during proliferation and differentiation. A) The total amount of BMM was counted after 2 d of proliferation with M-CSF. B) BMM differentiated for 5 d displayed increased size of multinucleated, TRAP+ (dark red/purple) osteoclast progenitor cells and showed enhanced signs of apoptosis (dashed lines, C). These observations (B,C) did not differ between cells from control and CIA animals. Numbers in parentheses indicate total number of samples analyzed. Box plots demonstrate the 10th (whisker), 25th, 50th (median), 75th, 90th (whisker) percentile. Abbreviations: CIA, collagen type II-induced arthritis; TRAP, tartrate resistant acid phosphatase.

2.6 In-vitro experiments with sympathetic ganglia, co-culture with osteoclast progenitors, immunofluorescence staining and image analysis

For the quantification of the fluorescence labeled markers TH and VAChT in mouse paravertebral sympathetic trunk ganglia an appropriate double staining technique had first to be established, also to exclude the possibility of false positive or high background staining. Here, successful double immunofluorescence staining was first established in mouse colon formalin fixed and frozen tissue, which exhibits both sympathetic TH expressing and cholinergic VAChT expressing nerve fibers and therefore was considered as a positive control for the double staining technique (**Figure 5**). This technique was then tested in mouse sympathetic ganglia and showed satisfactory results (**Figure 5**), being that Alexa

Fluor 488 indirectly labeled TH and Alexa Fluor 594 indirectly labeled VAChT could be separately excited and their fluorescence emission signal independently recorded via the use of fitting fluorescence filters in the microscope (Zeiss Axiovision).

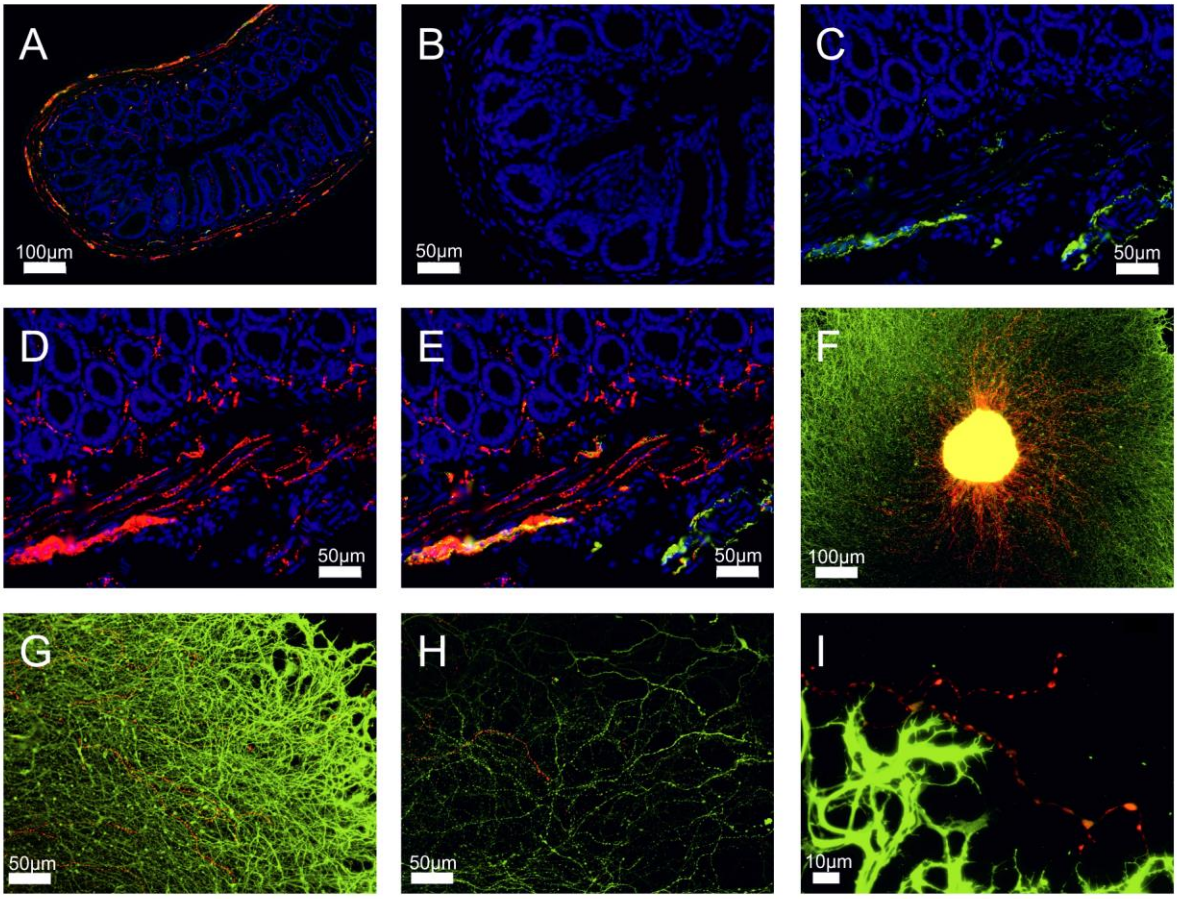

Figure 5. Establishing a double immuno fluorescence staining technique for tyrosine hydroxylase- and vesicular acetylcholine transporter-positive nerve fibers in mouse tissue. A,B,C,D,E) Double staining of TH and VAChT in mouse colon tissue (positive control) with A) showing an overview and B) showing a negative staining control, devoid of primary antibodies against TH and VAChT. C) Green fluorescence channel image depicting TH+ nerve fibers (green) and D) red fluorescence channel image depicting VAChT+ nerve fibers (red). E) Merged overlay image consisting of C) and D) showing distinct sets of nerve fibers (green=TH+, red=VAChT+) in submucosa and muscularis layers. F) Overview of a double staining of TH and VAChT in a mouse sympathetic trunk ganglion showing the soma in the center and radial outgrowth of TH+ (green) and VAChT+ (red) nerve fibers. G,H,I) Detailed images of sympathetic ganglia with depicting separate sets of TH+ and VAChT+ nerve fibers, demonstrating the specificity of the staining technique. Nerve fibers are stained in green (TH+) or red (VAChT+), cell bodies are counterstained with DAPI. Abbreviations: TH, tyrosine hydroxylase (key enzyme of catecholamine synthesis); VAChT, vesicular acetylcholine transporter (marker of cholinergic nerve fibers); DAPI, 4',6-diamidino-2-phenylindole.

Culture of paravertebral sympathetic trunk ganglia obtained from mice has been described recently (Fassold *et al.*, 2009; Fassold & Straub, 2010). Briefly, new born C57Bl/6J mice (postnatal day 2-4) were killed, and sympathetic trunk ganglia aseptically dissected under a stereo microscope (STEMI, Zeiss). After digestion and washing, ganglia were cultured for two days in medium with 100ng/ml

nerve growth factor (NGF) (cat.no. N0513, Sigma Aldrich) in 8-well chamber slides (8well µslide, ibidi GmbH, Martinsried, Germany), which were equipped with removable culture inserts made of silicone (cat.no. 80209, ibidi GmbH) (**Figure 6**).

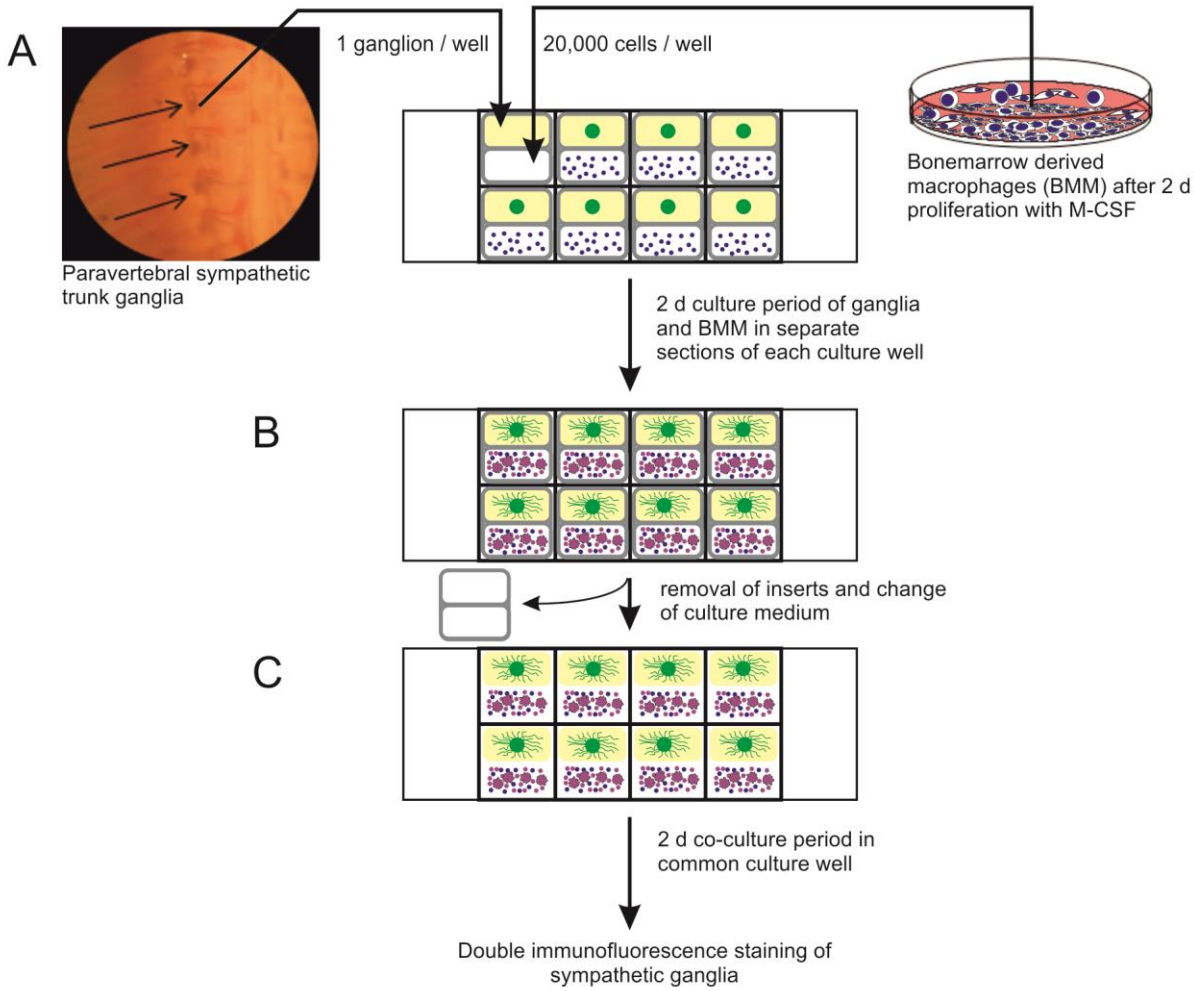

Figure 6. Scheme of the in-vitro co-culture system of sympathetic ganglia and osteoclast progenitor cells. A) Paravertebral sympathetic trunk ganglia are seeded into the poly-D-lysine coated half of a culture well which is physically separated from the uncoated half by a silicone insert. The uncoated half is being seeded with BMM. After 2 d culture period, sympathetic ganglia show a radial outgrowth of nerve fibers and BMM have differentiated into osteoclast progenitor cells in the presence of RANKL (B). C) Silicone inserts are removed and culture medium is being changed. Sympathetic ganglia and osteoclast progenitor cells are left in co-culture for 2 d. After 2 d, medium is removed, cells are washed, fixed with formalin and subsequently subjected to double immunofluorescence staining of TH and VAChT. Abbreviations: BMM, bone marrow derived macrophage; M-CSF, macrophage colony stimulating factor; RANKL, receptor activator of nuclear factor Kappa B ligand; TH, tyrosine hydroxylase; VAChT, vesicular acetylcholine transporter.

Half of the chamber divided by an insert was coated with a solution of poly-D-lysine (cat.no. 6407, Sigma Aldrich) to promote adhesion of sympathetic ganglia after seeding. The other half was seeded with arthritis-related cells of hematopoietic origin, which were obtained from either healthy or arthritic male mice (see above: 2.5, osteoclast progenitor cells, and 2.7, draining lymph node cells). After two

days, medium was aspirated, inserts were aseptically removed, and medium containing 25ng/ml of nerve growth factor, 20ng/mL M-CSF and 5ng/mL RANKL was added to the entire chamber.

After a co-culture period of 2 d, medium was aspirated, the chambers were briefly washed with PBS, and cells were fixed with 3.7% formalin. After washing, cells were blocked for 45 min (bovine serum albumin, fetal calf serum, goat serum, donkey serum, and 0.3% Triton X-100). Sympathetic ganglia were double stained for 12 hr using antibodies against TH (1:750, cat.no. 213004, guinea pig polyclonal, Synaptic Systems) and against VAChT (1:750, cat.no. 139103, rabbit polyclonal, Synaptic Systems). Alexa Fluor 488 and Alexa Fluor 594 conjugated secondary antibodies were used (both 1:500, donkey anti rabbit IgG, cat.no. A-21207, and goat anti guinea pig IgG, cat.no. A-11073, Molecular Probes). Cells were counterstained with 4',6-Diamidino-2-phenylindol (DAPI). Sympathetic ganglia were subsequently analyzed by fluorescence microscopy (Zeiss Axiovision, Zeiss, Jena, Germany).

Double stained ganglia were photographed in 4 to 9 representative regions of the nerve fiber outgrowth area (not in the area of the soma of the ganglion). To determine the amount of positive pixels of the green fluorescence channel (= area of TH+ immunoreactivity, Alexa Fluor 488) and the red fluorescence channel (= area of VAChT+ immunoreactivity, Alexa Fluor 594), the respective single channel images were analyzed by a color threshold function (Image J, Wayne Rasband, National Institutes of Health, USA, version 1.46). The same threshold value (126/255) which excluded false positive detection of background-staining and only allowed for the exclusive detection of specifically stained nerve fibers was used for all images analyzed. The ratios of VAChT+ divided by TH+ pixels were calculated for each image, which expresses the relative appearance of cholinergic to catecholaminergic sympathetic nerve fibers in this particular image.

In order to test possible effects of leukemia inhibitory factor (LIF) on the ratio of VAChT+ to TH+ nerve fibers, separate experiments without any additional cells were conducted (using 100ng/ml of recombinant mouse LIF; cat.no. A8831, AppliChem GmbH, Darmstadt, Germany). After 2 d of pure culture with 100ng/ml of nerve growth factor, LIF was administered in the presence of 25 or 10ng/ml of nerve growth factor (Sigma) for another 2 d. In a subset of stimulation experiments with LIF, the culture medium was devoid of progesterone (which is normally present in the culture medium for sympathetic ganglia at a concentration of $2x10^{-7}$M) to examine possible effects of sex steroids.

Additionally, also TIMP-1 (tissue inhibitor of metalloproteinase 1), biglycan and fibronectin, of which the transcripts in OCPs from healthy mice were elevated (see 3.4.1), were tested in this assay.

In these experiments, first, the effects of fibronectin as a coating agent and of RGDS (arginine-glycine-aspartate-serine tetra-peptide) as an agonist were tested. Due to the lack of murine full length protein, full length human fibronectin (cat.no. ab81743, abcam) was coated on top of self-coated poly-D-lysine (cat.no. 6407, Sigma Aldrich) coated 8-well chamber slides (ibidi) at a concentration of 10µg/mL in sterile PBS overnight at 4° Celsius. Sympathetic mouse ganglia were then cultivated in these slides for 2 d in culture medium containing 100ng/mL NGF.

For stimulation experiments with RGDS, TIMP-1 or biglycan, mouse sympathetic ganglia were cultured in poly-D-lysine coated slides for 2 d in presence of 100ng/mL NGF and then after change of culture medium for another 2 d in presence of 25ng/mL NGF and 100µg/mL RGDS (cat.no. 3498, Tocris/R&D systems), 100ng/mL TIMP-1 (cat.no. 980-MT, R&D systems) or 3µg/mL biglycan (cat.no. 8128-CM, R&D systems) respectively.

2.7 Isolation of draining lymph node cells

Draining lymph nodes were removed from healthy and arthritic C57Bl/6J mice. Inguinal draining lymph nodes, which are located near the hind limbs, were collected and aseptically processed through a 70 µm cell strainer and, then, cells were cultured in RPMI 1640 culture medium (10% FCS, 1% penicillin / streptomycin, 20mM HEPES, 50µM beta-mercaptoethanol, and 0.01% ascorbic acid; all from Sigma). Viability and number of cells were determined using the trypan blue exclusion method. A total of 20,000 cells were given to each of one half of well 8 well chamber slides analog to the set of experiments with osteoclast progenitor cells (see above, 2.6).

In a separate set of experiments, inguinal draining lymph node cells were also obtained from healthy and arthritic DBA1/J mice to check a possible strain specificity of the co-culture experiments of sympathetic ganglia and draining lymph node cells.

2.8 Gene expression profiling of osteoclast progenitor cells

For gene expression analysis, arthritis was induced in male DBA1/J mice (8-10weeks, see also 2.2) since severity and incidence is more reproducible than in C57Bl/6 mice and, additionally, less animals are needed. BMM from arthritic mice (n=3) with similar high clinical arthritis scores in both hind limbs (8 score points or more per limb out of a maximum of 13 score points per limb) as well as BMM from healthy control animals (n=3) of the exact same age were isolated and cultured as described above (2.5). Within 2h before noon of the same day the bone marrow of all animals was collected since the circadian rhythm can have an impact on overall gene expression and, therefore, all samples had to be

obtained in a time-matched manner. After 2 d, adherent cells were collected and 150,000 cells were seeded into each well of a 6-well plate (cat.no.3516, Corning Incorporated, NY, USA), containing medium with both M-CSF (20ng/ml) and RANK ligand (5ng/ml) (see above). After another 2 d, cells were lysed and whole RNA was isolated (RNeasy Mini Kit, Qiagen GmbH, Düsseldorf, Germany) according to the manufacturer's protocol. Quantity and quality of whole RNA was tested with a Nanodrop 2000 Spectrophotometer (Thermo Scientific, Wilmington, North Carolina) and a 2100 series Bioanalyzer (Agilent Technologies Inc., Santa Clara, California), respectively. Gene Chip® Mouse Gene 2.0 ST arrays were performed on the respective sets of whole RNA (cat.no. 902118, Affymetrix, Santa Clara, California). An authorized Affymetrix service provider (Kompetenzzentrum für Fluoreszente Bioanalytik (KFB), Regensburg, Germany) analyzed the array after validating the appropriate quality and quantity of RNA in the samples. Graphical color coded cluster image maps for selected genes taken from the microarray gene expression analysis were generated by using the public program CIMminer (http://discover.nci.nih.gov/cimminer/home.do , accessed Feb 15, 2015), provided by the National Cancer Institute (Scherf *et al.*, 2000; Weinstein *et al.*, 1997). For clustering, default settings (cluster rows, cluster columns, distance method: euclidean, cluster algorithm: average linkage) were used.

In a separate experiment, BMM from arthritic DBA1/J mice (n=2) with similar high clinical scores in both hind limbs (see above) as well as cells from healthy control animals (n=2) with the same age were isolated and cultured the same way as described above except that the phase of differentiation with M-CSF and RANK ligand lasted for 5 d instead of 2 d (see above). This experiment was performed to elucidate a possible influence of the duration of differentiation on the gene expression profile of OCP cells.

2.9 Proteome profiling of osteoclast progenitor cells

Since OCPs induced a shift of the ratio of cholinergic to catecholaminergic nerve fibers in co-culture with sympathetic ganglia and gene expression analysis of OCP cells revealed differences especially in cells differentiated for two days (given in 3. Results), respective cell culture supernatants were generated again and subsequently analyzed. For this purpose, bone marrow derived macrophages were obtained from highly arthritic (n=10) and age matched healthy control (n=10) DBA1/J male mice and were cultured and differentiated the same way as for the gene expression analysis of osteoclast progenitor cells (2 d proliferation with M-CSF and 2 d differentiation with M-CSF and RANK ligand) described above (2.8). After two days, supernatants were collected, pooled per animal, aliquoted and stored in cryotubes (Thermo Scientific) at -80°C until further analysis.

2.9.1 Proteome profile of osteoclast progenitor supernatants

For the purpose of an overall semi-quantitative screening, supernatants generated by OCP cells from healthy (n=4) and arthritic (n=4) mice (see above, 2.9) were analyzed by the use of the mouse cytokine proteome profiler technique according to the manufacturer's protocol (cat.no. ARY006, R&D Systems, Wiesbaden, Germany). Briefly, respective supernatants were incubated on separate membranes each of which contains a total of 40 bound antibodies raised against 40 different proteins. The signal produced by a chemiluminescent color compound is proportional to the amount of protein bound to the membrane and was recorded with the use of a Bio-Rad Chemidoc Imager XRS (Bio-Rad, Hercules, CA, USA) and analyzed with the volume tools function of the Image Lab software (Image Lab, version 4.0.1, Bio-Rad, USA). The mean pixel intensity per protein was then calculated relative to the mean pixel intensity of a positive control antibody present on every membrane set to 100%. The principle of this test is therefore semi-quantitative.

2.9.2 ELISA measurements of osteoclast progenitor supernatants

Suspected candidate proteins, which were up-regulated in the gene expression and proteome profiler analysis or which are known factors for sympathetic transition, were then quantitatively assayed with the use of individual ELISA tests: LIF, OSM, TIMP-1, Periostin/OSF-2 (osteoblast specific factor), progesterone, chemokine (C-C motif) ligand 2 (CCL2/MCP-1, monocyte chemoattractant protein-1), chemokine (C-C motif) ligand 3 (CCL3/MIP-1a, macrophage inflammatory protein-1a), chemokine (C-C motif) ligand 5 (CCL5/RANTES, regulated upon activation, normally T-cell expressed and presumably secreted), chemokine (C-C motif) ligand 7 (CCL7/MCP-3, monocyte chemoattractant protein-3), chemokine (C-X-C motif) ligand 2 (CXCL2/MIP-2a, macrophage inflammatory protein-2a), chemokine (C-X-C motif) ligand 10 (CXCL10), chemokine (C-X-C motif) ligand 12 (CXCL12/SDF-1, stromal cell derived factor) were assayed. For detailed information about the ELISA see **table 6** below. Assay ranges and sensitivities are given according to the manufacturer's protocol.

Table 6. Details of the ELISA tests used for the analysis of the proteome of osteoclast progenitor cells from control and arthritic mice.

Protein	Synonym	Manufacturer, cat. no.	Range [pg/mL]	Sensitivity [pg/mL]
LIF	-	R&D systems, MLF00	21.9 – 1,400	3.13
OSM	-	R&D systems, DY495-05	6.25 - 400	6.25
Periostin	OSF-2	R&D systems, DY2955	93.8 - 6000	93.8
TIMP-1	-	R&D systems, MTM100	37.5 – 2,400	3.5
Progesterone	-	IBL international, RE52231	300 – 40,000	45.0
CCL2	MCP-1	R&D systems, DY479-05	3.91 - 250	3.91
CCL3	MIP-1a	R&D systems, DY450-05	7.81 - 500	7.81
CCL5	RANTES	R&D systems, DY478-05	31.2 – 2,000	31.2
CCL7	MCP-3	Ebioscience, BMS6006INST	15.6 – 1,000	2.6
CXCL2	MIP-2a	R&D systems, DY452-05	15.6 – 1,000	15.6
CXCL10	-	R&D systems, DY466-05	62.5 – 4,000	62.5
CXCL12	SDF-1	R&D systems, DY460	46.9 – 3,000	46.9

2.10 Genetic analysis of the cholinergic gene locus

The cholinergic gene locus in the murine and human genome comprises the genes for both ChAT (choline acetyltransferase, the acetylcholine synthesizing enzyme) and VAChT (vesicular acetylcholine transporter) (Eiden, 1998; Eiden *et al.*, 2004; Erickson *et al.*, 1994; Lawal & Krantz, 2013). Investigation of possible steroid binding sites (response elements) at the cholinergic gene locus in the human and mouse genome was carried out within the so-called interdisciplinary Z-project of the FOR696 of the University Hospital of Regensburg (DFG-funded research unit). Possible response elements for steroids were checked within the cholinergic gene locus, which is located on chromosome 14 in the mouse genome (Pubmed: ChAT gene ID: 12647) and chromosome 10 in the human genome (Pubmed ChAT gene ID: 1103). In particular, possible binding sites within the VAChT gene (SLC18A3/Slc18a3, human/mouse respectively, solute carrier family 18 (vesicular monoamine), member 3) which is located within the ChAT locus at 10q11.2 (human, Pubmed VAChT gene ID: 6572) and 14 B; 14 19.4 cM (mouse, Pubmed VAChT gene ID: 20508) were checked. The Genomatix v2.4 (Mat-

Inspector Release professional 8.0.5, March 2011, database version ElDorado 08-2011, Matrix Family Library Version 8.4 (June 2011)) software suite was used (Cartharius *et al.*, 2005).

2.11 Presentation of data and statistical analysis

All data are given as mean ± SEM. Box plots give the 10th, 75th, 50th (median), 25th, and 10th percentile. We compared group medians by the non-parametric Mann-Whitney U test (Sigma Plot/Windows, version 11.0.0.75, Systat Software Inc). Due to the explorative nature of the study, we did not adjust for multiple use of the same data. Log2-signals in gene expression analysis were compared by using students' t-test. Correlation analysis was performed using Spearman's rank correlation (Sigma Plot). A p-value below 0.05 was considered as the significance level for all tests. Graphical interpretation of the signal intensities of selected genes in gene expression analysis is expressed in a color code, which is explained in the respective figure.

3 Results

3.1 Density of catecholaminergic tyrosine hydroxylase-positive and cholinergic vesicular acetylcholine transporter-positive nerve fibers in mice

With a latency of about 21 days post immunization, induction of collagen-induced arthritis in C57Bl/6 mice clinically resulted in swelling and erythema in toes, metatarsus and ankle joints of forepaws and hindpaws. Histologically, when compared to respective joints from healthy control mice (**Figure 7A**), arthritic joints demonstrated erosions of articular bone, destruction of articular cartilage, and inflammation of synovial tissue (**Figure 7B**). Sympathetic TH-positive (TH+) nerve fibers were detected in joints (**Figure 7C**) and in adjacent connective tissue surrounding blood vessels (**Figure 7D,E**). Cholinergic nerve fibers positive for the vesicular acetylcholine transporter (VAChT+) were primarily detected in muscle and skin tissue of the paws (**Figure 7F,G**).

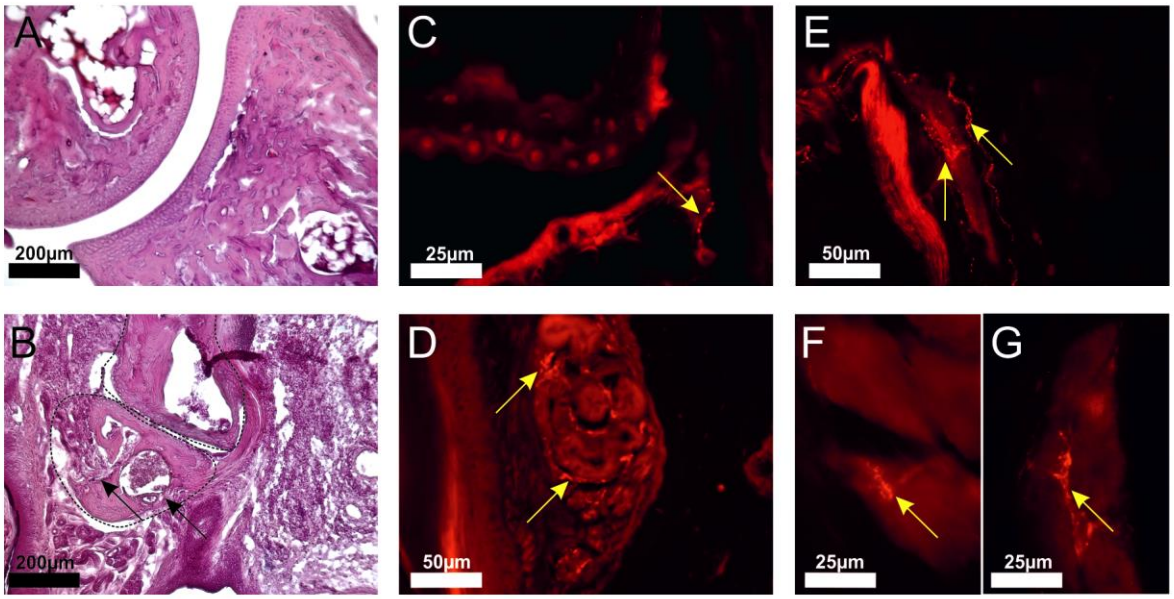

Figure 7. Catecholaminergic and cholinergic nerve fibers in mice. A) Histology of a normal joint in the C57Bl/6 mouse. Characteristic smooth cartilage surface at day 0 before immunization. B) Histology of arthritic joint in the C57Bl/6 mouse at day 35 post immunization showing erosion of bone (arrows). The dotted line indicates the typical anatomy of the normal non-inflamed joint for comparison. C,D,E) Catecholaminergic tyrosine hydroxylase (TH) - positive nerve fibers (arrow) in a joint (C) and surrounding blood vessels in the skin of mouse limbs (D,E). F,G) Cholinergic vesicular acetylcholine transporter (VAChT) - positive nerve fibers (arrows) in muscle (F) and skin (G) of an arthritic mouse paw. (Stangl *et al.*, 2015).

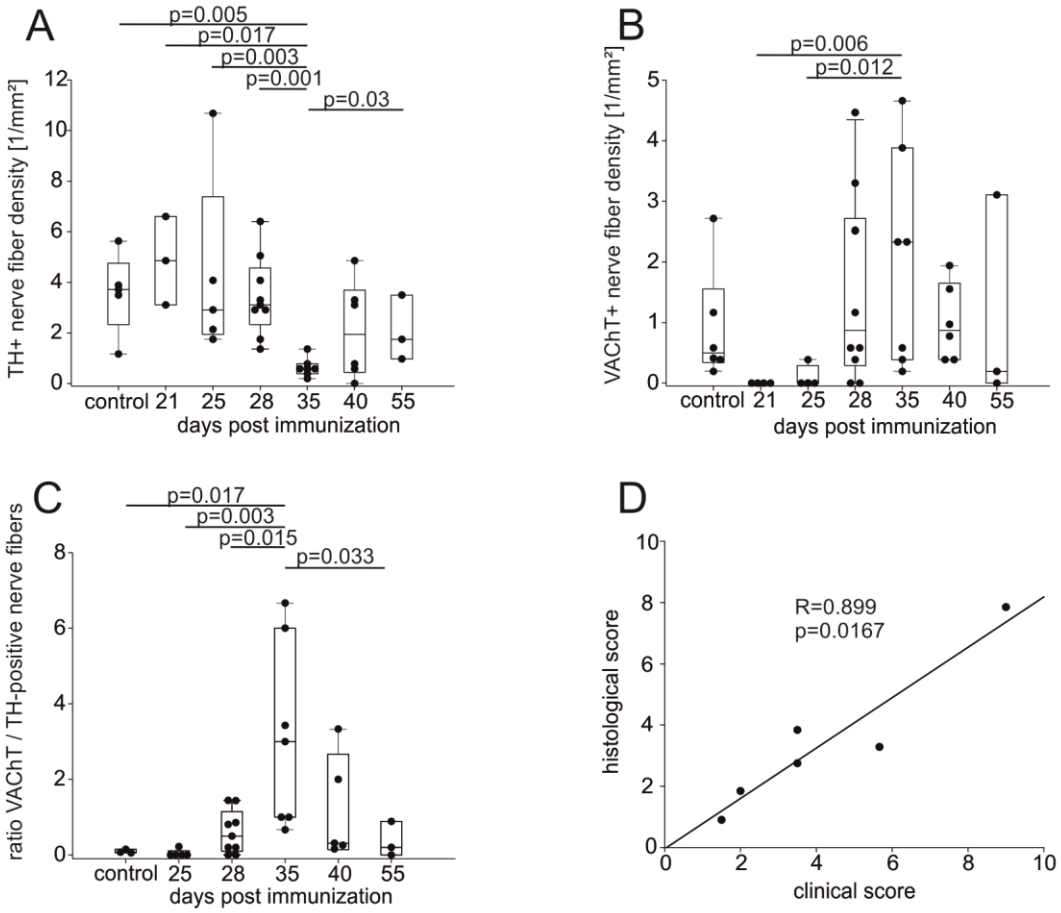

Figure 8. Density of catecholaminergic and cholinergic nerve fibers in inflamed paws of mice during collagen type II – induced arthritis (CIA). A) Density of catecholaminergic TH-positive nerve fibers. B) Density of cholinergic VAChT-positive nerve fibers. C) Ratio of cholinergic to catecholaminergic nerve fibers, calculated for each paw. A total of n=45 whole paws obtained from mice during CIA were collected at different time points post immunization. A,B,C) Each dot represents the nerve fiber density of one paw. Box plots demonstrate the 10th (whisker), 25th, 50th (median), 75th, 90th (whisker) percentile. D) Evaluation of inflamed paws: Spearman correlation of the mean clinical arthritis score and the mean histological arthritis score. One dot indicates the mean clinical score and mean histological score at a given day post immunization. Abbreviations see previous legends. (Stangl *et al.*, 2015).

Compared to paws from healthy mice with a density of about four sympathetic TH+ nerve fibers per square millimeter, the density of sympathetic TH+ nerve fibers in arthritic paws obtained on day 35 post immunization (p.i.) significantly decreased to a value below one nerve fiber per square millimeter (**Figure 8A**). Paws from day 35 p.i. also showed significantly decreased density of sympathetic TH+ nerve fibers compared to paws from day 21, 25 and 28 p.i. (**Figure 8A**). The density of TH+ nerve fibers however significantly increased again towards later stages of the disease (day 55 p.i., **Figure 8A**). During the course of arthritis, the density of cholinergic, VAChT+ nerve fibers in arthritic paws significantly increased on day 35 p.i. compared to day 21 and 25 when nearly no VAChT+ nerve fibers were detected (**Figure 8B**). The resulting ratios of densities of cholinergic VAChT+ nerve fibers divided

by the respective densities of sympathetic TH+ nerve fibers increased on day 35 p.i. when compared to ratios from control paws, day 25 and day 28 p.i. (**Figure 8C**). The ratio however decreased again to control level on day 55 p.i. (**Figure 8C**). The overall mean histological score which includes bone erosion, tissue inflammation and cell infiltration positively correlated with the mean clinical score (**Figure 8D**).

Cholinergic, VAChT+ nerve fibers were significantly more often found in less inflamed regions in the paw like in muscle or skin tissue compared to highly inflamed regions like in synovium or near focal bony erosions (**Figure 9**).

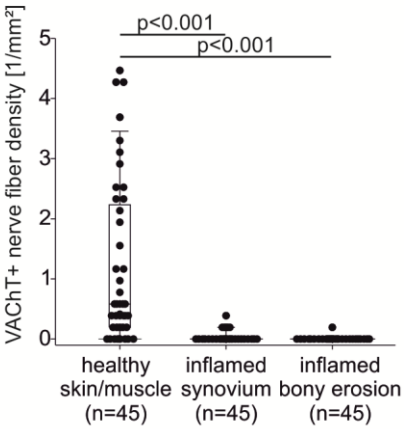

Figure 9. Localization of cholinergic nerve fibers in paws from arthritic C57Bl/6 mice. Each dot represents the nerve fiber density in one paw. Box plots demonstrate the 10th (whisker), 25th, 50th (median), 75th, 90th (whisker) percentile. Abbreviations: VAChT, vesicular acetylcholine transporter. (Stangl *et al.*, 2015).

3.2 Density of sympathetic TH-positive, cholinergic VAChT-positive and VIP-positive nerve fibers in osteoarthritis and rheumatoid arthritis

3.2.1 Innervation of finger joints

Cholinergic, VAChT+ and cholinergic VIP+ nerve fibers were detected in tissue samples obtained from OA and RA patients receiving finger arthrodesis surgery. The tissue samples were categorized into two basic groups: Samples mainly containing synovial and/or other types of connective tissue devoid of bone or cartilage and samples mainly containing articular bone and cartilage. Generally, VAChT+ and VIP+ nerve fibers were detected in both types of samples. In samples with connective tissue, VAChT+ nerve fibers (**Figure 10A**) were significantly more prevalent in samples obtained from OA patients compared to samples from RA patients (**Figure 10B**). No significant difference in the density of VIP+ nerve fibers (**Figure 10C**) was detected in connective tissue from finger joints from OA and RA patients (**Figure 10D**).

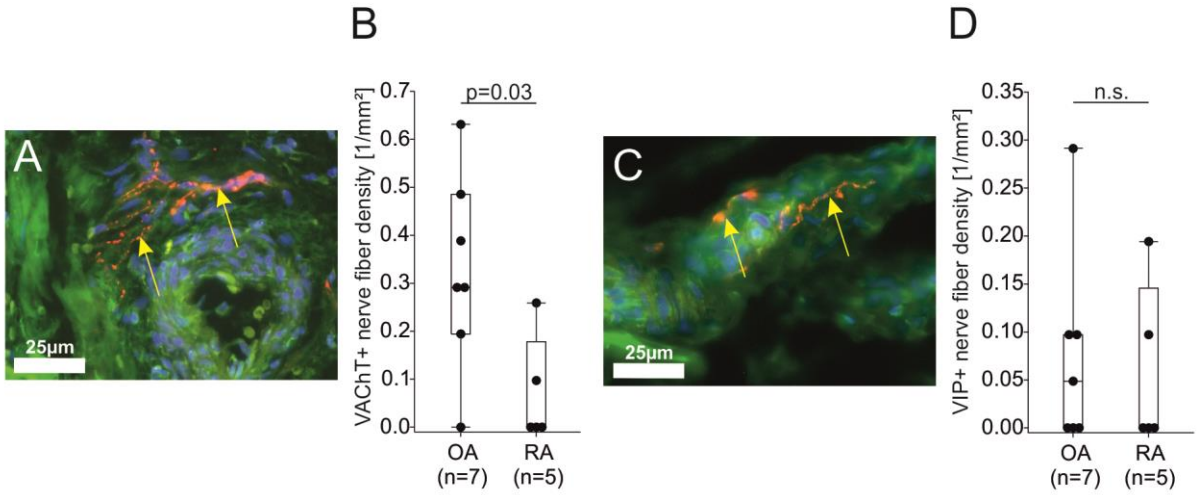

Figure 10. Cholinergic nerve fibers in connective tissue from OA and RA finger joints. A,C) Examples of cholinergic VAChT-positive nerve fibers (A, arrows) and cholinergic VIP-positive nerve fibers (C, arrows) in connective tissue from patients with arthritic finger joints receiving arthrodesis surgery. Magnification x400. Autofluorescence is displayed in green, stained nerve fibers are displayed in red. B,D) Comparison of cholinergic VAChT-positive (B) and cholinergic VIP-positive (D) nerve fibers in connective tissue from OA patients and patients with rheumatoid arthritis (RA). Each dot represents the nerve fiber density in the connective tissue of one finger joint of OA and RA patients (D,E). Box plots demonstrate the 10th (whisker), 25th, 50th (median), 75th, 90th (whisker) percentile. Abbreviations: OA, osteoarthritis; VAChT, vesicular acetylcholine transporter; VIP, vasoactive intestinal peptide; n.s., not significant. (Stangl *et al.*, 2015).

In samples primarily consisting of bone and cartilage, severity of cartilage damage and bone erosion was evaluated by the use of DMMB staining (for explanation, see 2.4). Cartilage in healthy condition with a high relative content of glycosaminoglycans is stained in a deep purple color (**Figure 11A**). The amount of glycosaminoglycans in the cartilage correlates with the color intensity of DMMB staining. In general, inflamed synovial tissue (**Figure 11B**), degradation of cartilage (**Figure 11B,C,D**), cells invading the joint space (**Figure 11C**), erosions of bone (**Figure 11B,D**) and pannus like structures (**Figure 11D**) were detected. Cholinergic VAChT+ and cholinergic VIP+ nerve fibers in bone containing tissue were detected (**Figure 11E,G**), but densities of these fibers (**Figure 11F,H**) were much lower than in connective tissue (**Figure 10B,D**). In contrast to finger joint samples containing connective tissue, no significant difference in VAChT+ nerve fiber density between bone samples obtained from OA patients compared to bone containing samples from RA patients was detected (**Figure 11F**). Similarly, no difference in VIP+ nerve fibers was observed (**Figure 11H**).

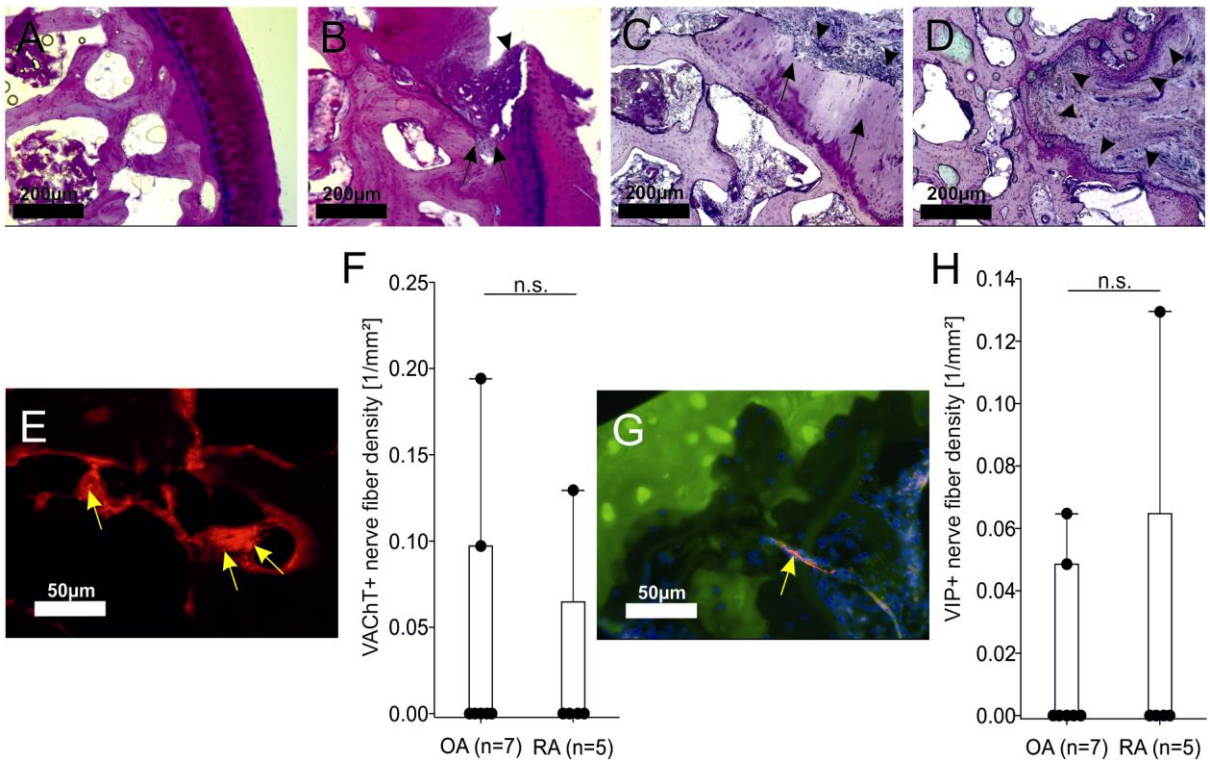

Figure 11. Cholinergic nerve fibers in bone tissue from finger joints in OA and RA patients. A,B,C,D) Representative DMMB (A,B) and HE (C,D) stainings of tissue from finger joints in OA and RA patients. A) Unharmed part of a joint. B,C) Connective tissue invading the joint space (arrow heads) and spots of bone erosion (B, arrows). Loss and change of cartilage (C, arrows). D) Pannus-like structure of connective tissue (arrow heads) invading bone tissue. E) Cholinergic VAChT-positive nerve fibers (arrows) adjacent to blood vessels in trabecular bone. G) Cholinergic VIP-positive nerve fiber (arrow) in subchondral bone. Autofluorescence displayed in green, cell nuclei in blue. F,H) Comparison of cholinergic VAChT-positive (F) and cholinergic VIP-positive (H) nerve fibers in bone tissue from OA and RA patient. Numbers in parentheses indicate total number of finger joints analyzed. Abbreviations: DMMB, 1,9-dimethyl-methylene blue; HE, hematoxylin-eosin. For explanation of other abbreviations and box plots see previous figures. (Stangl *et al.*, 2015).

Similarly, TH+ sympathetic nerve fibers were detected in OA and RA samples, but density of these nerve fibers did not differ between OA and RA samples neither in connective tissue containing material nor in mainly bone containing tissue (**Figure 12**).

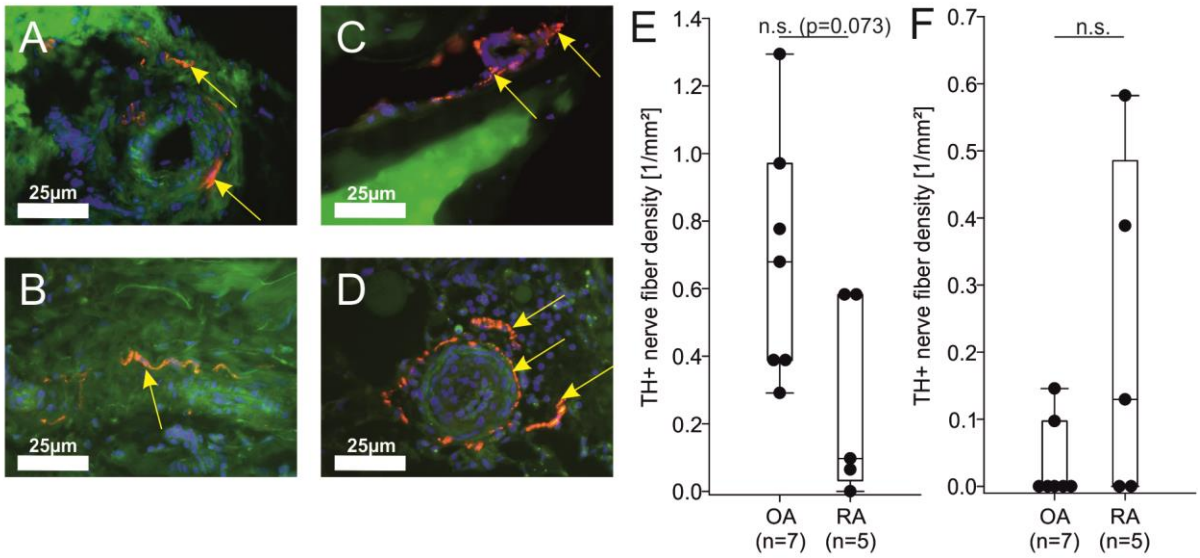

Figure 12. Sympathetic catecholaminergic nerve fibers in finger joint tissue from OA and RA patients. A,B) Examples of sympathetic TH-positive nerve fibers (A,B arrows) in samples from patients with OA receiving finger joint arthrodesis surgery. C,D) Examples of sympathetic TH-positive nerve fibers (C,D arrows) in samples from patients with RA receiving finger joint arthrodesis surgery. A,B,C,D) Magnification x400. Autofluorescence is displayed in green, TH+ stained nerve fibers are displayed in red. Comparison of the density of TH+ nerve fibers in samples devoid of bone tissue (E) and in bone tissue (F). Each dot represents the nerve fiber density in the tissue of one finger joint of OA and RA patients (D,E). Box plots demonstrate the 10th (whisker), 25th, 50th (median), 75th, 90th (whisker) percentile. Abbreviations: OA, osteoarthritis; RA, rheumatoid arthritis; TH, tyrosine hydroxylase; n.s., not significant.

3.2.2 Innervation of knee synovial tissue of OA and RA patients

In synovial tissue which was obtained from OA and RA patients undergoing total knee replacement surgery, VAChT+ (**Figure 13A**) and VIP+ (**Figure 13C**) nerve fibers with their typical bead like structure were detected. The densities of both, VAChT+ and VIP+ did not statistically differ. (**Figure 13B,D**). Density of TH+ nerve fibers in knee synovial tissue from OA and RA patients was not investigated since this has already been done in earlier studies.

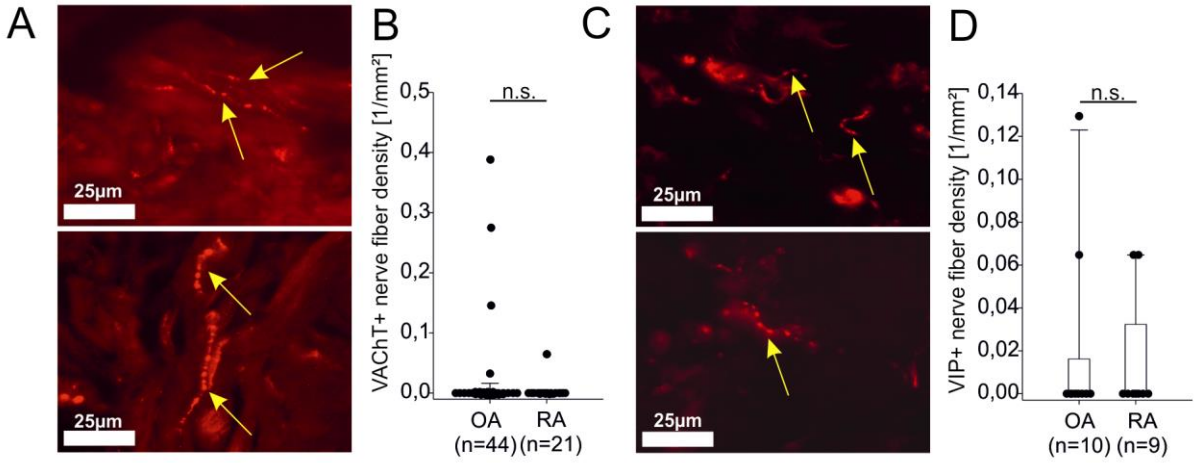

Figure 13. Cholinergic nerve fibers in synovial tissue from OA and RA patients. A,C) Examples of cholinergic VAChT-positive nerve fibers (A, arrows in upper and lower image) and cholinergic VIP-positive nerve fibers (C, arrows in upper and lower image) in synovial tissue from patients with osteoarthritis (OA) or rheumatoid arthritis (RA) undergoing total knee joint replacement surgery. Magnification x400. B) Comparison of cholinergic VAChT-positive nerve fibers in synovial tissue in the knee from OA patients and patients with RA. D) Comparison of cholinergic VIP-positive nerve fibers in synovial tissue in the knee from OA patients and patients with RA. One dot indicates the mean nerve fiber density in the synovial tissue of one patient. Box plots demonstrate the 10th (whisker), 25th, 50th (median), 75th, 90th (whisker) percentile. Abbreviations: VAChT, vesicular acetylcholine transporter; VIP, vasoactive intestinal peptide; n.s., not significant. (Stangl *et al.*, 2015).

3.2.3 Expression of the alpha-7 subtype-containing nicotinic acetylcholine receptor in fibroblast like synoviocytes

In a brief test, fibroblast-like synoviocytes (FLS) from OA patients (passage 2-4) were stained for the alpha-7 subtype-containing nicotinic acetylcholine receptor (α7nAChR). The α7nAChR stained cells exhibited a positive staining (**Figure 14A**) compared to immunoglobulin control (**Figure 14B**).

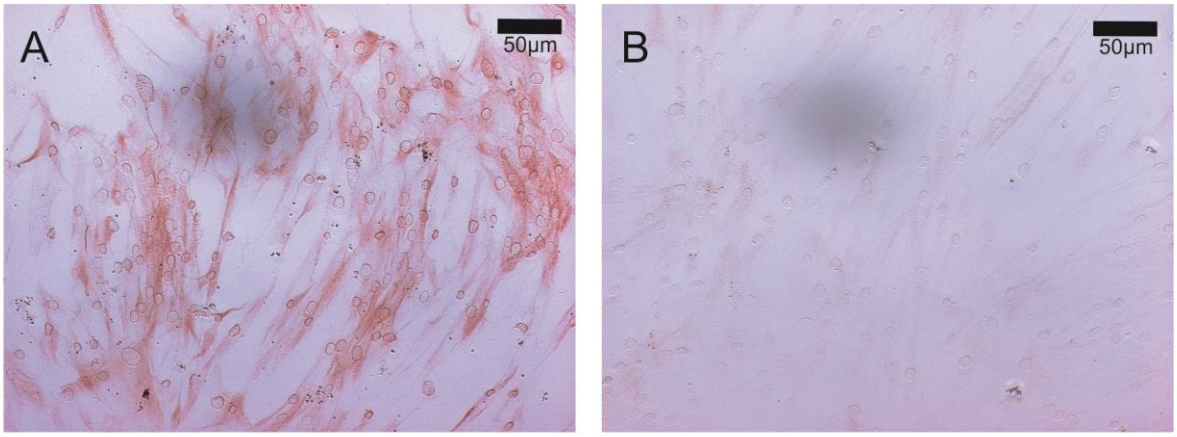

Figure 14. Expression of the alpha-7 subunit-containing nicotinic acetylcholine receptor (α7nAChR) in OA fibroblast-like synoviocytes. Example of fibroblast-like synoviocytes obtained from the synovial tissue of one OA patient undergoing knee replacement surgery. A) DAB staining of the α7nAChR in OA fibroblast-like synoviocytes. B) DAB staining of immunoglobulin control antibody. A,B) Magnification x200. Abbreviations: OA, osteoarthritis; DAB, 3,3'-diaminobenzidine.

3.3 Induction of the cholinergic phenotype of nerve fibers in mice sympathetic ganglia

To test a possible influence of different types of cells, namely draining lymph node cells and OCP cells from healthy and arthritic mice, on the frequency of VAChT-positive cholinergic nerve fibers in sympathetic mouse ganglia, the co-culture system shown in chapter **2.6** was used. In a second approach, candidate molecules, which were supposedly produced by OCPs, were tested.

3.3.1 Co-culture experiments

In many co-culture experiments, draining lymph node cells and OCP cells were migrating into the other half of the well after the insert was removed from the well. Nerve fibers from sympathetic ganglia and OCPs sometimes also came into direct contact (**Figure 15**). In some cases nerve fibers also formed basket shaped structures around these cells.

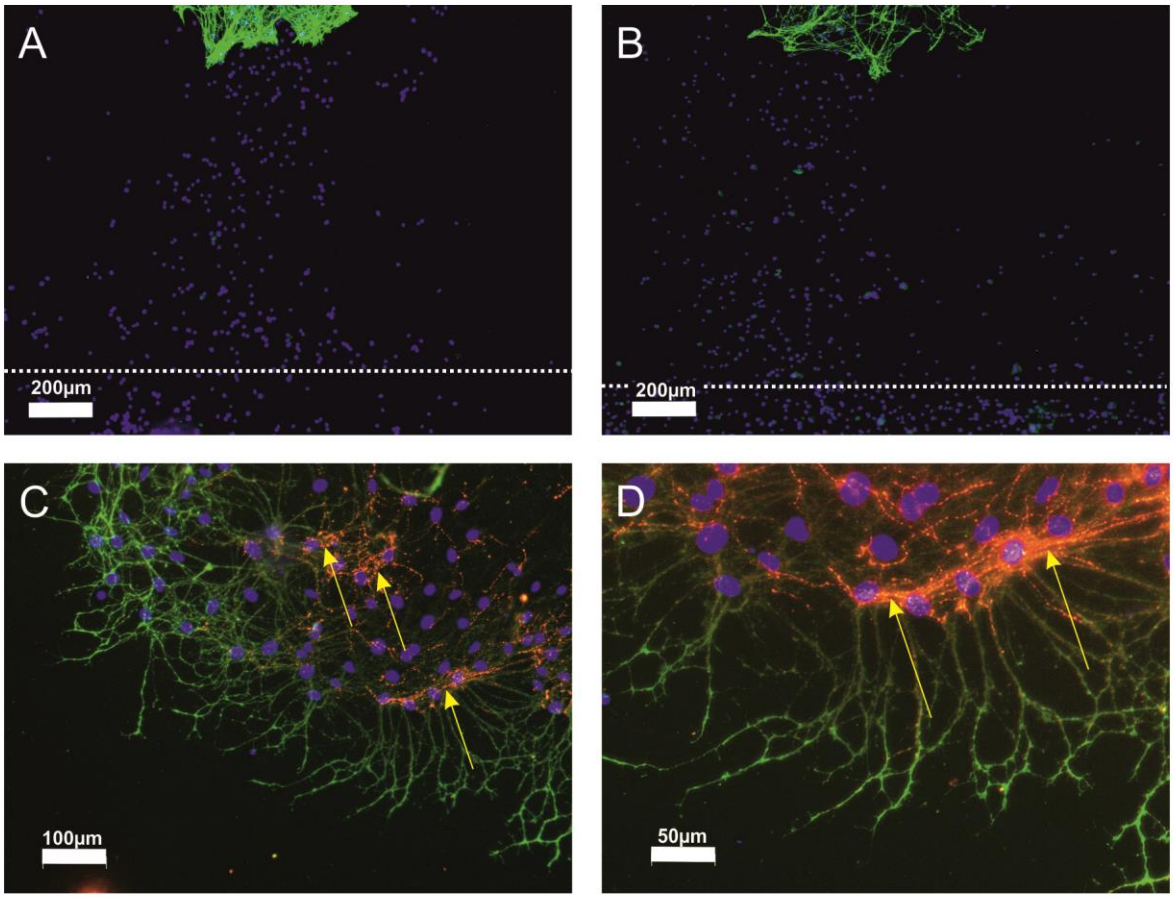

Figure 15. Chemotaxis and appearance of cholinergic nerve fibers in co-culture experiments with osteoclast progenitor cells and sympathetic ganglia. A,B) Examples of osteoclast progenitor cells migrating towards the radial nerve fiber outgrowth of sympathetic ganglia. The dotted lines indicate the border of the co-culture system when the silicone culture insert was still present. C,D) Sympathetic nerve fibers form basket like structures around osteoclast progenitor cells, in some cases the nerve fibers are VAChT positive (arrows).The culture medium contained nerve growth factor, macrophage colony-stimulating factor, and receptor activator of nuclear factor kappa-B ligand (RANKL). Coculture period lasted for two days. Catecholaminergic TH-positive fibers are displayed in green, cholinergic VAChT-positive fibers are stained in red, and osteoclast progenitor cells in blue. A,B) Magnification x50. C) Magnification x100. D) Magnification x200. Abbreviations see previous legends. (Stangl *et al.*, 2015).

In experiments with sympathetic ganglia from newborn C57Bl/6 mice in co-culture with draining lymph node cells from healthy and arthritic C57Bl/6 mice, no significant difference in the ratio of cholinergic to catecholaminergic nerve fibers was observed (**Figure 16A**). However, when OCP cells were used in the co-culture system, this ratio significantly increased to a mean value of above 0.5 in the case where

OCPs were obtained from healthy C57Bl/6 mice as compared to the same experiment with OCP cells from arthritic mice (**Figure 16A**). To check a possible strain specificity, the experiment setting was repeated only that draining lymph node cells and OCPs were now obtained from healthy and arthritic DBA1/J mice. Here, experiments with OCPs from healthy DBA1/J mice again resulted in higher ratios as compared to co-cultures with cells from mice with CIA (**Figure 16B**). In addition, in contrast to experiments in which both cell types were gathered from C57Bl/6 mice, assays with draining lymph node cells from healthy DBA1/J mice displayed significantly higher ratios compared to experiments with cells from arthritic mice (**Figure 16B**).

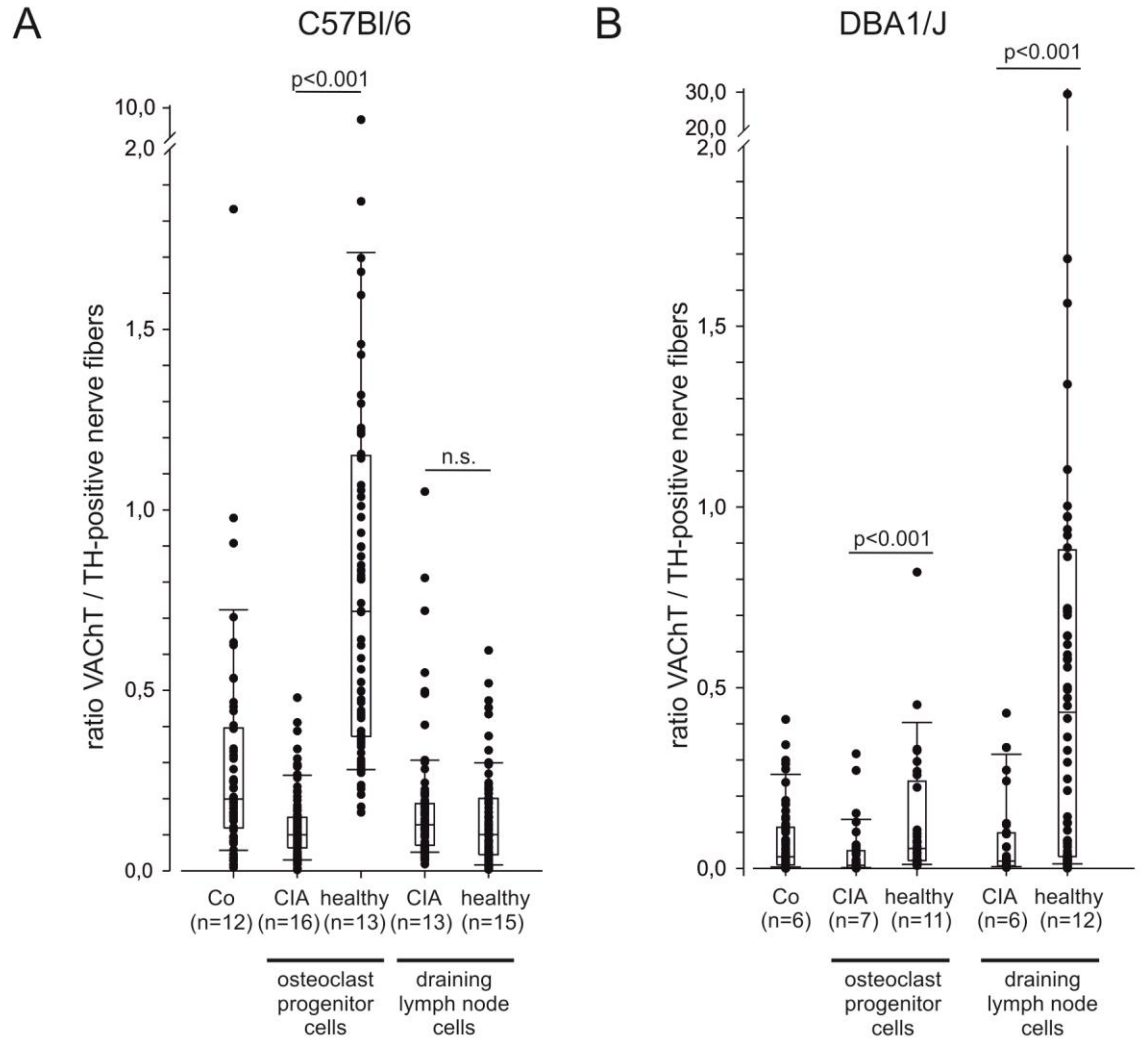

Figure 16. Ratio of cholinergic to catecholaminergic nerve fibers from sympathetic ganglia of newborn C57Bl/6 mice in co-culture experiments with osteoclast progenitor cells and draining lymph node cells from healthy and arthritic adult C57Bl/6 animals (A) or DBA1/J mice (B). The control situation reflects sympathetic ganglia only without osteoclast progenitor cells or draining lymph node cells. Each dot indicates the ratio of red pixel positivity for cholinergic VAChT-positive nerve fibers divided by green pixel positivity of sympathetic TH-positive nerve fibers of one digitally analyzed image. Numbers in parentheses indicate total number of sympathetic ganglia analyzed. Box plots demonstrate the 10th (whisker), 25th, 50th (median), 75th, 90th (whisker) percentile. Abbreviations: Co, control; CIA, collagen type II-induced arthritis; VAChT, vesicular acetylcholine transporter; TH, tyrosine hydroxylase. (Stangl *et al.*, 2015).

3.3.2 Stimulation of sympathetic ganglia

After the genome and proteome of the OCP cells from healthy and arthritic mice was analyzed (see 3.4 and 3.5) several candidate molecules were selected as possible soluble transition factors responsible for the increased frequency of VAChT+ cholinergic nerve fibers in sympathetic ganglia. First, LIF, which is a known transition factor for sympathetic nerve fibers, was identified as a possible molecule released by OCPs (see 3.4 and 3.5) and tested in the assay with sympathetic ganglia. Stimulation of sympathetic ganglia with 100ng/mL of LIF significantly increased the ratio of VAChT+ cholinergic to TH+ catecholaminergic nerve fibers (**Figure 17**). This effect was augmented if the stimulation with LIF was performed in culture medium containing progesterone since stimulations with LIF but without progesterone showed significantly lower ratios of VAChT+ to TH+ nerve fibers (**Figure 17**).

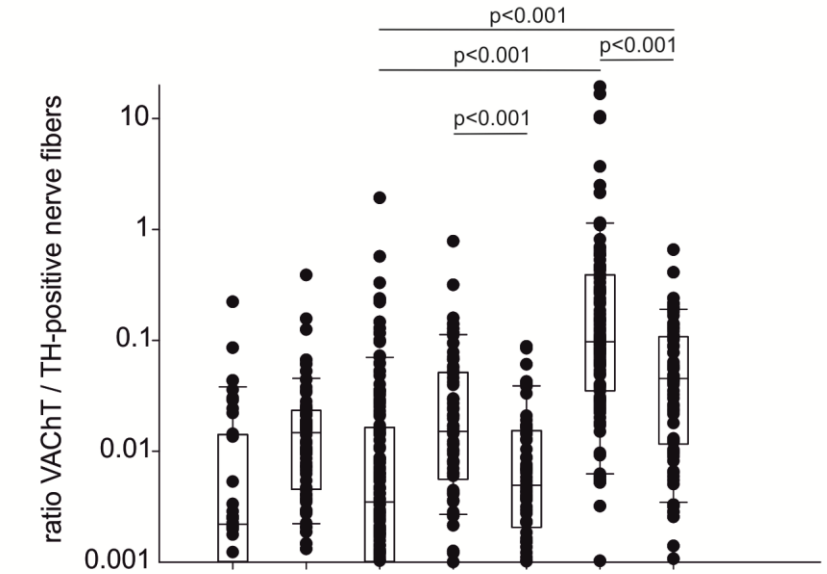

NGF 10ng/mL	+	+	-	+	+	-	-
NGF 25ng/mL	-	-	+	-	-	+	+
progesterone	+	-	+	+	-	+	-
LIF 100ng/mL	-	-	-	+	+	+	+
ganglia, n=	5	8	15	8	7	7	6

Figure 17. Stimulation of sympathetic ganglia with leukemia inhibitory factor (LIF) under different conditions. The effect of LIF on the ratio of VAChT+ cholinergic to TH+ catecholaminergic nerve fibers in sympathetic ganglia was tested with different concentrations of NGF. Additionally the effect of progesterone in the culture medium was tested. Sympathetic ganglia were grown for 2 d with or without progesterone with 100ng/mL of NGF and after 2 d received fresh culture medium with a lower concentration of NGF with or without progesterone and with or without LIF. After 2 d, ganglia were fixed, subjected to double immunofluorescence staining and subsequently digitally analyzed. Each dot indicates the ratio of red pixel positivity for cholinergic VAChT-positive nerve fibers divided by green pixel positivity of sympathetic TH-positive nerve fibers of one digitally analyzed image. Numbers in parentheses indicate total number of sympathetic ganglia analyzed. Box plots demonstrate the 10th (whisker), 25th, 50th (median), 75th, 90th (whisker) percentile. Abbreviations: NGF, nerve growth factor; other abbreviations see previous legends. (Stangl *et al.*, 2015).

In addition to experiments with LIF, further stimulation assays of sympathetic ganglia with TIMP-1 and BGN (biglycan) were conducted due to the fact that these two molecules showed enhanced expression in the gene expression analysis (see 3.4) and, in the case of TIMP-1, also in the proteome analysis of OCP cells. Stimulations with biglycan and TIMP-1 significantly enhanced the ratio of VAChT-positive to TH-positive nerve fibers in sympathetic ganglia (**Figure 18**) but not as strong as LIF (**Figure 17**) or in co-culture with OCP cells in (**Figure 16A**).

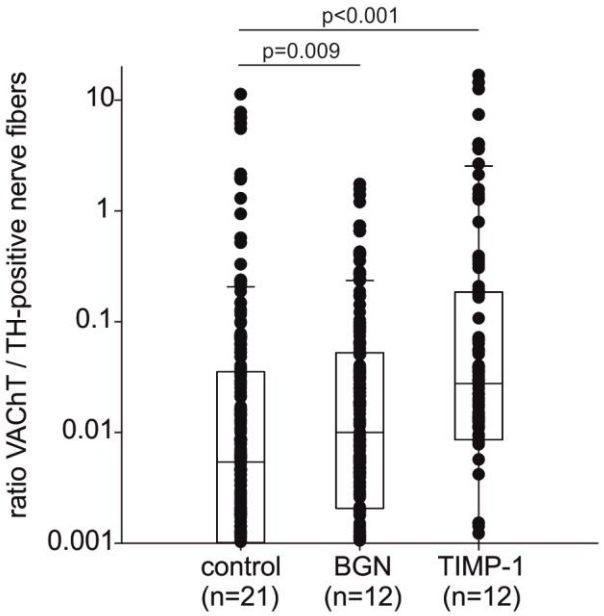

Figure 18. Stimulation of sympathetic ganglia with biglycan (BGN) or tissue inhibitor of metalloproteinase 1 (TIMP-1). The effect of BGN and TIMP-1 on the ratio of VAChT+ cholinergic to TH+ catecholaminergic nerve fibers in sympathetic ganglia was tested. Sympathetic ganglia were grown for 2 d with progesterone and 100ng/mL of NGF and after 2 d received fresh culture medium with 25ng/mL of NGF with progesterone and with BGN or TIMP-1, respectively. After 2 d, ganglia were fixed, subjected to double immunofluorescence staining and subsequently digitally analyzed. Each dot indicates the ratio of red pixel positivity for cholinergic VAChT-positive nerve fibers divided by green pixel positivity of sympathetic TH-positive nerve fibers of one digitally analyzed image. Numbers in parentheses indicate total number of sympathetic ganglia analyzed. Box plots demonstrate the 10th (whisker), 25th, 50th (median), 75th, 90th (whisker) percentile. Abbreviations: BGN, biglycan; TIMP-1, tissue inhibitor of metalloproteinase 1; other abbreviations see previous legends.

In contrast to the control situation with only poly-D-lysine coated chambers, coating with fibronectin and stimulation with RGDS tetra-peptide resulted in a very dense and overlapping, bundle-like outgrowth of sympathetic nerve fibers (**Figure 19B,C**). Due to this dense, overlapping outgrowth of nerve fibers, double immunofluorescence detection of VAChT+ and TH+ nerve fibers resulted in staining which was not suitable for quantification of VAChT and TH pixel positivity and respective results were regarded as not applicable for interpretation. Still, the observed effects of fibronectin and RGDS on the morphology of sympathetic nerve fiber outgrowth are noteworthy (**Figure 19**).

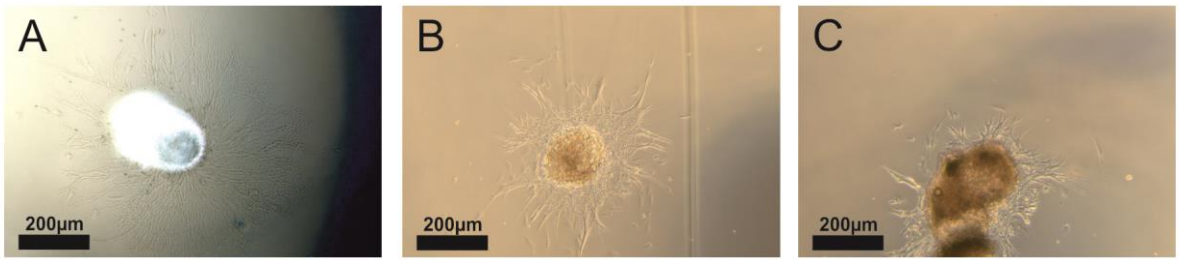

Figure 19. Effects of Fibronectin and RGDS on the outgrowth of nerve fibers from sympathetic ganglia. A) Control situation with standard poly-D-lysine coated chamber surface displays typical radial outgrowth of nerve fibers with nerve fibers showing individual and separate sprouting (image is color-inverted for better contrast). B) Stimulation of sympathetic ganglia with RGDS peptide leads to a more dense, overlapping and bundle like outgrowth of nerve fibers. C) Incidence of inhibited nerve fiber outgrowth and very intense clustered nerve fibers surrounding the ganglion soma is increased in fibronectin coated and RGDS stimulated ganglia. Abbreviations: RGDS, arginin-glycin-aspartate-serin tetrapeptide. Brightfield, magnification x50.

3.4 Gene expression levels of osteoclast progenitor cells

Based on the results from the co-culture experiments with OCP cells differentiated for 2 d which resulted in an enhanced frequency of cholinergic nerve fibers in sympathetic ganglia, the transcriptome of OCPs obtained from healthy control and arthritic mice was investigated. The results of cells differentiated for 2 d are highlighted on the left side of the table, while the gene expression values of cells differentiated for 5 d are for comparison displayed on the right part of the table (**Figure 20**) (Stangl *et al.*, 2015).

Gene symbol	Gene description	Gene accession	mean fold change (2 d Differentiation)	p-value (2 d Diff.)	mean fold change (5 d Differentiation)	p-value (5 d Diff.)
Bgn	biglycan	NM_007542	-5.19	0.0003	-3.01	0.0456
Tnc	tenascin C	NM_011607	-4.09	0.0003	-1.49	0.0005
Tspan7	tetraspanin 7	NM_019634	-3.44	0.006	-1.18	0.2130
Timp1	tissue inhibitor of metalloproteinase 1	NM_001044384	-3.41	0.006	-2.49	0.0174
Oscar	osteoclast associated receptor	NM_175632	-2.83	0.0065	-1.15	0.2450
Fn1	fibronectin 1	NM_010233	-2.75	0.0008	-2.60	0.0616
Tns1	tensin 1	NM_027884	-2.73	0.0004	+1.06	0.3190
Postn	periostin	NM_015784	-2.57	0.0078	-1.54	0.0622
Ctgf	connective tissue growth factor	NM_010217	-2.48	0.0023	-1.71	0.0555
Lif	leukemia inhibitory factor	NM_008501	-2.40	0.0041	-1.11	0.1510
Dcstamp	dentrocyte expressed seven transmembrane protein	NM_029422	-2.29	0.0085	-0.44	0.4300
Ocstamp	osteoclast stimulatory transmembrane protein	ENSMUST00000029213	-2.10	0.0048	-0.23	0.4010
Sparc	secreted acidic cysteine rich glycoprotein	NM_009242	-1.98	0.0000	-2.27	0.1130
Ccl8	chemokine (C-C motif) ligand 8	NM_021443	+3.28	0.0234	+1.54	0.2910
Il1a	interleukin 1alpha	NM_010554	+3.53	0.0014	-0.10	0.4630
Ccr5	chemokine (C-C motif) receptor 5	NM_009917	+3.63	0.0030	+1.17	0.3590
Cxcl3	chemokine (C-X-C motif) ligand 3	NM_203320	+3.67	0.0108	+1.27	0.0778
Ccl5	chemokine (C-C motif) ligand 5	NM_013653	+4.09	0.0013	-0.03	0.8740
Tnf	tumor necrosis factor	NM_013693	+4.14	0.0000	0.00	0.9990
Ccl12	chemokine (C-C motif) ligand 12	NM_011331	+5.06	0.0062	+1.17	0.1460
Ccl4	chemokine (C-C motif) ligand 4	NM_013652	+5.42	0.0000	+1.07	0.6470
Il1b	interleukin 1beta	NM_008361	+6.07	0.0008	+1.49	0.1770
Ccl3	chemokine (C-C motif) ligand 3	NM_011337	+6.37	0.0000	+0.05	0.7110
Ccl6	chemokine (C-C motif) ligand 6	NM_009139	+8.20	0.0003	-0.02	0.6580
Mmp8	matrix metalloproteinase 8	NM_008611	+9.61	0.0000	-1.24	0.1430
Cxcl2	chemokine (C-X-C motif) ligand 2	ENSMUST00000075433	+10.21	0.0003	-0.02	0.9680
Ccl2	chemokine (C-C motif) ligand 2	NM_011333	+11.18	0.0005	-0.26	0.5820
Marco	macrophage receptor with collagenous structure	NM_010766	+13.24	0.0000	-1.08	0.4280
Ccl7	chemokine (C-C motif) ligand 7	NM_013654	+18.31	0.0001	-0.23	0.6360
Saa3	serum amyloid A3	NM_011315	+52.86	0.0000	+1.24	0.3070

Figure 20. **Results from microarray gene expression analysis of osteoclast progenitors (OCP) from healthy and arthritic mice.** Whole RNA was isolated from OCPs obtained from arthritic (n=3) and age corresponding healthy control animals (n=3) (left table). OCPs were differentiated for 2 d with M-CSF and RANKL (left table). Negative values (bright background) in mean fold change indicate higher mRNA expression of the respective genes in cells obtained from healthy animals while positive values (dark background) indicate higher expression in cells from arthritic mice. For comparison, gene expression was also analyzed from OCPs obtained from arthritic (n=2) and corresponding healthy controls (n=2) which were differentiated for 5 d with M-CSF and RANKL (right table, white background). Isolated whole RNA was analyzed with the Affymetrix GeneChip mouse Gene 2.0 ST

array. Abbreviations: M-CSF, macrophage colony stimulating factor; RANKL, receptor activator of nuclear factor-kappa-B ligand. (Stangl *et al.*, 2015).

3.4.1 Gene expression in osteoclast progenitor cells from healthy mice

The gene expression values are given in mean fold changes, with signals from RNA obtained from arthritic mice being compared to signals from RNA obtained from healthy mice as control. This has the consequence that positive values in the mean fold change indicate an up-regulation of a given gene in cells from arthritic mice, while negative values indicate a relative up-regulation in cells from healthy control animals. Following transcripts were up-regulated in for 2 d differentiated OCP cells from healthy mice compared to cells from arthritic animals with an assumed threshold value for up-/down-regulation of approximately +/-2.0: *Biglycan* (-5.19), *tenascin C* (-4.09), *tetraspanin 7* (-3.44), *tissue inhibitor of metalloproteinase 1* (-3.41), *osteoclast associated receptor* (-2.83), *fibronectin 1* (-2.75), *tensin 1* (-2.73), *periostin* (-2.57), *connective tissue growth factor* (-2.48), *leukemia inhibitory factor* (-2.40), *dendrocyte expressed seven transmembrane protein* (-2.29), *osteoclast stimulatory transmembrane protein* (-2.10), *secreted acidic cysteine rich glycoprotein* (-1.98) (**Figure 20**). In cells differentiated for 5 d, transcripts for *Biglycan* (-3.01) and *tissue inhibitor of metalloproteinase 1* (-2.49) were still significantly up-regulated in cells from healthy mice, while a trend towards higher expression was observable for *fibronectin 1* (-2.60) and *secreted acidic cysteine rich glycoprotein* (-2.27) (**Figure 20**).

3.4.2 Gene expression in osteoclast progenitor cells from arthritic mice

In contrast, following transcripts of genes were significantly and markedly up-regulated in OCPs from arthritic mice: *Ccl8* (+3.28), *Il1a* (+3.53), *Ccr5* (+3.63), *Cxcl3* (+3.67), *Ccl5* (+4.09), *Tnf* (+4.14), *Ccl12* (+5.06), *Ccl4* (+5.42), *Il1b* (+6.07), *Ccl3* (+6.37), *Ccl6* (+8.20), *Mmp8* (+9.61), *Cxcl2* (+10.21), *Ccl2* (+11.18), *Marco* (+13.24), *Ccl7* (+18.31) and *Saa3* (+52.86) (for details and abbreviations see **Figure 20**). However, none of these gene transcripts was up-regulated in cells differentiated for 5 consecutive days (**Figure 20**).

3.4.3 Clustering of selected genes in osteoclast progenitor cells

In order to visualize the results given in **Figure 20**, a clustering algorithm was used to group subsets of genes resulting in a color coded image which indicates how strong the relation of expression signals of the respective genes to each other is (**Figure 21**).

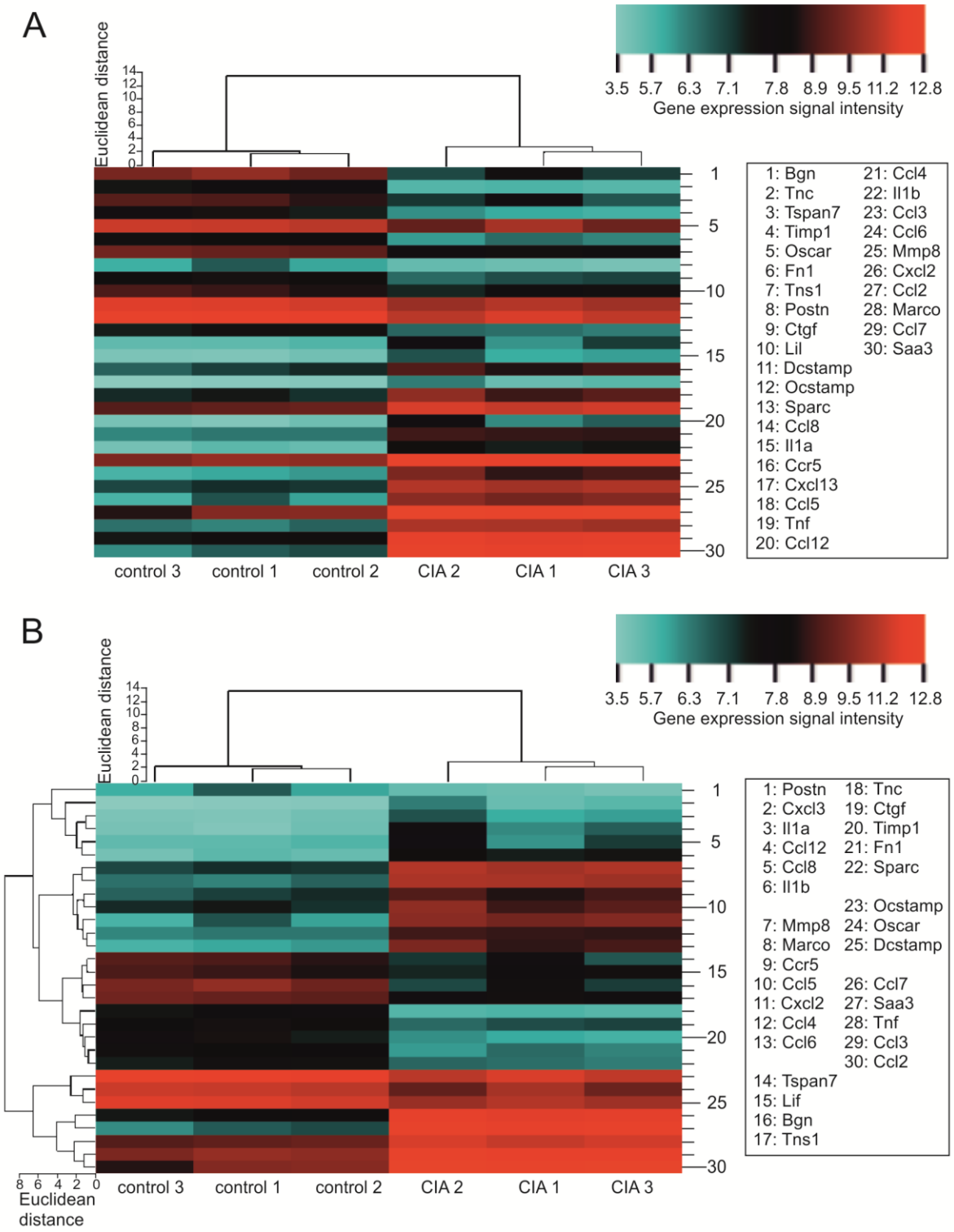

Figure 21. Clustered and color-coded heat map with clustering trees describing gene expression signal intensities from microarray analysis of osteoclast progenitor cells. A) Only the columns (=samples, control n=3, CIA n=3) are clustered; The given genes (1-30) are ordered after the mean fold change value of the respective gene (see previous figure). B) Columns (=samples) and rows (=genes) are clustered; Branching of the clustering tree indicates groups of genes with similar gene expression levels. A,B) Used clustering settings were Euclidean distance method and average linkage cluster algorithm. Abbreviations: see previous figure legends.

3.5 Proteome analysis of osteoclast progenitor cells

In the next step, cell culture supernatants of OCP cells obtained from healthy and arthritic mice were generated to check whether the observed changes in the gene expression also translated into changes of the respective protein concentrations. A general, relative expression screening with the help of the proteome profiler method was conducted, followed by quantitative ELISA measurements of single proteins.

3.5.1 Proteome profiler results

From the n=10 supernatants generated by OCP cells from healthy mice, n=4 were selected and subjected to the proteome profiler assay. Analogically, n=4 supernatants were picked from n=10 samples generated by OCPs from arthritic mice. A total of 40 proteins was screened with this technique. The results are displayed in two separate charts. In general, most of the cytokines investigated displayed a higher expression in supernatants harvested from OCP cells obtained from arthritic mice. In particular, interferon gamma (IFNγ), interleukins 1 alpha and beta, interleukins 3, 4, 6, 7, 10, 13, 16, 17, 23, 27, TREM-1 (all **Figure 22**), and chemokine (C-C motif) ligands 1, 2, 3, 5, and chemokine (C-X-C motif) ligands 9, 10, 11, 12, 13 showed stronger expressions (**Figure 23**).

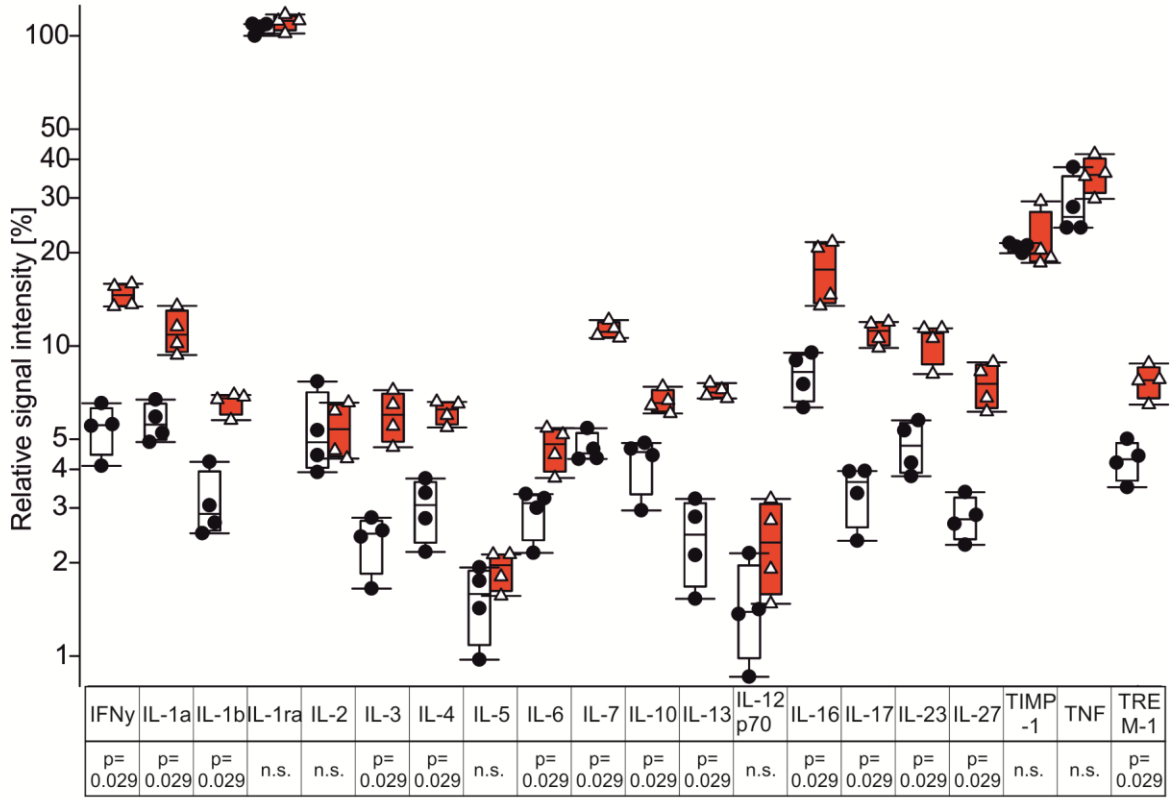

Figure 22. Cytokine profile (I) in supernatants of osteoclast progenitor cells. Proteome profiler mouse cytokine array panel A membranes were used for analysis of a total of 40 cytokines (see also figure 16). One dot or triangle indicates the relative signal intensity of one cytokine in the supernatant generated by cells from one animal. Black dots and white box plots indicate supernatants analyzed from control animals (n=4), whereas white triangles and red box plots indicate supernatants analyzed from arthritic animals (n=4). Box plots demonstrate the 10th (whisker), 25th, 50th (median), 75th, 90th (whisker) percentile. Abbreviations: IFNy, interferon gamma; IL, interleukin; IL-1a, interleukin 1alpha; IL-1b, interleukin 1beta; IL-1ra, interleukin 1 receptor antagonist; TIMP-1, tissue inhibitor of metalloproteinase 1; TNF, tumor necrosis factor; TREM-1, triggering receptor expressed on myeloid cells 1; n.s., not significant.

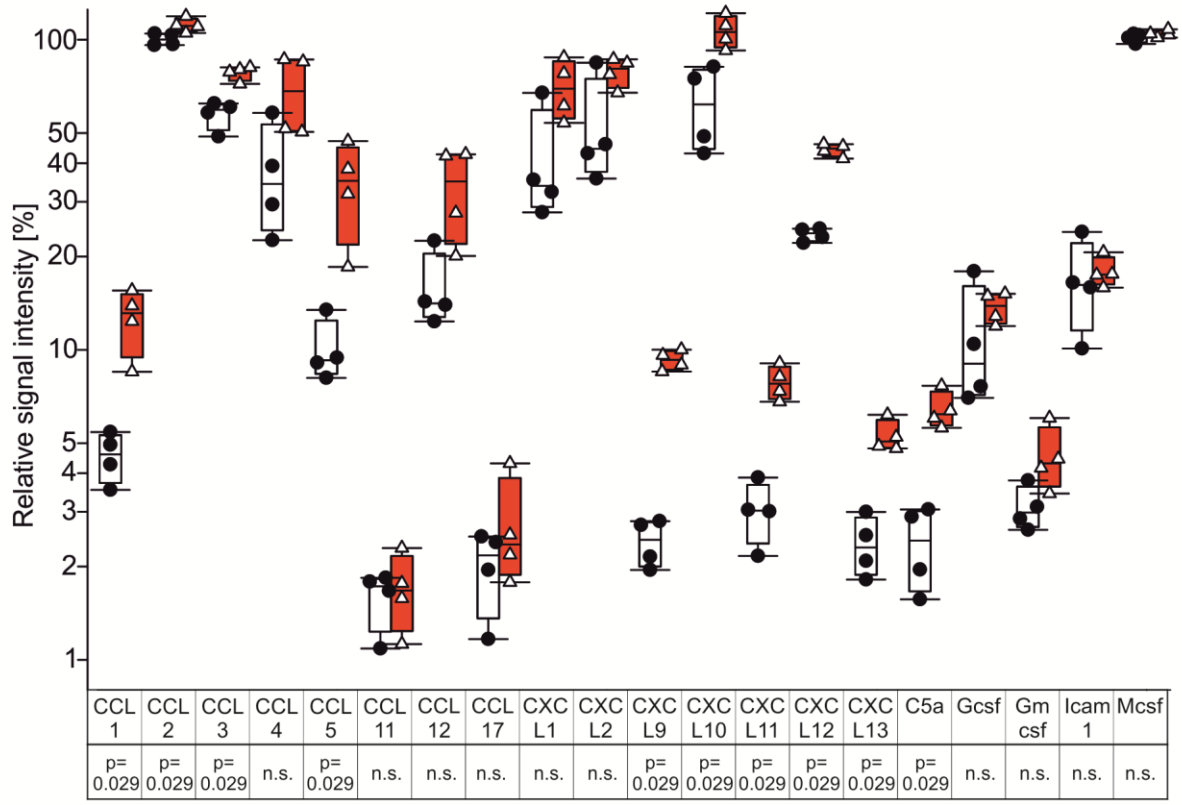

Figure 23. Cytokine profile (II) in supernatants of osteoclast progenitor cells. Proteome profiler mouse cytokine array panel A membranes were used for analysis of a total of 40 cytokines (see also previous figure 15). One dot or triangle indicates the relative signal intensity of one cytokine in the supernatant generated by cells from one animal. Black dots and white box plots indicate supernatants analyzed from control animals (n=4), whereas white triangles and red box plots indicate supernatants analyzed from arthritic animals (n=4). Box plots demonstrate the 10th (whisker), 25th, 50th (median), 75th, 90th (whisker) percentile. Abbreviations: CCL, chemokine (C-C motif) ligand; CXCL, chemokine (C-X-C motif) ligand; C5a, complement component 5a, in mouse known as Hc, hemolytic complement; Gcsf, colony stimulating factor 3 (granulocyte); Icam1, intercellular adhesion molecule 1; Mcsf, colony stimulating factor 1 (macrophage); n.s., not significant.

3.5.2 ELISA results of supernatants from osteoclast progenitor cells

3.5.2.1 Oncostatin M (OSM) and tissue inhibitor of metalloproteinase 1 (TIMP-1)

Oncostatin M (OSM) was detectable at very low concentrations in both kinds of supernatants (healthy and arthritic). Levels of OSM in samples of cells gathered from control mice were significantly higher than respective samples from arthritic mice (**Figure 24A**). TIMP-1 was detectable in both, control and CIA supernatants. Samples from cells obtained from healthy animals displayed significantly higher concentrations than samples from arthritic animals (**Figure 24B)**, which confirms gene expression studies.

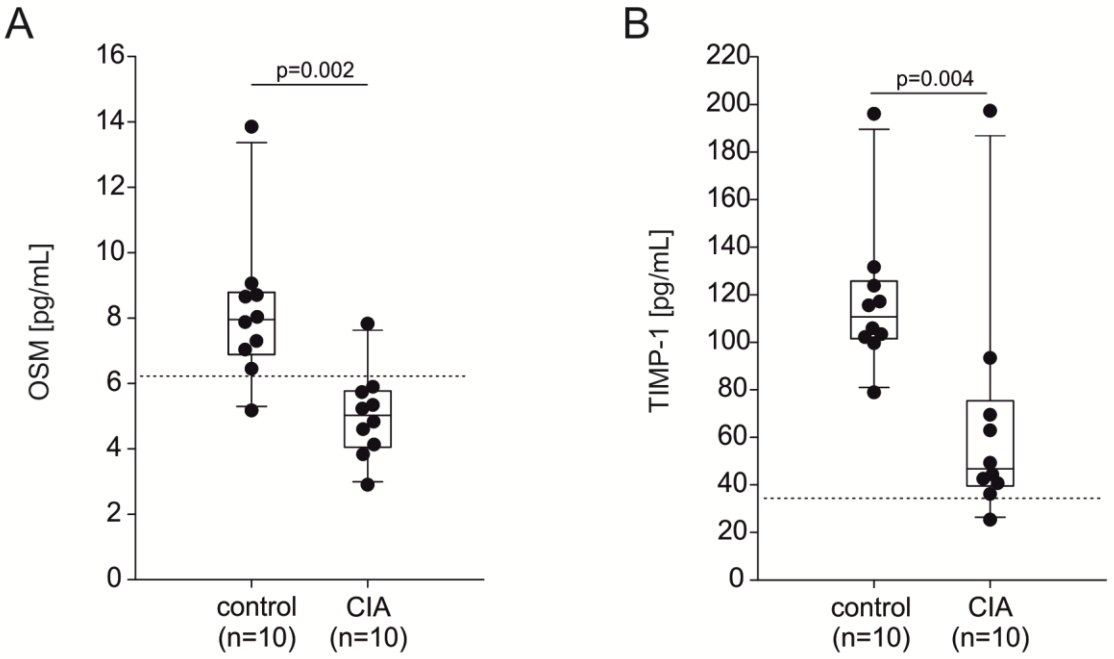

Figure 24. Levels of oncostatin M (OSM) and tissue inhibitor of metalloproteinase 1 (TIMP-1) in cell culture supernatants of osteoclast progenitor cells. One dot indicates the mean level of protein generated by cells from one animal. Numbers in parentheses indicate total number of samples analyzed. Box plots demonstrate the 10th (whisker), 25th, 50th (median), 75th, 90th (whisker) percentile. Abbreviations: OSM, oncostatin M; TIMP-1, tissue inhibitor of metalloproteinase 1; CIA, collagen type II-induced arthritis; A,B) The dotted line indicates the lowest standard used in the ELISA. (Stangl *et al.*, 2015).

3.5.2.2 LIF in cell culture supernatants of osteoclast progenitor cells

LIF was detectable in cell culture supernatants from OCP cells obtained from healthy control and arthritic mice. The amount of LIF did not significantly differ between the two groups (**Figure 25**). Due to the relevance of LIF as a potential transition factor of sympathetic nerve fibers, also cell lysates of BMM were measured. LIF was hardly detectable in these samples (**Figure 25**).

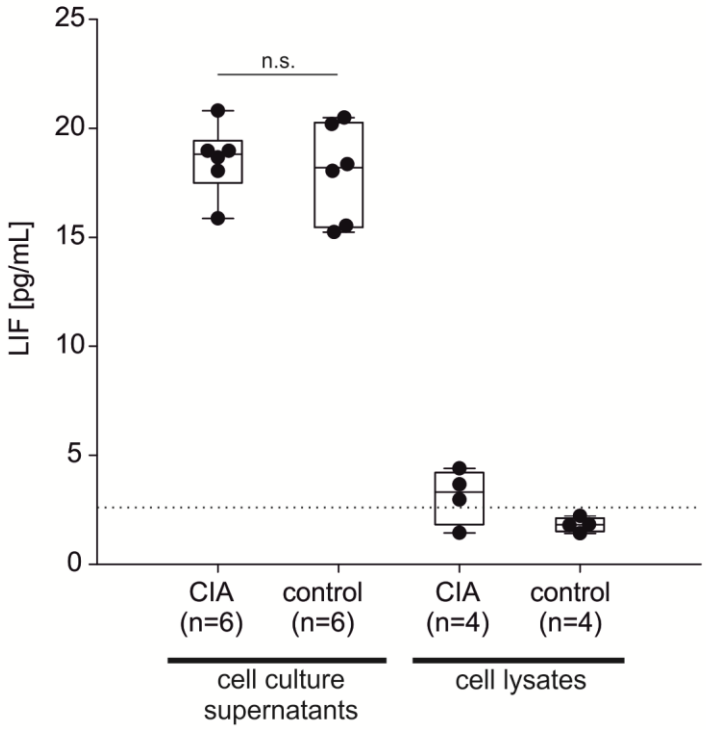

Figure 25. Levels of LIF in cell culture supernatants and cell lysates from osteoclast progenitor cells. One dot indicates the mean level per sample. Lower detection limit (~3 pg/mL) indicated by dashed line. Numbers in parentheses indicate number of samples analyzed. Box plots demonstrate the 10th (whisker), 25th, 50th (median), 75th, 90th (whisker) percentile. Abbreviations: LIF, leukemia inhibitory factor; CIA, collagen induced arthritis; n.s., not significant. (Stangl *et al.*, 2015).

3.5.2.3 Progesterone in cell culture supernatants of osteoclast progenitors and in synovial fluid of OA and RA patients

Since possible binding sites for steroids were detected within the cholinergic gene locus (see 3.6), supernatants of OCPs and synovial fluid of OA and RA patients were tested for progesterone. Progesterone was detectable in low concentrations (sensitivity 0.045ng/mL) in cell culture supernatants from OCP cells and in synovial fluid obtained from OA and RA patients. No significant difference was observed between control and arthritic samples or OA and RA samples respectively (**Figure 26A,B**).

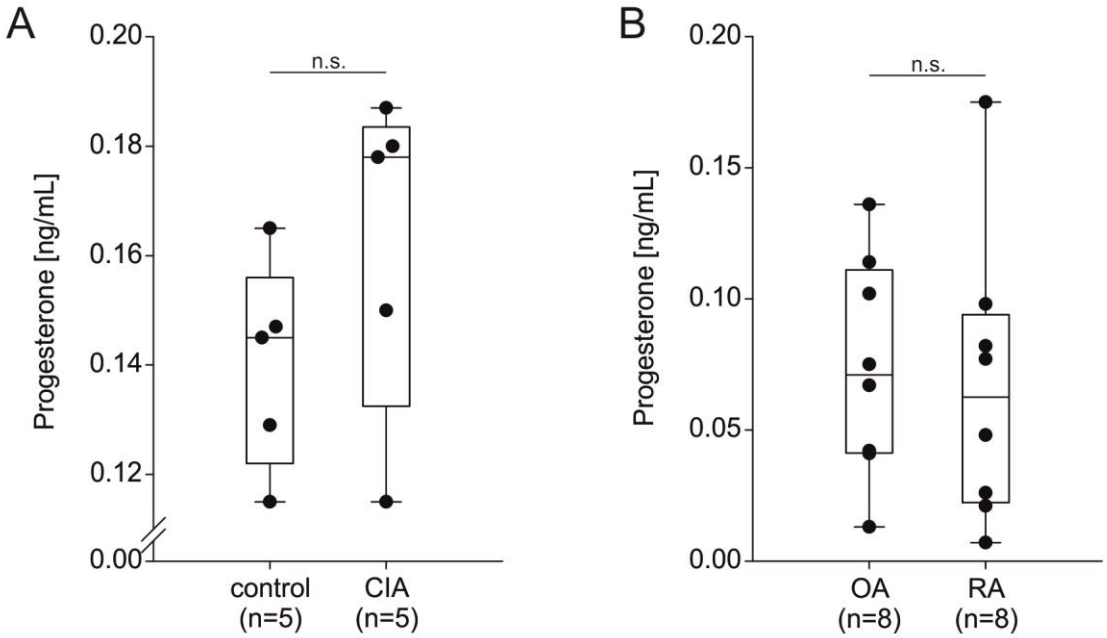

Figure 26. Levels of progesterone in cell culture supernatants of osteoclast progenitor cells (A) and synovial fluid of OA and RA patients (B). One dot indicates the mean level of protein per sample. Numbers in parentheses indicate total number of samples analyzed. Box plots demonstrate the 10th (whisker), 25th, 50th (median), 75th, 90th (whisker) percentile. Lowest standard used in the ELISA is 0.30 ng/mL and sensitivity is 0.045ng/mL according to the manufacturer‘s instructions. Abbreviations: OA, osteoarthritis; RA, rheumatoid arthritis; CIA, collagen type II-induced arthritis; n.s., not significant.

3.5.2.4 MCP-1 (CCL2) and MCP-3 (CCL7)

Since gene expression analysis showed enhanced expression of MCP-1 (CCL2) and MCP-3 (CCL7) transcripts in OCPs from arthritic mice, respective supernatants were tested for these proteins. Indeed, the two monocyte chemoattractant proteins MCP-1 (CCL2) and MCP-3 (CCL7) were detected in cell culture supernatants of both, healthy and arthritic cell cultures in high concentrations. Samples had to be diluted to reach the respective range of the ELISA. However, the measured concentrations did not significantly differ between control and CIA samples (**Figure 27A,B**).

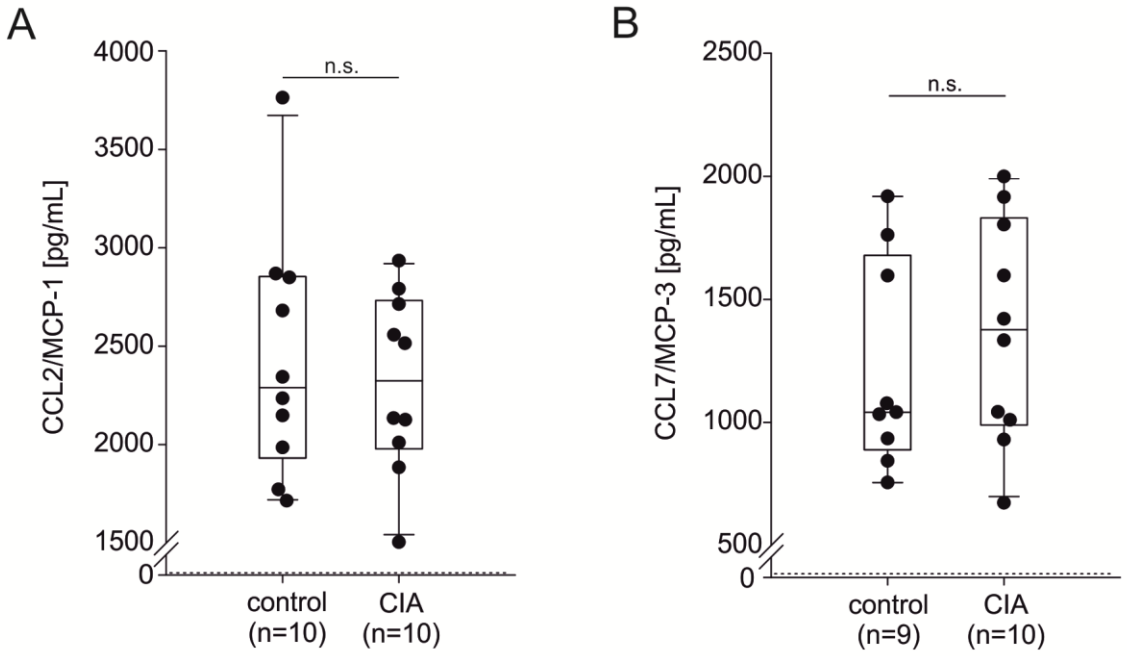

Figure 27. Levels of CCL2/MCP-1 (A) and CCL7/MCP-3 (B) in cell culture supernatants of osteoclast progenitor cells. One dot indicates the mean level of protein generated by cells from one animal. Numbers in parentheses indicate total number of samples analyzed. Box plots demonstrate the 10th (whisker), 25th, 50th (median), 75th, 90th (whisker) percentile. Abbreviations: CCL2, chemokine (C-C motif) ligand 2; MCP-1, monocyte chemoattractant protein-1; CCL7, chemokine (C-C motif) ligand 7; MCP-3, monocyte chemoattractant protein-3; CIA, collagen type II-induced arthritis; n.s., not significant. A,B) The dotted line indicates the lowest standard used in the ELISA.

3.5.2.5 CCL3/MIP-1a and CXCL2/MIP-2a

Since gene expression analysis showed enhanced expression of MIP-1a (CCL3) and MIP-2a (CXCL2) transcripts in OCPs from arthritic mice, respective supernatants were tested for these proteins. The two macrophage inflammatory proteins MIP-1a (CCL3) and MIP-2a (CXCL2) were both detected in cell culture supernatants from OCP cells. However, there was no significant difference between control and CIA samples (**Figure 28A,B**).

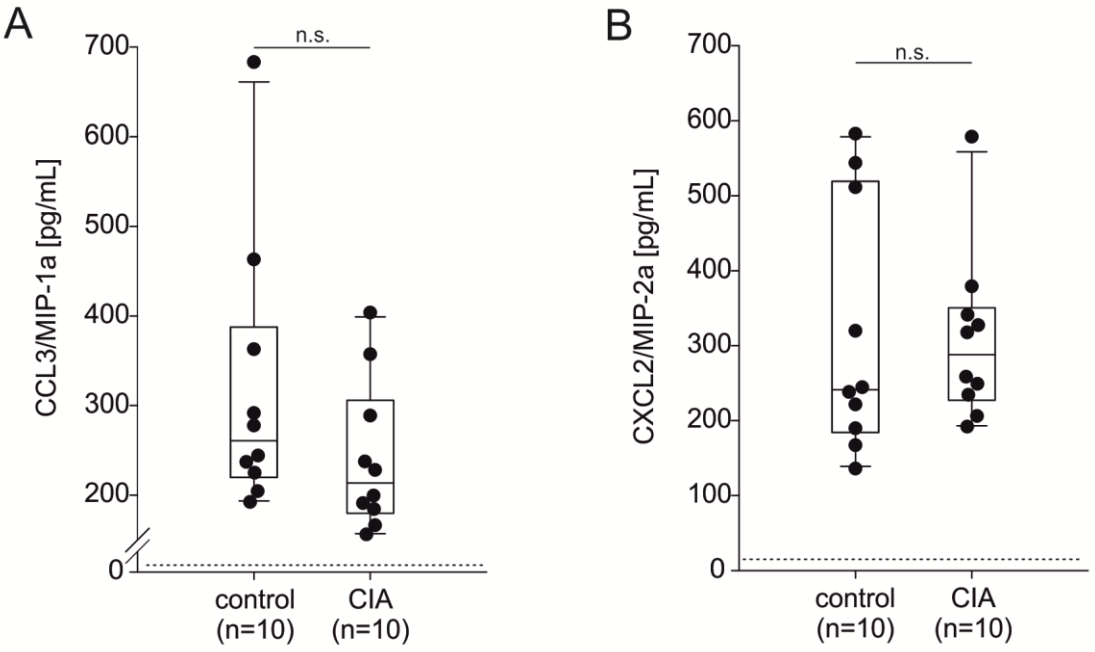

Figure 28. Levels of CCL3/MIP-1a (A) and CXCL2/MIP-2a (B) in cell culture supernatants of osteoclast progenitor cells. One dot indicates the mean level of protein generated by cells from one animal. Numbers in parentheses indicate total number of samples analyzed. Box plots demonstrate the 10th (whisker), 25th, 50th (median), 75th, 90th (whisker) percentile. Abbreviations: CCL3, chemokine (C-C motif) ligand 3; MIP-1a, macrophage inflammatory protein-1a; CXCL2, chemokine (C-X-C motif) ligand 2; MIP-2a, macrophage inflammatory protein-2a; CIA, collagen type II-induced arthritis; n.s., not significant. A,B) The dotted line indicates the lowest standard used in the ELISA.

3.5.2.6 CCL5/RANTES and CXCL10

Since gene expression and proteome analysis showed enhanced expression of RANTES (CCL5) and CXCL10 in OCPs from arthritic mice, respective supernatants were tested for these proteins with ELISA. The proteins CCL5/RANTES and CXCL10 were both detected in cell culture supernatants from OCP cells in control and CIA samples. Comparing the median values, concentrations of CCL5 in samples obtained from arthritic mice were significantly higher (p=0.002) than concentrations in control samples (**Figure 29A**). There was no significant difference in the amount of CXCL10 in control and CIA samples (**Figure 29B**).

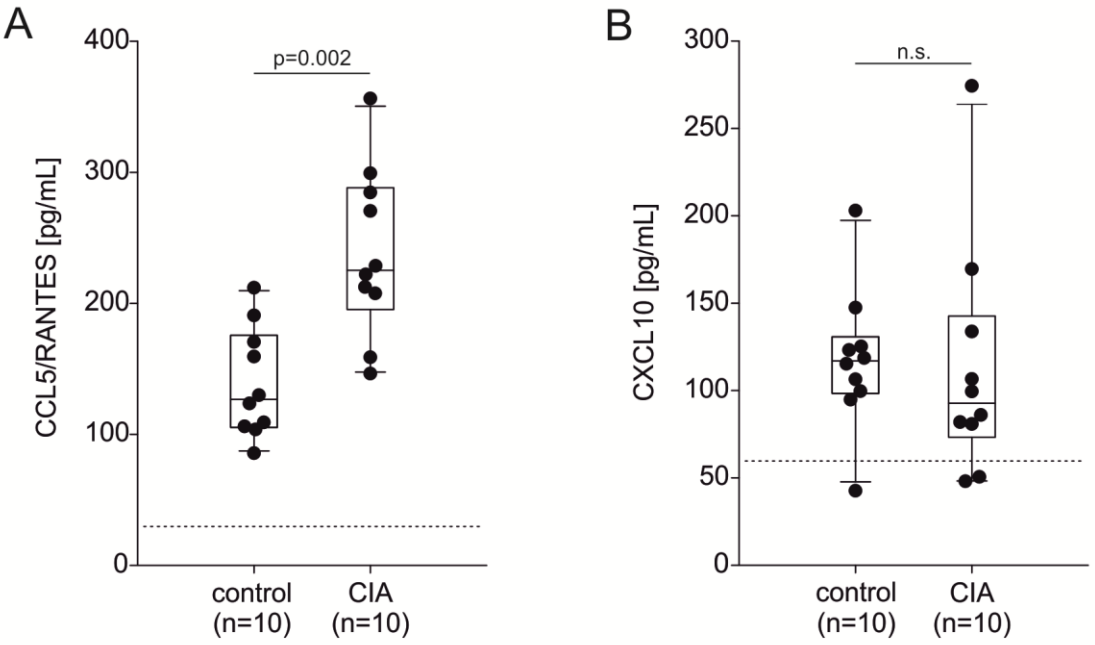

Figure 29. Levels of CCL5/RANTES (A) and CXCL10 (B) in cell culture supernatants of osteoclast progenitor cells. One dot indicates the mean level of protein generated by cells from one animal. Numbers in parentheses indicate total number of samples analyzed. Box plots demonstrate the 10th (whisker), 25th, 50th (median), 75th, 90th (whisker) percentile. Abbreviations: CCL5, chemokine (C-C motif) ligand 5; RANTES, regulated upon activation, normally T-cell expressed and presumably secreted; CXCL10, chemokine (C-X-C motif) ligand 10; CIA, collagen type II-induced arthritis; n.s., not significant. A,B) The dotted line indicates the lowest standard used in the ELISA.

3.5.2.7 Periostin/OSF2 and CXCL12/SDF-1

Since gene expression and proteome analysis suggested different expressions of Periostin/OSF2 and CXCL12/SDF-1 in OCPs obtained from arthritic and healthy control mice, supernatants of these cells were tested for these proteins with the help of specific ELISA. Although some samples produced extremely weak signals in the periostin and CXCL12 ELISA, both proteins were regarded as not detectable in cell culture supernatants from OCPs since the signals were far below the lowest standards which were used in the respective ELISA (**Figure 30**).

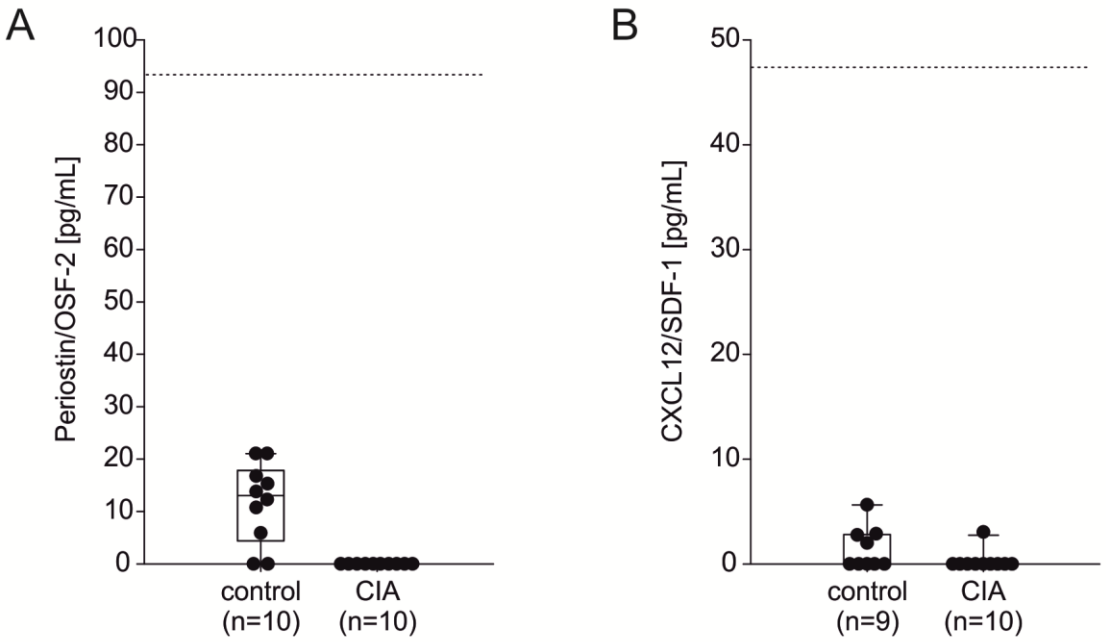

Figure 30. Levels of Periostin/OSF-2 (A) and CXCL12/SDF-1 (B) in cell culture supernatants of osteoclast progenitor cells. One dot indicates the mean level of protein generated by cells from one animal. Numbers in parentheses indicate total number of samples analyzed. Box plots demonstrate the 10th (whisker), 25th, 50th (median), 75th, 90th (whisker) percentile. Abbreviations: OSF-2, osteoblast specific factor; CXCL12, chemokine (C-X-C motif) ligand 12; SDF-1, stromal cell-derived factor 1; CIA, collagen type II-induced arthritis; A,B) The dotted line indicates the lowest standard used in the ELISA.

3.6 Analysis of promoter regions in the cholinergic gene locus in the murine and human genome

Binding elements for steroids within promoter regions of both VAChT (vesicular acetylcholine transporter) genes SLC18A3 (human) and slc18a3 (mouse), which are part of the cholinergic gene locus, were detected.

3.6.1 Detection of steroid binding sites in the promoter region of the murine vesicular acetylcholine transporter gene

In the mouse gene of VAChT (slc18a3) the base sequence *ctgcctccatcTGTTctcg* (bases in capital represent the four highest conserved bases of the respective matrix) was identified as a V$PRE.01 (progesterone receptor binding site) matrix belonging to the family of V$GREF (glucocorticoid responsive and related elements) matrices. This sequence was positioned on the minus strand at bases 39 – 57 with an anchor at base 48 out of a total of 601 bases representing the whole VAChT sequence. The matrix similarity, in which the algorithm of the software estimates matches and mismatches comparing the investigated sequence with the conserved sequence of the specific matrix, was rated with 0.888 out of a maximum of 1.0. The software algorithm sets an internal threshold for calculated results to 0.80, discarding any results below this value (Cartharius *et al.*, 2005).

3.6.2 Detection of steroid binding sites in the promoter region of the human vesicular acetylcholine transporter gene

Similar to the murine gene, in the human gene of VAChT (SLC18A3), the base sequence *ctgcgtccatcTGTTctcg* (bases in capital represent the four highest conserved bases of the respective matrix) was identified as a V$PRE.01 (progesterone receptor binding site) matrix belonging to the family of V$GREF (glucocorticoid responsive and related elements) matrices. This sequence was positioned on the minus strand at bases 28 – 46 with an anchor at base 37 out of a total of 601 bases representing the whole VAChT sequence. The matrix similarity was rated with 0.890 out of a maximum of 1.0. Additionally, the sequence *gagGGACatgctgttgccg,* positioned at bases 572 – 590 on the minus strand with an anchor at base 581, was identified as a V$GRE.02 (glucocorticoid receptor IR3 site) matrix also belonging to the family of V$GREF (glucocorticoid responsive and related elements) matrices. The matrix similarity was rated 0.879 out of a maximum of 1.0.

4 Discussion

4.1 Catecholaminergic and cholinergic nerve fibers in mouse limbs during experimental arthritis

In this chapter, the results are being discussed in respect to current literature dealing with the plasticity of sympathetic catecholaminergic and cholinergic nerve fibers in arthritis and other inflammatory conditions. Additionally, cholinergic signaling in cells and tissues relevant to arthritis is being discussed.

4.1.1 Plasticity of sympathetic nerve fibers in arthritis and other inflammatory conditions

In this study, the experiment with collagen induced arthritis in C57Bl/6 mice showed a gradually declining density of sympathetic, tyrosine hydroxylase-positive (TH+) nerve fibers with a minimum density of TH+ nerve fibers at day 35 post immunization (**Figure 8A**). This result is in concordance with earlier studies and marks a surprising turning point in the course of collagen type II induced arthritis in mice, at which the acute phase switches to a subacute transient state and an (early) chronic stage (Pongratz & Straub, 2013). These disease stages are typically characterized by relatively high clinical and histological scores, identified by strong edema, swelling of paw joints, inflamed synovial membrane, erosions of bone and infiltration of immune cells into the joint cavity and finally a subsequent destruction of the joint integrity. This loss of TH+ sympathetic catecholaminergic nerve fibers in tissues, which are characterized by high local inflammation like the synovial tissue in arthritic joints, is also a known phenomenon in RA (Miller *et al.*, 2000; Weidler *et al.*, 2005) and in animal models of arthritis, which have been thoroughly reviewed (Pongratz & Straub, 2013; Schaible & Straub, 2014; Straub, 2012; Straub *et al.*, 2013). Interestingly, the loss of sympathetic TH+ nerve fibers does not seem not to be restricted to highly inflamed joint tissues in arthritis but was also described in early inflamed pancreatic islands of BioBreeder diabetic rats (Mei *et al.*, 2002), in the spleen and in draining lymph nodes of arthritic rats and mice (Lorton *et al.*, 2005; Lorton *et al.*, 2009; Straub *et al.*, 2008b), chronic Charcot foot (Koeck *et al.*, 2009), colorectal adenomatous polyps (Graf *et al.*, 2012), in intratumoral arterioles in gastric cancer (Miyato *et al.*, 2011), in the myocardium after myocardial infarction (Parrish *et al.*, 2010), and in the colon wall of Crohn's patients (Straub *et al.*, 2008a). In chronic pruritus, prurigo nodularis and in infrapatellar fat pad from anterior knee pain patients, a relative loss of sympathetic innervation is observed because sensory innervation increases while the total amount of sympathetic nerve fibers

stays unchanged (Haas *et al.*, 2010; Lehner *et al.*, 2008). Yet, there are two studies describing an increase of sensory as well as sympathetic nerve fibers in the synovial membrane during the course of experimental arthritis in rodents (Jimenez-Andrade & Mantyh, 2012; Longo *et al.*, 2013). The authors of the first report show that the sprouting of sympathetic nerve fibers primarily takes place in joint-adjacent tissue like the skin as compared to sprouting of sensory nerves mainly in the synovial tissue (Longo *et al.*, 2013). However, an increase of sympathetic innervation in the joint might be a unique feature to the mono-arthritis model the authors used, featuring direct intra-articular injection of only CFA (complete Freund adjuvant) without a long-term antigen-driven inflammation like with type II collagen in the CIA model of arthritis or in RA in humans. Interestingly, a study in which the authors compared the synovial tissue from OA patients with control tissue from healthy animals, densities of both, sympathetic and sensory nerve fibers in OA synovium negatively correlated with the severity of inflammation, indicated by evaluating the Krenn score (Eitner *et al.*, 2013). In contrast, in fat tissue surrounding the synovial membrane of RA patients, an increased density of sympathetic nerves compared to OA has been reported (Straub *et al.*, 2011). To make things even more complex, in addition to an observed loss of TH-positive sympathetic nerve fibers, in inflamed synovial tissue from RA patients cells positive for TH appear (Capellino *et al.*, 2010; Capellino *et al.*, 2012; Miller *et al.*, 2000) seemingly to at least partially compensate for missing local supply with catecholamines (Schaible & Straub, 2014).

The reasons for the different changes of densities of sympathetic and sensory nerve fibers in inflammatory tissues are complex and seem to be driven by different mechanisms: First, nerve growth factor (NGF), a protein belonging to the neurotrophin familiy of growth factors, which is expressed by a variety of tissues and cell types, induces general sprouting and maintenance of sympathetic as well as sensory peripheral nerve fibers (Sofroniew *et al.*, 2001). NGF was found to be highly elevated in the synovial tissue of affected joints in an animal model of arthritis (Aloe *et al.*, 1993). This suggests a growth-promoting effect on both, sympathetic and sensory nerve fibers (Levi-Montalcini, 1952; Pongratz & Straub, 2013; Straub *et al.*, 2008b). The limiting of growth and the axon guidance of sympathetic nerves is tightly controlled by semaphorins, a class of proteins which, amongst various other functions, typically displays nerve fiber repellent characteristics (Pasterkamp, 2012). The semaphorin subtypes 3C and 3F were shown to be specific repellents for sympathetic but not sensory nerve fibers and they were shown to be increased in RA and Crohn's patients, which locally results in a net increase of sensory over sympathetic innervation in these diseases (Fassold *et al.*, 2009; Koeck *et al.*,

2009; Miller *et al.*, 2000; Miller *et al.*, 2004; Straub *et al.*, 2008a). In conditions in which also semaphorin 3A, a nerve fiber repellent capable of repelling also sensory nerves, is elevated, consequently also densities of both types of nerve fibers are decreased (Graf *et al.*, 2012). Recently, even other possible mechanisms for the loss of sympathetic nerve fibers have been proposed: In general, human and rat tyrosine hydroxylase, the key enzyme of catecholamine synthesis, can be degraded via phosphorylation of the residues serine 19 and 40 and subsequent proteasomal degradation by ubiquitination (Tekin *et al.*, 2014). More specifically, ubiquitination can be triggered by the gp130 class cytokines LIF and CNTF via an ERK1/2 (extracellular signal-regulated kinases-1/2) dependent pathway (Nakashima, 2012; Shi & Habecker, 2012; Tekin *et al.*, 2014). Additionally in rat neurons, CNTF also seems to inhibit Phox2a, an important transcription factor for the expression of noradrenergic markers TH and DBH (dopamine beta hydroxylase) (Dziennis & Habecker, 2004).

The observed increase of TH-positive sympathetic nerve fibers towards the end of the experiment of this study (day 55 post immunization) (**Figure 8A)** might resemble a beginning reverse or healing of inflammatory conditions in later more chronical stages of the disease. This might, due to decreasing concentrations of semaphorin subtypes 3F/C and possibly gp130 class cytokines, enable sympathetic nerve fibers to sprout back into the now less inflamed joint regions and to express TH.

Taken together, changes in the sympathetic innervation greatly depend on different aspects, like the type of disease or model of experimental arthritis, the time point of detection (acute, subacute, chronic), the inflammatory status and the exact type of the investigated tissue, density and type of vascularization (Haywood & Walsh, 2001), the target antigen (TH, DBH, VMAT [vesicular monoamine transporter, catecholaminergic marker], SP, CGRP), and presence of expression-promoting or inhibiting factors (all aspects reviewed in (Schaible & Straub, 2014)). However, this study and most of the literature back the hypothesis that during highly inflammatory episodes of arthritis, sympathetic nerve fibers positive for TH are being lost in the highly inflamed joint regions like the synovial tissue (Schaible & Straub, 2014).

4.1.2 Cholinergic nerve fibers in mouse limbs during arthritis

The aim of this study was to investigate a possible transition of sympathetic catecholaminergic TH-positive nerve fibers to a cholinergic phenotype of sympathetic nerve fibers, similar to the phenomena observed during the innervation of sweat glands and the periosteum (Asmus *et al.*, 2000; Asmus *et al.*, 2001; Landis *et al.*, 1988; Landis, 1996), which impressively demonstrate plasticity of sympathetic nerve fibers. Hence, it might well be that the observed loss of sympathetic nerve fibers is due to the

focus of sympathetic nerve fibers via detection of TH and that sympathetic nerve fibers as such remain and just loose TH but show cholinergic features.

So far, cholinergic nerve fibers in limbs have never been investigated in the aspect of experimental arthritis. The experiment in this study shows an increase of cholinergic VAChT-positive nerve fibers during the course of arthritis. Strikingly, this observation is most prominent on day 35 post immunization (**Figure 8B**), marking the same time point at which the limbs display a minimum of sympathetic innervation (**Figure 8A**). On day 35 post immunization, this shifted the ratio of innervation from a predominantly sympathetic to a predominantly cholinergic innervation of the investigated limbs (**Figure 8C**). Intriguingly, the density of VAChT-positive cholinergic nerve fibers in these limbs decreases towards the end of the observed time period (day 55 post immunization), at which the density of sympathetic nerve fibers increases (**Figure 8A,B**). This might, similar to the increasing amount of sympathetic nerves, be due to a declining severity of inflammation towards a late state of experimental arthritis, which could reverse the observed changes of innervation.

However, while sympathetic nerve fibers were found throughout the investigated limb in different kinds of tissues (skin, bone, synovial membrane and other connective tissues in the joint), most of all of the VAChT-positive, cholinergic nerve fibers occurred in joint-adjacent tissue like muscle or skin (**Figure 9**), which are minimally inflamed regions of the arthritic limbs. Apart from the well documented cholinergic innervation of sweat glands in rodent paws (Landis *et al.*, 1988; Landis, 1996), VAChT-positive, cholinergic nerve fibers in rodent limbs were also shown in other studies: VAChT immunoreactive nerve fibers were detected at the motor endplate of skeletal muscles in limbs (Guidry & Landis, 2000; Guidry *et al.*, 2005). Regarding VAChT-positive nerve fibers adjacent to vasculature in rodent muscles, which were not found in mouse experiments of this present study, there are contradictory reports (Guidry & Landis, 2000; Schafer *et al.*, 1998). The few VAChT-positive cholinergic nerve fibers which were directly located in highly inflamed regions in the synovial tissue or near bony erosions (**Figure 9**) can be explained by the cholinergic innervation of the periosteum (Asmus *et al.*, 2000; Asmus *et al.*, 2001; Bjurholm *et al.*, 1988; Hill & Elde, 1991; Hohmann *et al.*, 1986), the recently described VAChT-positive cholinergic nerve fibers in trabecular bone of the femoral metaphysis from mice (Bajayo *et al.*, 2012), and studies reporting cholinergic VIP immunoreactivity alongside catecholaminergic sympathetic markers (NPY, DBH) in the synovial tissue and bone of rats (Bjurholm *et al.*, 1988; Bjurholm *et al.*, 1990; Sisask *et al.*, 1996) (reviewed in (Eimar *et al.*, 2013)). In addition, in a very recent study, VAChT-positive cholinergic nerve fibers have also been found in bone defects in an osteoporosis model of the

rat (Lips *et al.*, 2014). Interestingly, the sympathetic nature of cholinergic (VIP-positive) nerve fibers in the periosteum was proven by treatment of animals with guanethidine, a substance which is specifically toxic for sympathetic nerves (Cherruau *et al.*, 2003; Hill & Elde, 1991). This was confirmed by others, who demonstrated the sympathetic origin of cholinergic innervation of the periosteum by ganglionectomy of sympathetic ganglia (Hohmann *et al.*, 1986).

These studies clearly demonstrate that along sympathetic catecholaminergic innervation there also exists a cholinergic innervation of the bone. Yet it remains unclear why VAChT-positive nerve fibers seem to increase during the course of experimental arthritis in rather healthy (skin and muscle) but not in highly inflamed tissue such as the inflamed synovial membrane, since in synovial fluid of OA and RA patients the presence of gp130 class cytokines like LIF or OSM, which are capable of inducing sympathetic transition, has been shown (Lotz *et al.*, 1992; Tsuchida *et al.*, 2014) (reviewed in (Kapoor *et al.*, 2011; Westacott & Sharif, 1996)). One might also argue that, even if sympathetic catecholaminergic nerve fibers in highly inflamed regions like the synovial tissue displayed the phenomenon of a transition to a cholinergic type of sympathetic nerves, they might still be repelled by semaphorins 3F and 3C, which are present in inflamed synovial tissue and are specific for sympathetic nerve fibers (Fassold *et al.*, 2009; Miller *et al.*, 2004). Another possible reason could be that sympathetic nerves might be in fact as such entirely lost in highly inflamed tissues during arthritis and, hence, can not switch their phenotype: Two earlier studies that investigated sensory nerve fibers and nerves positive for PGP (protein gene product) 9.5, a cytoskeletal and hence general marker of nerve fibers, in the synovium of arthritic rats suggested a general loss of all these nerve fibers in inflamed synovial tissue (Hukkanen *et al.*, 1991; Konttinen *et al.*, 1990).

Yet, there is a technical issue with elucidating sympathetic transition with this type of investigation which remains problematic: With the means of immunostaining of ex vivo tissue samples one can not precisely detect sympathetic transition in the exact same nerve fiber which in theory should display a decrease of adrenergic properties and at the same time gather cholinergic properties, similar to the phenomenon in developing sweat glands (Landis *et al.*, 1988; Landis, 1996). This is still a challenge, at least by the use of tissue fixation and subsequent immunofluorescent staining of two marker proteins. Even with the means of double immunofluorescence techniques it remains uncertain whether a single nerve fiber changed its whole phenotype including functional properties over a given time. For example, in certain cardiac sympathetic nerves both phenotypes (adrenergic and cholinergic) seem to exist at the same time (Felder & Dechant, 2007). This indicates a co-expression or a transition rather

than a switch. A possible solution for overcoming this obstacle might be a mouse strain which expresses two different fluorescent proteins, one under the control of a promoter for TH and the other under control of a promoter for ChAT or VAChT, similar to the principle of Felder and Dechant (Felder & Dechant, 2007). This might allow detection of both markers in one and the same nerve fiber over a certain period of time *in vivo*.

4.2 Cholinergic and sympathetic articular innervation in patients with OA and RA

In joint-related tissues obtained from patients with OA and RA, so far sensory and sympathetic nerve fibers have been investigated (reviewed in (Pongratz & Straub, 2013; Schaible & Straub, 2014)). It was demonstrated that in highly inflamed tissues like the synovial tissue a preponderance of sensory over sympathetic innervation exists due to suggested reasons discussed in the previous chapter (4.1). To check a potential transition of sympathetic nerve fibers in OA and RA, this study focused particularly on a possible cholinergic innervation of tissues relevant to arthritis in the knee and in finger joints of OA and RA patients, especially the synovial membrane of finger joints and the knee joint. Due to the different surgical needs and procedures in this study, the innervation of the knee could only be tested in the synovial tissue while in samples from finger joints, an analysis was possible that differentiates between connective (synovial) tissue and bone tissue.

To date, cholinergic nerve fibers in the human synovial tissue have not been found. In this study, for the first time existence of VAChT-positive cholinergic nerve fibers was demonstrated in synovial tissue of finger joints (**Figure 10A, B**) and of the knee (**Figure 13A, B**) from OA and RA patients.

In finger joint synovial tissue, density of VAChT-positive cholinergic nerve fibers was significantly higher in OA than in RA (**Figure 10B**), while in knee synovial tissue only a trend was observed (**Figure 13B**). Additionally, presence of nerve fibers positive for VIP, an important co-transmitter and marker of cholinergic nerve fibers was demonstrated in synovial tissue from finger joints (**Figure 10C, D**) as well as from knee joints (**Figure 13C, D**). This finding correlates to a study in which VIP+ nerve fibers were also demonstrated in the synovial membrane in Sprague Dawley rats (Bjurholm *et al.*, 1990). Sympathetic TH-positive nerve fibers in the synovial membrane of finger joints were also detected (**Figure 12A, B, D**). The densities however did not differ between OA and RA (**Figure 12E**) although a trend towards higher densities in OA patients was visible, and a statistical power problem can not be excluded.

Further, in bone tissue of finger joints from OA and RA patients, cholinergic VAChT-positive (**Figure 11E**) and VIP-positive (**Figure 11G**) nerve fibers were detected. However, both VAChT, and VIP densities did not statistically differ between OA and RA (**Figure 11F, H**). VIP containing nerve fibers in the bone were also found by others who demonstrated the existence of these fibers in the epiphysis and in the periosteum of rat bone (Bjurholm *et al.*, 1988; Hill & Elde, 1991; Hohmann *et al.*, 1986) alongside with sympathetic NPY-positive nerve fibers. Nerve fibers positive for TH and NPY, a known co-transmitter of sympathetic nerves, are distributed throughout the bone and influence bone turnover (Bjurholm *et al.*, 1988; Elefteriou, 2005; Imai & Matsusue, 2002). This is consistent with the sympathetic TH-positive nerve fibers which were also detected in bone tissue of OA and RA patients in this study (**Figure 12F**).The presence of cholinergic VAChT-positive nerve fibers in bone tissue presented in this study confirms results from others who just very recently have shown existence of nerve fibers positive for VAChT in trabecular bone of the murine femur and in bone defects in an osteoporosis model of the rat (Bajayo *et al.*, 2012; Lips *et al.*, 2014).

The results of this study and the current literature clearly indicate cholinergic innervation of the bone and joint in both rodents and humans. In the periosteum, the sympathetic nature of cholinergic innervation has been demonstrated by means of chemical sympathectomy, selective sympathetic ganglioectomy, and retrograde staining (Hill & Elde, 1991; Hohmann *et al.*, 1986). However, cholinergic innervation of the femur seems to be controlled by the parasympathetic nervous system indicated by retrograde labeling with pseudorabies virus (Bajayo *et al.*, 2012). In other studies, it remains to be elucidated whether cholinergic signaling is controlled via the SNS or the parasympathetic nervous system. This would be of great value because a cholinergic innervation controlled by the SNS provides further evidence of a catecholaminergic-to-cholinergic transition of sympathetic nerve fibers, like in the periosteum or in sweat glands. Additionally, activation of a sympathetic cholinergic part of the peripheral nervous systems in the bone would require different mechanisms than a parasympathetic cholinergic innervation of bone. However, in respect to current literature, one has to assume that in bone cholinergic innervation is used by both, the sympathetic and the parasympathetic nervous system but future studies are needed to further elucidate both systems of cholinergic innervation of bone.

The homeostasis of bone formation and resorption, also termed bone turnover, is tightly balanced by the hormone system and the peripheral nervous system. The balance of bone formation, mainly mediated by osteoblasts, and bone resorption achieved by osteoclasts, plays a key role in these processes and is relevant to arthritis due to activated osteoclasts in focal bony erosions of affected joints. The

two main neurotransmitters released by cholinergic nerve fibers in bone are acetylcholine (ACh) and vasoactive intestinal peptide (VIP) (Eimar *et al.*, 2013; Persson & Lerner, 2011). While activation of the peripheral sympathetic catecholaminergic nervous system seems to mainly inhibit bone formation and to favor bone loss by increased osteoclast formation and differentiation via β2-adrenoceptor signaling (Aitken *et al.*, 2009; Cherruau *et al.*, 2003) (reviewed in (Elefteriou, 2005; Straub, 2012; Togari & Arai, 2008)), an activation of VIP signaling in bone seems to mainly favor bone accrual by directly inhibiting osteoclasts through activation of VPAC1 receptors on these cells (Lerner & Persson, 2008). Additionally, VIP counteracts an up-regulation of RANKL by vitamin-D3 and PTH (parathyroid hormone) and a decrease of OPG (osteoprotegerin) caused by VitD3 (Lerner & Persson, 2008). Actions of VIP on osteoblasts are bimodal because VIP is also able to enhance RANKL production in osteoblasts via mainly VPAC2 receptor activation, which in turn leads to up-regulated differentiation and activity of osteoclasts (Lerner & Persson, 2008). On the other hand, activation of VPAC2 receptors by VIP on osteoblasts leads to increased differentiation of osteoblasts and direct activation of ALP (alkaline phosphatase), an important enzyme for bone mineralization and therefore bone formation (Lerner & Persson, 2008; Lundberg *et al.*, 1999).

In addition to the overall promotion of bone formation by VIP signaling in osteoblasts and osteoclasts, also direct anti-inflammatory effects of VIP have been reported as reviewed in (Chandrasekharan *et al.*, 2013; Delgado & Ganea, 2008; Lerner & Persson, 2008): In microglia, VIP was shown to directly influence inflammation by inhibiting the pro-inflammatory cytokines IL-1β, IL-6, IL-12 and TNF, and nitric oxides, as well as inhibiting the pro-inflammatory prostaglandine E2 (PGE2) produced by cyclooxygenase type 2 (COX-2) in macrophages and dentritic cells (Delgado *et al.*, 2003; Gonzalez-Rey & Delgado, 2008). VIP is also locally synthesized by immune cells and in a paracrine/autocrine way of signaling seems to direct the immune response towards a rather T helper cell type 2 (Th-2) response and to up-regulate T regulatory (Treg) cells (Gonzalez-Rey *et al.*, 2006; Pozo & Delgado, 2004). The anti-inflammatory potential of VIP has also been shown in experimental arthritis (Delgado *et al.*, 2001; Delgado *et al.*, 2008b) and the use of VIP is proposed as a possible agent for the treatment of RA (Chandrasekharan *et al.*, 2013; Delgado *et al.*, 2001; Delgado *et al.*, 2008b; Delgado & Ganea, 2008; Gonzalez-Rey *et al.*, 2007). The important role of the VIP receptor VPAC1 has been demonstrated in experimental arthritis and in immune cells from RA patients (Delgado *et al.*, 2008a).

Acetylcholine, the main neurotransmitter of the cholinergic nervous system conveys its signals via a variety of receptors, which can be divided into two main groups: Muscarinic, G-protein-coupled seven

transmembrane domain receptors (type M1 through M5) (Eglen, 2006), and nicotinic ligand gated ion channels consisting of a pentamer of different subunits (Lukas *et al.*, 1999). In the context of arthritis, especially the homo-pentamer α7-subunit containing nicotinic acetylcholine receptor (α7nAChR) has gained attention since its anti-inflammatory potential in inhibiting TNF release from macrophages was described (Wang *et al.*, 2003). The anti-inflammatory potential of stimulating the α7nAChR in experimental arthritis (van Maanen *et al.*, 2009a) and in fibroblast like synoviocytes (FLS) from RA patients has been shown (van Maanen *et al.*, 2009b). Yet, there is conflicting data regarding these effects in an α7nAChR knock-out mouse model (van Maanen *et al.*, 2009b; Westman *et al.*, 2010). Here, the presence of the α7nAChR in fibroblast like synoviocytes (FLS) is demonstrated (**Figure 14**), which is in line with the results of others who have shown the expression of this receptor in FLS as well as in synovial tissue from OA and RA patients (Forsgren, 2012; van Maanen *et al.*, 2009b; Waldburger *et al.*, 2008; Westman *et al.*, 2009). Moreover, further parts of the cholinergic machinery, like mRNA for and protein of high affinity choline transporter (ChT) and choline transporter like protein (CTL1&2), but absence of VAChT mRNA (Beckmann *et al.*, 2015), and presence of ChAT mRNA (Forsgren, 2012; Schubert *et al.*, 2012) have been found in the synovial tissue of arthritis patients. Beckman and Lips suggest a local non-neuronal cholinergic system (Beckmann & Lips, 2013) similar to the non-neuronal system, which has been demonstrated to play a key role in the communication of lymphocytes reviewed by Kawashima and coworkers (Fujii *et al.*, 2008; Kawashima & Fujii, 2000; Kawashima & Fujii, 2003; Kawashima & Fujii, 2004; Kawashima *et al.*, 2012).

However, the results of this very study suggest that due to the expression of VAChT, a typical axonal marker of cholinergic nerve fibers, and the typical bead like structure of the detected VIP- and VAChT-positive nerve fibers, also a direct neuronal innervation of the synovial tissue in humans and mice is as well possible.

4.3 Transition of nerve fibers from a catecholaminergic to a cholinergic phenotype in vitro

After the identification of previously unknown cholinergic nerve fibers in joint tissue obtained from arthritic mice and humans, the study aimed to investigate on possible cell types and molecules being responsible for the putative transition of the well documented catecholaminergic type of sympathetic nerve fibers to a cholinergic type.

4.3.1 Transition in the co-culture system of sympathetic ganglia

For this purpose, the assay of sympathetic ganglia as a model for catecholaminergic sympathetic nerve fibers was redesigned as a co-culture system of sympathetic ganglia and cells relevant to arthritis, like OCP cells obtained from BMM, and lymphocytes from inguinal draining lymph nodes. It was also intended that fibroblasts obtained from subcutaneous connective tissue in the paw and from the periosteum, according to protocols for the isolation of periostal cells and synovial fibroblasts of mice (Gao *et al.*, 2006; Kawanami *et al.*, 2009; Korb-Pap *et al.*, 2012; van *et al.*, 2012) were tested, but respective cells failed to display the ability of being passaged and transferred to the co-culture chamber slides in a sufficient amount.

First, sympathetic ganglia without any stimulation or contact to other cells, which reflects the control situation, always show a little amount of cholinergic marker expression (reviewed in (Francis & Landis, 1999)) which was also found in this present study (**Figure 16A,B,** control).

The co-culture experiments were divided into two subsets: The first set comprised sympathetic ganglia, OCPs and lymphocytes obtained entirely from C57Bl/6 mice (**Figure 16A)**. In the second set, OCP cells and lymphocytes were obtained from DBA1/J mice (**Figure 16B**) in order to test a possible mouse-strain specificity. In both subsets of experiments, co-cultures of sympathetic ganglia and osteoclast progenitors obtained from healthy control animals displayed a higher frequency of VAChT-positive cholinergic nerve fibers in the ganglia (**Figure 16A,B**), while only in the subset with lymphocytes obtained from healthy DBA1/J mice, respective experiments displayed this phenomenon (**Figure 16B**). This might be due to the presence of immunocompetent cells like resident macrophages or microglia capable of expressing major histocompatibility complex (MHC) class II molecules (Kiefer *et al.*, 2001). These might interact with lymphocytes obtained from a different mouse strain and in turn, after activation by these lymphocytes, alter expression of cholinergic markers in the neurons of the ganglia since glial cells are able to release trophic factors (reviewed in (Hanani, 2010; Jessen, 2004). Interestingly, in co-culture experiments with OCP cells, these cells migrated in a chemotactic fashion towards the sympathetic ganglion located in the other half of the well (**Figure 15A,B**). This confirms results from an earlier study showing chemotactic potential of neurotransmitters released by sympathetic nerve endings on monocytes (Straub *et al.*, 2000). A direct communication between osteoblasts and osteoclasts in co-culture with neurons obtained from the superior cervical ganglion (a sympathetic ganglion) has demonstrated α_1-adrenoceptor signaling between these two cell types (Obata *et al.*, 2007; Suga *et al.*, 2010). These findings support the principle concept of this co-culture system using

OCP cells together with sympathetic ganglia. A direct effect of bone marrow derived cells has so far mostly been described for bone marrow derived stromal cells, which are isolated in a similar way compared to the bone marrow macrophage isolation (Takeshita *et al.*, 2000). For example, stromal cells were shown to release chemokines like SDF-1 (stromal derived factor), which are capable of inducing dopaminergic neuronal differentiation (Schwartz *et al.*, 2012). Co-culture experiments demonstrated an up-regulation of cholinergic properties in neuronal cells when cultured together with heart cells (Yamamori *et al.*, 1989), periostal cells (Asmus *et al.*, 2001), and cells obtained from eccrine sweat glands (Habecker *et al.*, 1997), which all suggest gp130 class cytokines as being the responsible factors for cholinergic differentiation. In this study, sympathetic ganglia in co-cultures with OCPs from healthy mice displayed an overall higher ratio of VAChT-positive to TH-positive nerve fibers, as well as locally enhanced VAChT expression where nerve fibers were in direct contact with OCP cells (**Figure 15**, **Figure 16**). These observations can be interpreted as an effect dependent on a soluble factor released by OCP cells or a direct contact of sympathetic nerve fibers with extracellular matrix (ECM) components produced by OCPs.

In order to elucidate the differences between OCP cells obtained from healthy control mice and OCPs from mice with CIA, cells were subjected to gene expression analysis and proteome profiling.

4.3.2 Identification of possible transition factors of osteoclast progenitor cells via gene expression analysis

Gene expression analysis of OCP cells revealed differences in genes that can be generally attributed to extracellular matrix related genes, genes related to inflammation like chemokines and cytokines but also genes coding for proteins known for transition of sympathetic nerves to a cholinergic phenotype. Respective genes are discussed in context of the expression in macrophage/osteoclast lineage of cells and their possible influence on the nervous system.

4.3.2.1 Up-regulated gene transcripts in osteoclast progenitors from healthy mice

4.3.2.1.1 Biglycan (Bgn)

The most prominent up-regulation in cells from healthy control mice was found for biglycan *(BGN)* (**Figure 20**). The multiple functions of biglycan, which is regarded as a small leucine rich proteoglycan (SLRP) or chondroitin sulfate proteoglycan (CSPG) and is part of the extra cellular matrix (ECM) have

recently been reviewed (Nastase *et al.*, 2012): Generally being seen as a rather pro-inflammatory signaling molecule, triggering production of interleukin 1beta (IL1b), tumor necrosis factor (TNF) and other pro-inflammatory cytokines (via activation of toll like receptors TLR2/4 and purinergic receptor P2X7 on macrophages), it also plays an important role in bone homeostasis as it promotes osteoblast differentiation by activating receptors of bone morphogenetic proteins and transforming growth factor beta. This is supported by the fact that biglycan-deficient mice show an osteoporosis like phenotype (reviewed in (Nastase *et al.*, 2012)). Hence, an elevated expression of biglycan by OCP cells in healthy mice (as suggested by the gene expression results of this study) would favor bone formation in a crosstalk between osteoclasts and osteoblasts, while a lack of biglycan in arthritic animals would promote bone loss. It has been shown that activated macrophages are able to express and release biglycan (reviewed in (Nastase *et al.*, 2012)). Another report proposes also an anti-inflammatory role of biglycan by inhibiting pro-inflammatory effects of the activated complement protein C1q (Groeneveld *et al.*, 2005). Further functions of biglycan include its induction of collagen matrix formation in adaptive remodeling processes after myocardial infarction (Ahmed *et al.*, 2003; Westermann *et al.*, 2008), maintenance of stability of cholinergic synapses at the neuromuscular junction (Amenta *et al.*, 2012), transient inhibition of outgrowth of sensory neurons (Lemons *et al.*, 2005), and acting as a neurotrophic factor in neocortical rat neurons as well as activating ventral pallidal-neocortical cholinergic neurons in the rat brain (Huston *et al.*, 2000). Thus, it might be a good candidate to induce catecholaminergic-to-cholinergic transition demonstrated in this study.

4.3.2.1.2 Tenascin C (Tnc)

Another up-regulated gene transcript was *Tnc* (**Figure 20**), coding for Tenascin C, which belongs to the family of ECM glycoproteins and is expressed in bone, cartilage, tendon and nervous system amongst other tissues. It has been assigned a variety of functions like modulation of cell adhesion, migration and guidance of axonal growth depending on expression of different functional subdomains due to alternative splicing (reviewed in (Chiquet-Ehrismann, 2004; Chiquet-Ehrismann & Tucker, 2004; Joester & Faissner, 2001)). Expression of tenascin C in the ECM is thought to be up-regulated after injuries, during inflammatory and remodeling processes like after myocardial infarction (Milting *et al.*, 2008). Interestingly, the inflammatory property of tenascin C has been demonstrated in a study in which RA patients displayed significantly higher serum concentrations of tenascin C compared to healthy controls: The amount of tenascin C positively correlated with the severity of bone erosions in affected joints in these patients and therefore was suggested as a possible marker for disease activity

in RA (Page *et al.*, 2012). These observations are supported by the fact that tenascin C-deficient mice develop a less severe experimental arthritis (reviewed in (Chiquet-Ehrismann *et al.*, 2014)) and disturbed motor coordination properties (Joester & Faissner, 2001). This indicates an important role of tenascin C in organizing the ECM during arthritis and different functions in the nervous system.

4.3.2.1.3 Fibronectin 1 (Fn1)

Similar to tenascin C, also the gene coding for fibronectin *(Fn1)* was elevated in OCPs from healthy mice (**Figure 20**). Fibronectin and tenascin C are evolutionarily closely related since they are only found in chordates, tenascin C features similar type III functional subdomains like fibronectin, and tenascin C is able to modulate fibronectin function (Chiquet-Ehrismann & Tucker, 2011). Yet in contrast to tenascin C, which rather inhibits cell adhesion by inhibiting cells to bind to fibronectin and rather fosters cell motility (Chiquet-Ehrismann, 2004), fibronectin itself promotes cell adhesion due to the high affinity of its RGD motif containing type III domains, which bind to different heterodimers of integrins expressed on cells (Lowin & Straub, 2011). A further important function of fibronectin is the formation of insoluble fibrils, which are a major component of a scaffold for the ECM (Lowin & Straub, 2011). Importantly, since fibronectin conveys cell adhesion via integrin binding, it plays also a significant role for the invasive potential of fibroblasts, because its expression is enhanced in the synovial fluid of OA patients and in the synovial lining layer in RA patients (Lowin & Straub, 2011). Thought to be produced mainly by non-neuronal cells like Schwann cells, fibronectin is also described as an important factor for adhesion and guidance of growing or regenerating peripheral nerve fibers (reviewed in (Gardiner, 2011; Webber & Zochodne, 2010). In a report investigating the conditioned medium of astrocytes stimulated by a cholinergic agonist, fibronectin was shown to be up-regulated, suggesting that it plays a role in modeling the ECM of cholinergic neurons (Moore *et al.*, 2009). Since it is a factor of ECM in bone, fibronectin also seems to be capable of influencing size and shape of osteoclasts (Gramoun *et al.*, 2010).

4.3.2.1.4 Connective tissue growth factor (Ctgf)

Another gene related to the ECM and up-regulated in osteoclasts from healthy control mice was *Ctgf*, coding for connective tissue growth factor (**Figure 20**). It was demonstrated that gene expression of Ctgf is involved in the development of the cardiovascular system, of tissue adjacent to bone and cartilage, and of certain neurons in the brain (Friedrichsen *et al.*, 2003). Furthermore serum Ctgf was shown to be elevated in RA compared to healthy controls as well as in activated RA compared to inac-

tive RA, and to promote osteoclastogenesis *in vitro*, suggesting a pro-inflammatory role in RA (Nozawa *et al.*, 2009). In a mouse model for hypertrophic cardiomyopathy and heart failure, increased gene expression for Ctgf was observed together with tissue inhibitor of metalloproteinase 1 (TIMP-1), fibronectin, tenascin C, and periostin (Tsoutsman *et al.*, 2013), which are also up-regulated in OCPs from healthy mice in this study (**Figure 20**), underlining their importance in ECM remodeling. This finding is also supported by the fact that in this study these genes were up-regulated in a similar way since they were grouped together by gene clustering in analyzing the microarray results (**Figure 21**).

4.3.2.1.5 Tissue inhibitor of metalloproteinase 1 (TIMP-1)

TIMP-1, a pleiotropic molecule and first member of a family comprising a total of four different TIMPs was characterized by its function of inhibiting matrix metalloproteinases (MMPs), which are responsible for the breakdown of protein based ECM components but also cleavage and, hence, activation or deactivation of endogenous signaling peptides (Moore & Crocker, 2012; Ries, 2014). Apart from this classical inhibition of MMPs, quite recently additional and alternative functions for TIMP-1 have been suggested since not all observed effects by TIMP-1 could be assigned to the well characterized inhibition of MMPs: In human mesenchymal stem cells (hMSCs) an inhibition of β-catenin signaling in these cells was shown to be mediated by a newly discovered receptor for TIMP-1, CD63 (Moore & Crocker, 2012; Ries, 2014). In addition to this cytokine-like direct signaling pathway, TIMP-1 can also elicit signaling by binding to proMMP-9, one of the main targets of TIMP-1, and subsequent binding of this complex to a cell surface-bound receptor, CD44 (Moore & Crocker, 2012; Ries, 2014). Further still unknown cell surface receptors for TIMP-1 are being proposed.

The here described effect of TIMP-1 on sympathetic ganglia in vitro (**Figure 18**) might be assigned to a yet unknown, but direct signaling of TIMP-1 on neuronal or non-neuronal cells present in the ganglia. In relation to bone and nervous system, TIMP-1 was shown to be expressed by osteoblasts and osteoclasts (Bord *et al.*, 1999; Grassi *et al.*, 2004; Hill *et al.*, 1994), and it has a protective influence on the nervous system by ensuring effective myelination (Moore *et al.*, 2011). In RA, it is suggested that in synovial fluid the balance between MMP9 and its specific counterpart TIMP-1 is shifted towards MMP9, which results in increased breakdown of collagen in the joints (Tchetverikov *et al.*, 2004). Similar to biglycan, Ctgf, tenascin C and fibronectin, TIMP-1 seems to be involved in the cardiac remodeling of the ECM after heart failure (Vanhoutte & Heymans, 2010). Thus there can be a common reason why it was up-regulated together with these genes in OCPs from healthy mice (**Figure 20**).

4.3.2.1.6 Tensin 1 (Tns1)

Less is known about tensin 1 in respect to an involvement in arthritis and the peripheral nervous system, but it is generally regarded as an integrin adaptor protein and, hence, it is involved in cellular adhesion processes and seems to be important for invasiveness of tumor cells (reviewed in (Haynie, 2014)). This again makes sense since tensin was also up-regulated together with other ECM related gene transcripts (**Figure 20**) in OCPs from healthy animals. Expression of tensin has also been shown in the podosome-like extensions of osteoclasts, confirming its relevance to cell adhesion processes and it was further suggested as a differentiation marker of osteoclasts because of its proposed role in fusion processes of osteoclast progenitors (Hiura *et al.*, 1995).

4.3.2.1.7 Tetraspanin 7 (Tspan7)

Similar to tensin 1, relatively little is known about tetraspanin 7, especially in regards to arthritis and nervous system. Generally, tetraspanins are proteins consisting of four transmembrane domains and intracellular and extracellular loops, the latter carrying typical highly conserved motifs which are important for characteristic dynamic interaction of several tetraspanin molecules and further transmembrane proteins, referred to as the 'tetraspanin-web' (reviewed in (Levy & Shoham, 2005b; Levy & Shoham, 2005a). These processes are important during cell-cell interactions like during communication of immune cells or in fusion of cells (Levy & Shoham, 2005b; Levy & Shoham, 2005a), which is critical in the transition of OCP cells to mature osteoclasts although tetraspanins are thought not to be responsible for the fusion themselves but rather to modulate the fusion process (Fanaei *et al.*, 2011).

4.3.2.1.8 Periostin (Postn)

Periostin, a matricellular protein, the expression of which was first discovered in the periosteum, possesses different specific binding domains for tenascin C, collagen type I and fibronectin and it was suggested as a modulator of collagen-I-crosslinking, and incorporation of tenascin C hexameres into a fibronectin collagen I based ECM, thereby establishing a meshwork (Kii *et al.*, 2010). Mouse strains deficient for periostin or tenascin C display similar phenotypes with regions of bone loss, and expression of periostin and tenascin C in wildtype mice was seen in similar areas, highlighting the functional relationship to tenascin C and the ECM in general (Kii *et al.*, 2010). Apart from its promotion of bone turnover and development, involvement of periostin has also been shown in remodeling processes in the ECM of the myocardium after infarction, in lung tissue after puncture, in lung and respiratory tissue in asthmatic and allergic diseases, in skin diseases and wound healing, and in promoting invasiveness

of tumor cells and of RA synoviocytes (Conway *et al.*, 2014; Kudo, 2011; You *et al.*, 2014). Interestingly, just like in the transcriptome of OCPs in this study, periostin was also elevated together with TIMP-1 in a gene expression analysis of an osteoarthritis mouse model (Loeser *et al.*, 2012), again emphasizing its role in remodeling of the ECM. Additionally, in a very recent study, Shih and colleagues could show that periostin also participates in axonal regeneration after injury (Shih *et al.*, 2014). Transcriptional expression of periostin by osteoclasts seems novel since it has so far been shown only by one very recent study (Merle *et al.*, 2014).

4.3.2.1.9 Sparc

Secreted protein acidic and rich in cysteine (SPARC, also referred to as osteonectin or BM-40) is known to be expressed in bone and to have an overall promoting effect on bone accrual, and an inhibiting effect on bone resorption, as shown in a SPARC knock-out mouse (Delany & Hankenson, 2009). Due to its collagen binding capabilities, SPARC is also involved in ECM assembly and remodeling, which is of major importance not only in processes like in bone turnover (Alford & Hankenson, 2006) but similar to tenascin C and periostin also in cardiac remodeling (McCurdy *et al.*, 2010; Schellings *et al.*, 2004). In addition, a synergistic neurotrophic effect together with BDNF (brain derived neurotrophic factor) on retinal ganglion cells (Ma *et al.*, 2010), and an activation of the STAT3 (signal transducer and activator of transcription 3) pathway has been reported, leading to increased expression of neuronal markers in medullablastoma cells (Bhoopathi *et al.*, 2011).

4.3.2.1.10 DC-stamp and OC-stamp

Both gene transcripts were up-regulated in OCP cells from healthy control mice and code for the two seven transmembrane proteins dentrocyte expressed seven transmembrane protein (DC-stamp) and osteoclast stimulatory transmembrane protein (OC-stamp). Fusion of OCPs and pre-osteoclasts to multinucleated cells is one of several requirements for functional bone resorbing osteoclasts and it was shown *in vitro* and *in vivo* that expression of both proteins, DC-stamp and OC-stamp, which is inducible by RANKL, is required for successful fusion (Miyamoto *et al.*, 2012). Further, OC-stamp, the expression of which is assumed to be regulated via protein kinase B/AKT or PKCβ (protein kinase C beta) signaling, seems to be not only involved in osteoclast fusion but also in differentiation of osteoclasts (Kim *et al.*, 2011).

4.3.2.1.11 Oscar

The expression of Oscar (osteoclast associated receptor) on the osteoclast cell linage in mice and humans has been shown previously (reviewed in (Nemeth *et al.*, 2011)). It was demonstrated that Oscar activation acts as an important co-stimulus in osteoclastogenesis and that Oscar possesses collagen binding domains, suggesting an interaction with the ECM, which Barrow and colleagues indeed were able to show (Barrow *et al.*, 2011; Nemeth *et al.*, 2011). In RA, expression of Oscar was detected in osteoclasts at focal erosions, in synovial cells and in circulating blood monocytes, the latter of which showed enhanced expression in active RA compared to monocytes from RA patients in remission, suggesting a relation between Oscar expression and disease activity (Herman *et al.*, 2008b; Crotti *et al.*, 2012). A soluble form of Oscar was demonstrated in similar amounts in synovial fluid from RA and OA patients (Crotti *et al.*, 2012) and in serum, in which Oscar was elevated in RA compared to healthy controls (Herman *et al.*, 2008b). Here it remains unclear, why Oscar displayed an elevated gene transcript expression in OCPs from healthy control mice compared to arthritic animals (**Figure 20**).

4.3.2.1.12 LIF

Gp130 class cytokines like LIF, OSM, IL-6, CT-1 and CNTF seem to be major players in regulating bone mass accrual and resorption in a paracrine fashioned communication between osteoblasts and osteoclasts (reviewed in (Auernhammer & Melmed, 2000; Sims & Walsh, 2010; Sims & Johnson, 2012)). *In vivo*, LIF leads to an up-regulation of both bone formation and resorption, and it was confirmed *in vitro* that this is mainly due to a direct stimulation of osteoblast lineage cells, which increases bone accrual and release of RANK ligand, which in turn indirectly enhances osteoclast differentiation and activity, resulting in an overall increased bone turnover ((Palmqvist *et al.*, 2002; Sims & Johnson, 2012)). Expression of LIF receptor was shown on osteoblasts but not on osteoclasts and, until recently, expression of LIF by osteoclasts was regarded as not existing (Auernhammer & Melmed, 2000; Sims & Walsh, 2010). However, results of this study and two other studies of osteoclast-like cells indicate that OCPs or osteoclast-like cells might under certain circumstances be able to express LIF (Gouin *et al.*, 1999; Ota *et al.*, 2013) (**Figure 20**, **Figure 25**). In contrast, one study showed up-regulation of LIF gene expression in total subchondral bone of a chronic joint pain OA model in rats (Dawes *et al.*, 2013), but this might be explained by the different animal model of a different disease (OA joint pain), and gene expression analysis of total tissue instead of isolated and differentiated BMM. Interestingly, in co-culture experiments of osteoclast-like cells and sympathetic ganglion cells,

Suga and colleagues could demonstrate an up-regulation of the gp130 cytokine IL-6 upon activation of the α_{1A}-adrenoceptor (α_{1A} AR) which is present on osteoclasts (Suga *et al.*, 2010). Hence, it might well be that activation of (α_{1A} AR) on osteoclast progenitors by norepinephrine, which is spontaneously released by sympathetic ganglia, led to an up-regulation and release of LIF (**Figure 20**, **Figure 25**) and/or other gp130 class cytokines like OSM (**Figure 24**), which in turn promoted the well described transition from a sympathetic to a cholinergic phenotype in neurons of sympathetic ganglia elicited by these cytokines (Bamber *et al.*, 1994; Geissen *et al.*, 1998; Rao *et al.*, 1992; Yamamori *et al.*, 1989).

4.3.2.2 Up-regulated gene transcripts in osteoclast progenitors from arthritic mice

In contrast to the gene transcripts, which were up-regulated in OCPs from healthy control mice, the genes which displayed higher expression in cells from arthritic animals, generally are related to the cytokine and chemokine (especially CCL and CXCL) families of molecules, which makes sense given that arthritis is an inflammatory disease, in which bone marrow macrophages and osteoclasts are involved (McInnes & O'Dell, 2010; Schett & Firestein, 2010; Firestein, 2003; Straub *et al.*, 2013; McInnes & Schett, 2011; McInnes & Schett, 2007).

4.3.2.2.1 SAA3

The gene transcript with the highest induction seen in osteoclasts from mice with CIA was *SAA3* (serum amyloid A3), which is known to be released from LPS (lipopolysaccharide) stimulated macrophages (Meek *et al.*, 1992) alongside with MIP-1a (macrophage inflammatory protein-1a, CCL3) and MIP-1b (macrophage inflammatory protein-1b, CCL4) (Meheus *et al.*, 1993), which both also displayed enhanced expression in OCPs from arthritic mice (**Figure 20**). In RA, it was suggested that up-regulation of SAA3 in the synovium plays a role in the pathogenesis of the disease (Geurts *et al.*, 2011; O'Hara *et al.*, 2004). Additionally, SAA3 also seems to influence bone homeostasis by affecting osteoblast differentiation and osteoclastogenesis (Thaler *et al.*, 2014) as well as having the ability of inducing the expression of pro-inflammatory TNF and several matrix metalloproteinases, rendering it as a possible marker of disease activity (Connolly *et al.*, 2012).

4.3.2.2.2 CCL2, CCL7, CCL5, CCL12, CCR5

The chemokine C-C motif ligand 7 (CCL7), also termed MCP-3 (monocyte chemoattractant protein-3), showed the highest up-regulation of several CC and CXC chemokines in OCPs from arthritic mice (**Figure 20**). Similar to CCL2 (MCP-1), CCL7 was shown to enhance formation and differentiation of

multinucleated osteoclasts via activation of CCR2 (Binder *et al.*, 2009; Yu *et al.*, 2004) and to be expressed in synovial tissue of RA patients (Haringman *et al.*, 2006). The importance of these two cytokines in activation and differentiation of osteoclasts was demonstrated in experiments by Binder et al., who showed that activation of CCR2 via CCL2 or CCL7 leads to bone loss via an increased RANK signaling, which was abrogated in a CCR2 knock-out mouse (Binder *et al.*, 2009). Interestingly, in an arthritis mouse model expression of CCL2 and CCL7 in affected joints was shown and inhibition of both CCL2 and CCL7 ameliorated the disease severity (Chen *et al.*, 2015). However, several studies investigating experimental arthritis in mice indicated that deletion of the receptors CCR2 and CCR5 (a chemokine receptor for chemokines CCL5, 3 and 7) unexpectedly did not ameliorate arthritis (Fujii *et al.*, 2011; Quinones *et al.*, 2004; Rampersad *et al.*, 2011), and it was even suggested that chemokine receptors might have a protective role during arthritis (Doodes *et al.*, 2009; Fujii *et al.*, 2011; Quinones *et al.*, 2004; Rampersad *et al.*, 2011). This is in line with several clinical trials in which treatment of RA patients by chemokine receptor antagonists failed to improve the disease (Asquith *et al.*, 2015; Lebre *et al.*, 2011). However, the chemokines CCL2 and CCL7 were implicated to also play a role in the nervous system, since they were shown to promote dopaminergic differentiation (Edman *et al.*, 2008) and activity (Guyon *et al.*, 2009; Semple *et al.*, 2010). Further, CCL2 was also shown to influence nociception in dorsal root ganglia (Biber & Boddeke, 2014; Jung *et al.*, 2008), to be co-expressed with its receptor CCR2 in certain dopaminergic and cholinergic neurons of the CNS (Banisadr *et al.*, 2005; Melik-Parsadaniantz & Rostene, 2008), and to be expressed in sympathetic ganglia upon axotomy (Schreiber *et al.*, 2001). Hence it might well be that CCL2 or even other chemokines released by OCPs from arthritic mice support expression of the existing dopaminergic phenotype of most of the neurons in sympathetic ganglia and prevent a possible up-regulation of cholinergic markers like in co-culture experiments with OCPs from healthy control mice (**Figure 16**). CCL12 (or MCP-5, monocyte chemoattractant protein-5) is structurally and functionally very closely related to CCL2 (MCP-1) (Sarafi *et al.*, 1997), since they signal via the same receptor CCR2. Interestingly they both are induced under hypoxia in astrocytes (Mojsilovic-Petrovic *et al.*, 2007), and it was also suggested that CCL12 has a decisive role in joint development (Longobardi *et al.*, 2012), highlighting an involvement in the skeletal and nervous system.

4.3.2.2.3 CCL3, CCL4, CCL6, CCL8, CXCL2, CXCL3

Similar to this study (**Figure 20**, **Figure 28**), expression of CCL3/MIP-1a (macrophage inflammatory protein-1a) was also detected in supernatants of OCPs obtained from BALB/C mice and from a murine

osteoclast-like cell line (Lee *et al.*, 2007; Yu *et al.*, 2004). Further, CCL3 was shown to foster differentiation and motility but not activity of osteoclasts (Fuller *et al.*, 1995; Oba *et al.*, 2005; Yu *et al.*, 2004). The here demonstrated presence of CXCL2/MIP-2a (macrophage inflammatory protein-2a) expressed by OCPs (**Figure 20**, **Figure 28**) confirms earlier studies which show that CXCL2 gene and protein expression in OCPs treated with RANKL or LPS is enhanced and it was suggested that CXCL2 increases osteoclastogenesis (Ha *et al.*, 2010; Ha *et al.*, 2011; Tanaka *et al.*, 2013). Since elevated presence of CXCL2 was shown in synovial fluid and serum from RA patients compared to OA (Ha *et al.*, 2010), and the deletion of only CXCR2 (the main receptor of CXCL2) but not any other chemokine receptors improved autoantibody-induced arthritis, the CXCL2/CXCR2 and CXCL10 signaling pathways remain promising targets for future studies and clinical trials in RA (Asquith *et al.*, 2015; Jacobs *et al.*, 2010). In the CNS and in immune cells, expression of CXCR2 has been shown (reviewed in (Veenstra & Ransohoff, 2012)), but no expression in sympathetic ganglia has been described yet although CXCL2/CXCR2 axis signaling seems to play a key role in recruiting immune cells to sensory ganglia (Stock *et al.*, 2014). Not so much is known about CXCL3, which is another ligand for CXCR2 (Jacobs *et al.*, 2010) and hence might display similar properties as CXCL2.

CCL6, also known as C10/MRP-1, has been demonstrated to be produced by BMM treated with either IL-4, GM-CSF, or M-CSF (Orlofsky *et al.*, 1994), and since its expression was also shown in microglia, it was suggested that CCL6 might also be involved in immune-system-CNS crosstalk (Kanno *et al.*, 2005).

Similar effects of CCL4 (MIP-1b) and CCL3 (MIP-1a) were suggested in bone marrow cells from multiple myeloma patients, as they both enhanced osteoclast activity by an elevated secretion of RANKL and both signal via the same receptor CCR5 (Abe *et al.*, 2002). Gene expression analysis in a human osteoclast cell line indicated up-regulation of CCL4 along with CCL2, CCL3 and CCL5 upon stimulation with M-CSF and RANKL (Morrison *et al.*, 2014). Interestingly, in a study examining RA patients during anti-TNF therapy, a decrease of the chemokines CCL2, CCL4 and CXCL10 in the patients' blood was observed within the initial two weeks of treatment (Eriksson *et al.*, 2013). In another study, presence of CCL2 (MCP-1), CCL5, CCL7 and CCL8 (MCP-2) alongside CCR5 (a receptor for CCL3 and CCL4) was demonstrated in synovial tissue of RA patients (Haringman *et al.*, 2006).

4.3.2.2.4 IL1-α, IL1-β, TNF, MMP-8, Marco

Elevated expression of TNF, IL-1α and IL-1β, as found in OCPs of arthritic mice in this study (**Figure 20**) was not surprising since these cytokines are known to be expressed in the bone marrow (Van

Bezooijen *et al.*, 1998) and by (bone marrow) macrophages (Braun & Zwerina, 2011; Kwan *et al.*, 2004; Li *et al.*, 2003), and are up-regulated in animal models of arthritis and in RA (Braun & Zwerina, 2011; Schett, 2011). In general, the net effect of these three cytokines is regarded as rather pro-inflammatory and pro-osteoclastogenic, leading to enhanced bone loss and erosions in arthritis (Braun & Zwerina, 2011; Schett, 2011).

Although circulating levels of matrix metalloproteinase 8 (MMP-8), a collagenase, were associated with a higher risk of mortality due to respiratory diseases in patients with RA (Mattey *et al.*, 2012), knock-out models for MMP-8 showed exacerbation of experimental arthritis, suggesting also a protective role for MMP-8 in arthritis (Cox *et al.*, 2010; Garcia *et al.*, 2010).

Marco, a transmembrane class A scavenger receptor on macrophages (Kraal *et al.*, 2000), was found to be a receptor especially for bacterial compounds such as LPS, but it also recognizes whole living or heat killed bacteria (Chen *et al.*, 2010; Kraal *et al.*, 2000; Sankala *et al.*, 2002) such as mycobacterium tuberculosis (Bowdish *et al.*, 2009), which was also used for the induction of experimental arthritis in this study (2.3). This might be a reason for the up-regulated gene expression of Marco in OCPs from arthritic animals (**Figure 20**).

To summarize the results of the gene expression analysis in this study, OCPs obtained from healthy control mice displayed an up-regulation of genes which apart from *LIF*, a known factor for cholinergic transition, are related to remodeling processes of the ECM *(TIMP-1, Bgn, Tnc, Fn1, Ctgf, Tspan7, Tns, Sparc, Postn)*, but some feature also influences on the nervous system *(Bgn, Tnc, Fn1, Sparc, Postn)* or osteoclast fusion processes *(Tns, Tspan7, Dcstamp, Ocstamp)*. On the other hand, OCPs obtained from mice with CIA, display an up-regulation in gene transcripts which mainly code for inflammatory cytokines and chemokines, some of which also play a role in neuronal differentiation *(CCL2, CCL7)*. These results suggest that LIF, possibly augmented by ECM related molecules, enhanced expression of cholinergic markers in co-culture experiments with OCPs from control mice, while up-regulated chemokines might have inhibited this transition in experiments with OCPs from CIA mice (**Figure 16**). Additionally, the fusion process of OCPs seems to be differently regulated in healthy and arthritic mice.

4.3.3 Identification of possible transition factors of osteoclast progenitor cells by proteome analysis

Following gene expression analysis, supernatants from OCPs obtained from healthy control and arthritic mice were first subjected to semi quantitative cytokine profiling, followed by quantitative ELISA measurements of promising candidate proteins.

In the cytokine profile (I) (**Figure 22**), most of the investigated proteins displayed relative weak signal intensities between 1 and 20%. Notably, if there was a difference, signals were consistently higher in samples from CIA compared to control. This is reasonable for cytokines like interleukin 1α/β, 6, 7, 12p70, 17, 23, and, in part, 27 which are generally regarded as pro-inflammatory and present in inflamed joints (reviewed in (Firestein, 2003; Herman *et al.*, 2008a; McInnes & Schett, 2007)) but not so much for interleukins 4, 10 or 13 which were shown to be down-regulated under inflammatory conditions and are regarded as rather anti-inflammatory cytokines (reviewed in (Firestein, 2003; Herman *et al.*, 2008a; McInnes & Schett, 2007)). Interestingly, no difference in TNF, TIMP-1 expression was seen with the profiling technique, which might be a problem of low statistical power (n=4 vs. n=4). C-C and C-X-C motif chemokine protein expression levels were generally higher, which makes sense since many of these chemokines play a role in the monocyte/macrophage lineage of cells. Strong protein expression (more than 20% relative signal intensity) was detected for CCL2, 3, 4, 5 and CXCL1, 2, 10 and 12 (cytokine profile (II) **Figure 23**).

First, TIMP-1 and LIF, which displayed elevated gene expression were assayed with ELISA, followed by OSM, which was not up-regulated in the gene expression analysis but is a known gp130 class cytokine for sympathetic transition and normally present in bone (see 4.3.2.1.12). Strikingly, TIMP-1, LIF and OSM were indeed present in low levels in the supernatants of both, control and CIA OCPs, with TIMP-1 and OSM showing higher levels in supernatants from control OCPs (**Figure 24**). LIF was also present in of both supernatants but at equally low levels (**Figure 25**). The significance of TIMP-1 and LIF in bone and the nervous system has been discussed above (4.3.2.1.5 and 4.3.2.1.12, respectively).

So far an expression of OSM in fully developed osteoclasts has not been reported (reviewed in (Heymann & Rousselle, 2000; Sims & Walsh, 2010)), but just recently it has been found that OSM can be expressed not only in osteoblasts and osteocytes (both mesenchymal cells) but also macrophages (hematopoietic cells) (Guihard *et al.*, 2015). Since OCPs in this study were shown to express OSM

(**Figure 24**), and these OCPs were generated from BMM (hematopoietic cells), it might well be that different stages of developing osteoclast precursors indeed do express OSM protein. As a special gp130 class cytokine, OSM seems to play an ambivalent role in bone since it uniquely mediates its signals through two different receptor combinations (gp130+OSM receptor complex, gp130+LIF receptor complex) which are expressed on different bone cells (osteoblasts, osteocytes), acting directly on osteoblasts and indirectly on osteoclasts via osteoblasts (reviewed in (Heymann & Rousselle, 2000; Sims & Walsh, 2010)): It was demonstrated that OSM enhances osteoclast differentiation and activity (Richards *et al.*, 2000), which was shown to be an indirect effect of increased RANKL expression in osteoblasts which in turn stimulated osteoclasts (Palmqvist *et al.*, 2002; Sims & Walsh, 2010). Additionally, OSM also fosters osteoprotegerin (OPG) expression which favors bone formation (Palmqvist *et al.*, 2002). To make things even more complex, it was suggested that OSM, when signaling via the OSM receptor complex, leads to enhanced bone turnover via RANKL induced bone resorption and OPG induced bone formation (Walker *et al.*, 2010). However, there seems to be an independent pathway mediated via the LIF receptor complex leading to enhanced bone formation by inhibition of sclerostin in osteoblasts (Walker *et al.*, 2010). Interestingly and in line with observations in this study, OSM up-regulation coincided also with an increase in TIMP-1 expression (**Figure 24**), which was also seen in human cardiac myocytes and fibroblasts (Weiss *et al.*, 2005), in human synovial lining cells (Gatsios *et al.*, 1996) and osteoblasts (reviewed in (Heymann & Rousselle, 2000)) and it was suggested that an up-regulation of TIMP-1 might be counter-regulatory to limit tissue destruction by increased MMP activity in heart remodeling (Weiss *et al.*, 2005). In the joint however, OSM was shown to be mainly pro-inflammatory, enhancing tissue damage, although the net effect depends on the local receptor constellation for OSM and corresponding target cells which mediate the effects (Hui *et al.*, 2003; Langdon *et al.*, 2000; Moran *et al.*, 2009; Richards, 2013; Rowan *et al.*, 2003). The influence of OSM and other gp130 class cytokines on sympathetic ganglia has been discussed (4.3.2.1.12), and the elevated concentration of OSM in supernatants from control OCPs might be a reason for the observed increase in VAChT/TH ratio in sympathetic ganglia in co-culture with control OCPs (**Figure 16**), since an elevated expression of LIF in OCPs from control mice as suggested by gene expression analysis (**Figure 20**) could not be demonstrated by measuring LIF protein (**Figure 25**). The expression of LIF protein by OCPs however is novel (see also 4.3.2.1.12). The protein expression of several macrophage and osteoclast related chemokines (CCL2/MCP-1, CCL7/MCP-3, CCL3/MIP-1a, CXCL2/MIP-2a, CCL5/RANTES and CXCL10) was confirmed with ELISA (**Figure 27**, **Figure 28**, **Figure 29**). However, only CCL5/RANTES displayed higher protein expression in OCPs generated from CIA mice, rendering

this specific chemokine as a possible inhibitor of the sympathetic transition seen in co-cultures with OCPs from healthy controls (**Figure 16**), similar to CCL2 and CCL7, which were described to enhance dopaminergic properties in neurons (see 4.3.2.2.2). The proteins periostin and CXCL12 were rated as non-detectable since they displayed sub-standard signals in the ELISA assay (**Figure 30**). The significance of all these factors in bone and in the nervous system has already been discussed above (see 4.3.2). However, one can not exclude that other soluble factors supported the observed cholinergic transition of sympathetic ganglia in co-culture with OCPs. For example, the expression of Satb2 was shown to be crucial in the cholinergic transition of sympathetic neurons and at the same time it is expressed by osteoblast lineage cells, and is involved in skeletal development and osteoblast differentiation (Apostolova *et al.*, 2010; Dobreva *et al.*, 2006). Future studies will be needed to further clarify the observed differences.

4.3.4 Identification of possible transition factor DNA binding sites by genomic analysis

In this study, progesterone was found to augment LIF induced cholinergic transition of sympathetic ganglia (**Figure 17**), which is not in contrast to earlier literature which suggested that the glucocorticoid corticosterone and the mineralocorticoid aldosterone but not the sex steroid progesterone inhibit an up-regulation of cholinergic markers in sympathetic ganglia in culture (McLennan *et al.*, 1984). This inhibition of cholinergic transition was blocked by RU38486 (Mifepristone), a glucocorticoid receptor and progesterone receptor antagonist (Hendry *et al.*, 1987). It was suggested that non-neuronal cells present in the ganglia are *in vivo* controlled by steroids, which prevents them from releasing soluble factors that would elicit cholinergic switching of neurons in the ganglia (Fukada, 1980; McLennan *et al.*, 1980). These inhibitory effects of glucocorticoids have been later confirmed by others (Berse & Blusztajn, 1997) and presence of progesterone and its receptor has been demonstrated in neurons (Chan *et al.*, 2000). It was further suggested that within the VAChT cholinergic gene locus there exists a response element for glucocorticoid receptors (Cervini *et al.*, 1995) which is confirmed by results of this very study, predicting the presence of progesterone receptor and glucocorticoid receptor binding sites in promoter regions of VAChT (see 3.6). Quite recently, it was also shown for the sex steroid estrogen to up-regulate cholinergic ChAT transcriptome in a neuronal cell line *in vitro* (Yamamuro & Aizawa, 2010). These observations and the presence of progesterone in the medium of ganglia experiments, a possible yet unknown local production of progesterone by BMM/OCPs and its presence in

the synovial fluid of OA and RA patients (**Figure 26**) might possibly also be supporting an up-regulation of cholinergic markers in sympathetic peripheral nerve fibers.

4.3.5 Transition of sympathetic ganglia by stimulation with single molecules

To investigate possible influences of candidate molecules on frequency of the cholinergic marker VAChT in sympathetic nerve fibers, these molecules were tested in stimulation experiments with sympathetic ganglia. In line with previous work of others (see 4.3.2.1.12), expectedly LIF increased the VAChT/TH ratio in nerve fibers of sympathetic ganglia (**Figure 17**). Interestingly, this effect was supported by the presence of progesterone, which has been discussed above (4.3.4). Also biglycan and TIMP-1 enhanced the frequency of cholinergic immunoreactivity in sympathetic ganglia, which might render novel functions of these molecules, which were discussed in 4.3.2.1. RGDS and fibronectin displayed an effect on the morphology of nerve fiber growth which supports their influence in adhesion processes (discussed in 4.3.2.1.3).

5 Conclusion

First, this study confirms earlier observations that in highly inflamed regions of the joint like the synovium and near focal bony erosions, sympathetic TH-positive nerve fibers are lost. This was shown in earlier studies of RA patients and in experimental arthritis of mice (CIA) in this study. A suspected transition to a cholinergic phenotype of sympathetic nerve fibers was not demonstrated in these regions. This phenomenon of cholinergic transition is only known for sympathetic catecholaminergic nerve fibers and not for sensory nerve fibers, which are often increased in highly inflamed tissue.

Secondly and unexpectedly, an increase of cholinergic, VAChT-positive nerve fibers in rather healthy tissue (skin and muscle) was detected at the same time (day 35 p.i.) in experimental arthritis at which TH-positive nerve fibers were lost. This supports the concept by Pongratz and Straub who suggested an overall change of innervation and conditions in inflamed joints in CIA at this very point of time (Pongratz & Straub, 2013), marking a transition from acute to chronic inflammation. In concordance with this observation, cholinergic VAChT-positive fibers were more prevalent in joint tissue from OA patients compared to RA, with OA being generally considered as a disease with a lower degree of local and systemic inflammation. Furthermore, cholinergic transition of sympathetic nerve fibers could be induced *in vitro*, but only by bone marrow derived cells from healthy control and not from arthritic animals, supporting the above mentioned results. Importantly, the possibility of a direct innervation by VAChT-positive and VIP-positive cholinergic nerve fibers in the synovial tissue of RA and OA patients and humans in general was demonstrated here for the first time.

Thirdly, in addition to previously known transition factors LIF and OSM, an influence on transition by ECM-related factors, progesterone, and possibly chemokines was demonstrated. In respect to extensive work of others and results of this very study, early concepts of static and purely adrenergic or cholinergic nerve fiber phenotypes seem obsolete.

In conclusion, presence of cholinergic innervation would provide the required neurotransmitters ACh and VIP for anti-inflammatory signaling elicited by local expression of α7nAChRs and VIP receptors on immune cells and synovial cells, which would support a therapy concept for arthritis in enhancing and exploiting these anti-inflammatory signaling pathways.

6 Appendix

6.1 List of literature

Reference List

1. Abe, M, Hiura, K, Wilde, J, Moriyama, K, Hashimoto, T, Ozaki, S, Wakatsuki, S, Kosaka, M, Kido, S, Inoue, D & Matsumoto, T. (2002). Role for macrophage inflammatory protein (MIP)-1alpha and MIP-1beta in the development of osteolytic lesions in multiple myeloma. *Blood*, **100**, 2195-2202.

2. Ahmed, MS, Oie, E, Vinge, LE, Yndestad, A, Andersen, GG, Andersson, Y, Attramadal, T & Attramadal, H. (2003). Induction of myocardial biglycan in heart failure in rats--an extracellular matrix component targeted by AT(1) receptor antagonism. *Cardiovasc Res*, **60**, 557-568.

3. Aitken, SJ, Landao-Bassonga, E, Ralston, SH & Idris, AI. (2009). Beta2-adrenoreceptor ligands regulate osteoclast differentiation in vitro by direct and indirect mechanisms. *Arch Biochem Biophys*, **482**, 96-103.

4. Aletaha, D, Neogi, T, Silman, AJ, Funovits, J, Felson, DT, Bingham, CO, III, Birnbaum, NS, Burmester, GR, Bykerk, VP, Cohen, MD, Combe, B, Costenbader, KH, Dougados, M, Emery, P, Ferraccioli, G, Hazes, JM, Hobbs, K, Huizinga, TW, Kavanaugh, A, Kay, J, Kvien, TK, Laing, T, Mease, P, Menard, HA, Moreland, LW, Naden, RL, Pincus, T, Smolen, JS, Stanislawska-Biernat, E, Symmons, D, Tak, PP, Upchurch, KS, Vencovsky, J, Wolfe, F & Hawker, G. (2010). 2010 Rheumatoid arthritis classification criteria: an American College of Rheumatology/European League Against Rheumatism collaborative initiative. *Arthritis Rheum*, **62**, 2569-2581.

5. Alford, AI & Hankenson, KD. (2006). Matricellular proteins: Extracellular modulators of bone development, remodeling, and regeneration. *Bone*, **38**, 749-757.

6. Aloe, L, Probert, L, Kollias, G, Bracci-Laudiero, L, Spillantini, MG & Levi-Montalcini, R. (1993). The synovium of transgenic arthritic mice expressing human tumor necrosis factor contains a high level of nerve growth factor. *Growth Factors*, **9**, 149-155.

7. Amenta, AR, Creely, HE, Mercado, ML, Hagiwara, H, McKechnie, BA, Lechner, BE, Rossi, SG, Wang, Q, Owens, RT, Marrero, E, Mei, L, Hoch, W, Young, MF, McQuillan, DJ, Rotundo, RL & Fallon, JR. (2012). Biglycan is an extracellular MuSK binding protein important for synapse stability. *J Neurosci*, **32**, 2324-2334.

8. Apostolova, G & Dechant, G. (2009). Development of neurotransmitter phenotypes in sympathetic neurons. *Auton Neurosci*, **151**, 30-38.

9. Apostolova, G, Loy, B, Dorn, R & Dechant, G. (2010). The sympathetic neurotransmitter switch depends on the nuclear matrix protein Satb2. *J Neurosci*, **30**, 16356-16364.

10. Arnett, FC, Edworthy, SM, Bloch, DA, McShane, DJ, Fries, JF, Cooper, NS, Healey, LA, Kaplan, SR, Liang, MH & Luthra, HS. (1988). The American Rheumatism Association 1987 revised criteria for the classification of rheumatoid arthritis. *Arthritis Rheum*, **31**, 315-324.

11. Asmus, SE, Parsons, S & Landis, SC. (2000). Developmental changes in the transmitter properties of sympathetic neurons that innervate the periosteum. *J Neurosci*, **20**, 1495-1504.

12. Asmus, SE, Tian, H & Landis, SC. (2001). Induction of cholinergic function in cultured sympathetic neurons by periosteal cells: cellular mechanisms. *Dev Biol*, **235**, 1-11.

13. Asquith, DL, Bryce, SA & Nibbs, RJ. (2015). Targeting cell migration in rheumatoid arthritis. *Curr Opin Rheumatol*, **27**, 204-211.

14. Auernhammer, CJ & Melmed, S. (2000). Leukemia-inhibitory factor-neuroimmune modulator of endocrine function. *Endocr Rev*, **21**, 313-345.

15. Bajayo, A, Bar, A, Denes, A, Bachar, M, Kram, V, Attar-Namdar, M, Zallone, A, Kovacs, KJ, Yirmiya, R & Bab, I. (2012). Skeletal parasympathetic innervation communicates central IL-1 signals regulating bone mass accrual. *Proc Natl Acad Sci U S A*, **109**, 15455-15460.

16. Bamber, BA, Masters, BA, Hoyle, GW, Brinster, RL & Palmiter, RD. (1994). Leukemia inhibitory factor induces neurotransmitter switching in transgenic mice. *Proc Natl Acad Sci U S A*, **91**, 7839-7843.

17. Banisadr, G, Gosselin, RD, Mechighel, P, Kitabgi, P, Rostene, W & Parsadaniantz, SM. (2005). Highly regionalized neuronal expression of monocyte chemoattractant protein-1 (MCP-1/CCL2) in rat brain: evidence for its colocalization with neurotransmitters and neuropeptides. *J Comp Neurol*, **489**, 275-292.

18. Barrow, AD, Raynal, N, Andersen, TL, Slatter, DA, Bihan, D, Pugh, N, Cella, M, Kim, T, Rho, J, Negishi-Koga, T, Delaisse, JM, Takayanagi, H, Lorenzo, J, Colonna, M, Farndale, RW, Choi, Y & Trowsdale, J. (2011). OSCAR is a collagen receptor that costimulates osteoclastogenesis in DAP12-deficient humans and mice. *J Clin Invest*, **121**, 3505-3516.

19. Beckmann, J & Lips, KS. (2013). The non-neuronal cholinergic system in health and disease. *Pharmacology*, **92**, 286-302.

20. Beckmann, J, Schubert, J, Morhenn, HG, Grau, V, Schnettler, R & Lips, KS. (2015). Expression of choline and acetylcholine transporters in synovial tissue and cartilage of patients with rheumatoid arthritis and osteoarthritis. *Cell Tissue Res*, **359**, 465-477.

21. Bencherif, M, Lippiello, PM, Lucas, R & Marrero, MB. (2011). Alpha7 nicotinic receptors as novel therapeutic targets for inflammation-based diseases. *Cell Mol Life Sci*, **68**, 931-949.

22. Berse, B & Blusztajn, JK. (1997). Modulation of cholinergic locus expression by glucocorticoids and retinoic acid is cell-type specific. *FEBS Lett*, **410**, 175-179.

23. Bhoopathi, P, Chetty, C, Dontula, R, Gujrati, M, Dinh, DH, Rao, JS & Lakka, SS. (2011). SPARC stimulates neuronal differentiation of medulloblastoma cells via the Notch1/STAT3 pathway. *Cancer Res*, **71**, 4908-4919.

24. Biber, K & Boddeke, E. (2014). Neuronal CC chemokines: the distinct roles of CCL21 and CCL2 in neuropathic pain. *Front Cell Neurosci*, **8**, 210.

25. Binder, NB, Niederreiter, B, Hoffmann, O, Stange, R, Pap, T, Stulnig, TM, Mack, M, Erben, RG, Smolen, JS & Redlich, K. (2009). Estrogen-dependent and C-C chemokine receptor-2-dependent pathways determine osteoclast behavior in osteoporosis. *Nat Med*, **15**, 417-424.

26. Bjurholm, A, Kreicbergs, A, Ahmed, M & Schultzberg, M. (1990). Noradrenergic and peptidergic nerves in the synovial membrane of the Sprague-Dawley rat. *Arthritis Rheum*, **33**, 859-865.

27. Bjurholm, A, Kreicbergs, A, Terenius, L, Goldstein, M & Schultzberg, M. (1988). Neuropeptide Y-, tyrosine hydroxylase- and vasoactive intestinal polypeptide-immunoreactive nerves in bone and surrounding tissues. *J Auton Nerv Syst*, **25**, 119-125.

28. Bord, S, Horner, A, Beeton, CA, Hembry, RM & Compston, JE. (1999). Tissue inhibitor of matrix metalloproteinase-1 (TIMP-1) distribution in normal and pathological human bone. *Bone*, **24**, 229-235.

29. Borovikova, LV, Ivanova, S, Zhang, M, Yang, H, Botchkina, GI, Watkins, LR, Wang, H, Abumrad, N, Eaton, JW & Tracey, KJ. (2000). Vagus nerve stimulation attenuates the systemic inflammatory response to endotoxin. *Nature*, **405**, 458-462.

30. Bowdish, DM, Sakamoto, K, Kim, MJ, Kroos, M, Mukhopadhyay, S, Leifer, CA, Tryggvason, K, Gordon, S & Russell, DG. (2009). MARCO, TLR2, and CD14 are required for macrophage cytokine responses to mycobacterial trehalose dimycolate and Mycobacterium tuberculosis. *PLoS Pathog*, **5**, e1000474.

31. Boyle, DL, Soma, K, Hodge, J, Kavanaugh, A, Mandel, D, Mease, P, Shurmur, R, Singhal, AK, Wei, N, Rosengren, S, Kaplan, I, Krishnaswami, S, Luo, Z, Bradley, J & Firestein, GS. (2014). The JAK inhibitor tofacitinib suppresses synovial JAK1-STAT signalling in rheumatoid arthritis. *Ann Rheum Dis*, **74**, 1311-1316.

32. Braun, T & Zwerina, J. (2011). Positive regulators of osteoclastogenesis and bone resorption in rheumatoid arthritis. *Arthritis Res Ther*, **13**, 235.

33. Brennan, C, Rivas-Plata, K & Landis, SC. (1999). The p75 neurotrophin receptor influences NT-3 responsiveness of sympathetic neurons in vivo. *Nat Neurosci*, **2**, 699-705.

34. Capellino, S, Cosentino, M, Wolff, C, Schmidt, M, Grifka, J & Straub, RH. (2010). Catecholamine-producing cells in the synovial tissue during arthritis: modulation of sympathetic neurotransmitters as new therapeutic target. *Ann Rheum Dis*, **69**, 1853-1860.

35. Capellino, S, Weber, K, Gelder, M, Harle, P & Straub, RH. (2012). First appearance and location of catecholaminergic cells during experimental arthritis and elimination by chemical sympathectomy. *Arthritis Rheum*, **64**, 1110-1118.

36. Cartharius, K, Frech, K, Grote, K, Klocke, B, Haltmeier, M, Klingenhoff, A, Frisch, M, Bayerlein, M & Werner, T. (2005). MatInspector and beyond: promoter analysis based on transcription factor binding sites. *Bioinformatics*, **21**, 2933-2942.

37. Cervini, R, Houhou, L, Pradat, PF, Bejanin, S, Mallet, J & Berrard, S. (1995). Specific vesicular acetylcholine transporter promoters lie within the first intron of the rat choline acetyltransferase gene. *J Biol Chem*, **270**, 24654-24657.

38. Chan, JR, Rodriguez-Waitkus, PM, Ng, BK, Liang, P & Glaser, M. (2000). Progesterone synthesized by Schwann cells during myelin formation regulates neuronal gene expression. *Mol Biol Cell*, **11**, 2283-2295.

39. Chandrasekharan, B, Nezami, BG & Srinivasan, S. (2013). Emerging neuropeptide targets in inflammation: NPY and VIP. *Am J Physiol Gastrointest Liver Physiol*, **304**, G949-G957.

40. Chen, W, Foo, SS, Taylor, A, Lulla, A, Merits, A, Hueston, L, Forwood, MR, Walsh, NC, Sims, NA, Herrero, LJ & Mahalingam, S. (2015). Bindarit, an inhibitor of monocyte chemotactic protein synthesis, protects against bone loss induced by chikungunya virus infection. *J Virol*, **89**, 581-593.

41. Chen, Y, Wermeling, F, Sundqvist, J, Jonsson, AB, Tryggvason, K, Pikkarainen, T & Karlsson, MC. (2010). A regulatory role for macrophage class A scavenger receptors in TLR4-mediated LPS responses. *Eur J Immunol*, **40**, 1451-1460.

42. Cherruau, M, Morvan, FO, Schirar, A & Saffar, JL. (2003). Chemical sympathectomy-induced changes in TH-, VIP-, and CGRP-immunoreactive fibers in the rat mandible periosteum: influence on bone resorption. *J Cell Physiol*, **194**, 341-348.

43. Chiquet-Ehrismann, R. (2004). Tenascins. *Int J Biochem Cell Biol*, **36**, 986-990.

44. Chiquet-Ehrismann, R, Orend, G, Chiquet, M, Tucker, RP & Midwood, KS. (2014). Tenascins in stem cell niches. *Matrix Biol*, **37**, 112-123.

45. Chiquet-Ehrismann, R & Tucker, RP. (2004). Connective tissues: signalling by tenascins. *Int J Biochem Cell Biol*, **36**, 1085-1089.

46. Chiquet-Ehrismann, R & Tucker, RP. (2011). Tenascins and the importance of adhesion modulation. *Cold Spring Harb Perspect Biol*, **3**, a004960.

47. Connolly, M, Mullan, RH, McCormick, J, Matthews, C, Sullivan, O, Kennedy, A, Fitzgerald, O, Poole, AR, Bresnihan, B, Veale, DJ & Fearon, U. (2012). Acute-phase serum amyloid A regulates tumor necrosis factor alpha and matrix turnover and predicts disease progression in patients with inflammatory arthritis before and after biologic therapy. *Arthritis Rheum*, **64**, 1035-1045.

48. Conway, SJ, Izuhara, K, Kudo, Y, Litvin, J, Markwald, R, Ouyang, G, Arron, JR, Holweg, CT & Kudo, A. (2014). The role of periostin in tissue remodeling across health and disease. *Cell Mol Life Sci*, **71**, 1279-1288.

49. Cox, JH, Starr, AE, Kappelhoff, R, Yan, R, Roberts, CR & Overall, CM. (2010). Matrix metalloproteinase 8 deficiency in mice exacerbates inflammatory arthritis through delayed neutrophil apoptosis and reduced caspase 11 expression. *Arthritis Rheum*, **62**, 3645-3655.

50. Crotti, TN, Dharmapatni, AA, Alias, E, Zannettino, AC, Smith, MD & Haynes, DR. (2012). The immunoreceptor tyrosine-based activation motif (ITAM) -related factors are increased in synovial tissue and vasculature of rheumatoid arthritic joints. *Arthritis Res Ther*, **14**, R245.

51. Dawes, JM, Kiesewetter, H, Perkins, JR, Bennett, DL & McMahon, SB. (2013). Chemokine expression in peripheral tissues from the monosodium iodoacetate model of chronic joint pain. *Mol Pain*, **9**, 57.

52. Del Rey, A, Wolff, C, Wildmann, J, Randolf, A, Straub, RH & Besedovsky, HO. (2010). When immune-neuro-endocrine interactions are disrupted: experimentally induced arthritis as an example. *Neuroimmunomodulation*, **17**, 165-168.

53. Delany, AM & Hankenson, KD. (2009). Thrombospondin-2 and SPARC/osteonectin are critical regulators of bone remodeling. *J Cell Commun Signal*, **3**, 227-238.

54. Delgado, M, Abad, C, Martinez, C, Juarranz, MG, Arranz, A, Gomariz, RP & Leceta, J. (2002). Vasoactive intestinal peptide in the immune system: potential therapeutic role in inflammatory and autoimmune diseases. *J Mol Med (Berl)*, **80**, 16-24.

55. Delgado, M, Abad, C, Martinez, C, Leceta, J & Gomariz, RP. (2001). Vasoactive intestinal peptide prevents experimental arthritis by downregulating both autoimmune and inflammatory components of the disease. *Nat Med*, **7**, 563-568.

56. Delgado, M & Ganea, D. (2008). Anti-inflammatory neuropeptides: a new class of endogenous immunoregulatory agents. *Brain Behav Immun*, **22**, 1146-1151.

57. Delgado, M, Leceta, J & Ganea, D. (2003). Vasoactive intestinal peptide and pituitary adenylate cyclase-activating polypeptide inhibit the production of inflammatory mediators by activated microglia. *J Leukoc Biol*, **73**, 155-164.

58. Delgado, M, Robledo, G, Rueda, B, Varela, N, O'Valle, F, Hernandez-Cortes, P, Caro, M, Orozco, G, Gonzalez-Rey, E & Martin, J. (2008a). Genetic association of vasoactive intestinal peptide receptor with rheumatoid arthritis: altered expression and signal in immune cells. *Arthritis Rheum*, **58**, 1010-1019.

59. Delgado, M, Toscano, MG, Benabdellah, K, Cobo, M, O'Valle, F, Gonzalez-Rey, E & Martin, F. (2008b). In vivo delivery of lentiviral vectors expressing vasoactive intestinal peptide complementary DNA as gene therapy for collagen-induced arthritis. *Arthritis Rheum*, **58**, 1026-1037.

60. Dobreva, G, Chahrour, M, Dautzenberg, M, Chirivella, L, Kanzler, B, Farinas, I, Karsenty, G & Grosschedl, R. (2006). SATB2 is a multifunctional determinant of craniofacial patterning and osteoblast differentiation. *Cell*, **125**, 971-986.

61. Doodes, PD, Cao, Y, Hamel, KM, Wang, Y, Rodeghero, RL, Kobezda, T & Finnegan, A. (2009). CCR5 is involved in resolution of inflammation in proteoglycan-induced arthritis. *Arthritis Rheum*, **60**, 2945-2953.

62. Duong, CV, Geissen, M & Rohrer, H. (2002). The developmental expression of vasoactive intestinal peptide (VIP) in cholinergic sympathetic neurons depends on cytokines signaling through LIFRbeta-containing receptors. *Development*, **129**, 1387-1396.

63. Dziennis, S & Habecker, BA. (2004). Ciliary neurotrophic factor suppresses Phox2a in sympathetic neurons. *Neuroreport*, **15**, 33-36.

64. Edman, LC, Mira, H & Arenas, E. (2008). The beta-chemokines CCL2 and CCL7 are two novel differentiation factors for midbrain dopaminergic precursors and neurons. *Exp Cell Res*, **314**, 2123-2130.

65. Eglen, RM. (2006). Muscarinic receptor subtypes in neuronal and non-neuronal cholinergic function. *Auton Autacoid Pharmacol*, **26**, 219-233.

66. Eiden, LE. (1998). The cholinergic gene locus. *J Neurochem*, **70**, 2227-2240.

67. Eiden, LE, Schafer, MK, Weihe, E & Schutz, B. (2004). The vesicular amine transporter family (SLC18): amine/proton antiporters required for vesicular accumulation and regulated exocytotic secretion of monoamines and acetylcholine. *Pflugers Arch*, **447**, 636-640.

68. Eimar, H, Tamimi, I, Murshed, M & Tamimi, F. (2013). Cholinergic regulation of bone. *J Musculoskelet Neuronal Interact*, **13**, 124-132.

69. Eitner, A, Pester, J, Nietzsche, S, Hofmann, GO & Schaible, HG. (2013). The innervation of synovium of human osteoarthritic joints in comparison with normal rat and sheep synovium. *Osteoarthritis Cartilage*, **21**, 1383-1391.

70. Elefteriou, F. (2005). Neuronal signaling and the regulation of bone remodeling. *Cell Mol Life Sci*, **62**, 2339-2349.

71. Erickson, JD, Varoqui, H, Schafer, MK, Modi, W, Diebler, MF, Weihe, E, Rand, J, Eiden, LE, Bonner, TI & Usdin, TB. (1994). Functional identification of a vesicular acetylcholine transporter and its expression from a "cholinergic" gene locus. *J Biol Chem*, **269**, 21929-21932.

72. Eriksson, C, Rantapaa-Dahlqvist, S & Sundqvist, KG. (2013). Changes in chemokines and their receptors in blood during treatment with the TNF inhibitor infliximab in patients with rheumatoid arthritis. *Scand J Rheumatol*, **42**, 260-265.

73. Ernsberger, U & Rohrer, H. (1999). Development of the cholinergic neurotransmitter phenotype in postganglionic sympathetic neurons. *Cell Tissue Res*, **297**, 339-361.

74. Fanaei, M, Monk, PN & Partridge, LJ. (2011). The role of tetraspanins in fusion. *Biochem Soc Trans*, **39**, 524-528.

75. Fassold, A, Falk, W, Anders, S, Hirsch, T, Mirsky, VM & Straub, RH. (2009). Soluble neuropilin-2, a nerve repellent receptor, is increased in rheumatoid arthritis synovium and aggravates sympathetic fiber repulsion and arthritis. *Arthritis Rheum*, **60**, 2892-2901.

76. Fassold, A & Straub, RH. (2010). A new assay for nerve fiber repulsion. *Ann N Y Acad Sci*, **1193**, 43-47.

77. Felder, E & Dechant, G. (2007). Neurotrophic factors acutely alter the sorting of the vesicular acetyl choline transporter and the vesicular monoamine transporter 2 in bimodal sympathetic neurons. *Mol Cell Neurosci*, **34**, 1-9.

78. Firestein, GS. (2003). Evolving concepts of rheumatoid arthritis. *Nature*, **423**, 356-361.

79. Forsgren, S. (2012). Presence of ChAT mRNA and a very marked alpha7nAChR immunoreaction in the synovial lining layer of the knee joint. *Life Sci*, **91**, 1043-1047.

80. Francis, N, Farinas, I, Brennan, C, Rivas-Plata, K, Backus, C, Reichardt, L & Landis, S. (1999). NT-3, like NGF, is required for survival of sympathetic neurons, but not their precursors. *Dev Biol*, **210**, 411-427.

81. Francis, NJ, Asmus, SE & Landis, SC. (1997). CNTF and LIF are not required for the target-directed acquisition of cholinergic and peptidergic properties by sympathetic neurons in vivo. *Dev Biol*, **182**, 76-87.

82. Francis, NJ & Landis, SC. (1999). Cellular and molecular determinants of sympathetic neuron development. *Annu Rev Neurosci*, **22**, 541-566.

83. Friedrichsen, S, Heuer, H, Christ, S, Winckler, M, Brauer, D, Bauer, K & Raivich, G. (2003). CTGF expression during mouse embryonic development. *Cell Tissue Res*, **312**, 175-188.

84. Fujii, H, Baba, T, Ishida, Y, Kondo, T, Yamagishi, M, Kawano, M & Mukaida, N. (2011). Ablation of the Ccr2 gene exacerbates polyarthritis in interleukin-1 receptor antagonist-deficient mice. *Arthritis Rheum*, **63**, 96-106.

85. Fujii, T, Takada-Takatori, Y & Kawashima, K. (2008). Basic and clinical aspects of non-neuronal acetylcholine: expression of an independent, non-neuronal cholinergic system in lymphocytes and its clinical significance in immunotherapy. *J Pharmacol Sci*, **106**, 186-192.

86. Fujii, T, Watanabe, Y, Inoue, T & Kawashima, K. (2003). Upregulation of mRNA encoding the M5 muscarinic acetylcholine receptor in human T- and B-lymphocytes during immunological responses. *Neurochem Res*, **28**, 423-429.

87. Fukada, K. (1980). Hormonal control of neurotransmitter choice in sympathetic neurone cultures. *Nature*, **287**, 553-555.

88. Fuller, K, Owens, JM & Chambers, TJ. (1995). Macrophage inflammatory protein-1 alpha and IL-8 stimulate the motility but suppress the resorption of isolated rat osteoclasts. *J Immunol*, **154**, 6065-6072.

89. Gao, B, Calhoun, K & Fang, D. (2006). The proinflammatory cytokines IL-1beta and TNF-alpha induce the expression of Synoviolin, an E3 ubiquitin ligase, in mouse synovial fibroblasts via the Erk1/2-ETS1 pathway. *Arthritis Res Ther*, **8**, R172.

90. Garcia, S, Forteza, J, Lopez-Otin, C, Gomez-Reino, JJ, Gonzalez, A & Conde, C. (2010). Matrix metalloproteinase-8 deficiency increases joint inflammation and bone erosion in the K/BxN serum-transfer arthritis model. *Arthritis Res Ther*, **12**, R224.

91. Gardiner, NJ. (2011). Integrins and the extracellular matrix: key mediators of development and regeneration of the sensory nervous system. *Dev Neurobiol*, **71**, 1054-1072.

92. Gatsios, P, Haubeck, HD, Van de Leur, E, Frisch, W, Apte, SS, Greiling, H, Heinrich, PC & Graeve, L. (1996). Oncostatin M differentially regulates tissue inhibitors of metalloproteinases TIMP-1 and TIMP-3 gene expression in human synovial lining cells. *Eur J Biochem*, **241**, 56-63.

93. Geissen, M, Heller, S, Pennica, D, Ernsberger, U & Rohrer, H. (1998). The specification of sympathetic neurotransmitter phenotype depends on gp130 cytokine receptor signaling. *Development*, **125**, 4791-4801.

94. Genovese, MC, Jarosova, K, Cieslak, D, Alper, J, Kivitz, A, Hough, DR, Maes, P, Pineda, L, Chen, M & Zaidi, F. (2015). Apremilast in patients with active rheumatoid arthritis: A phase II, multicenter, randomized, double-blind, placebo-controlled, parallel-group study. *Arthritis Rheumatol*, Accepted article, doi: 10.1002/art.39120.

95. Geurts, J, Vermeij, EA, Pohlers, D, Arntz, OJ, Kinne, RW, van den Berg, WB & van de Loo, FA. (2011). A novel Saa3-promoter reporter distinguishes inflammatory subtypes in experimental arthritis and human synovial fibroblasts. *Ann Rheum Dis*, **70**, 1311-1319.

96. Gonzalez-Rey, E, Chorny, A, Fernandez-Martin, A, Ganea, D & Delgado, M. (2006). Vasoactive intestinal peptide generates human tolerogenic dendritic cells that induce CD4 and CD8 regulatory T cells. *Blood*, **107**, 3632-3638.

97. Gonzalez-Rey, E & Delgado, M. (2008). Vasoactive intestinal peptide inhibits cyclooxygenase-2 expression in activated macrophages, microglia, and dendritic cells. *Brain Behav Immun*, **22**, 35-41.

98. Gonzalez-Rey, E, Varela, N, Chorny, A & Delgado, M. (2007). Therapeutical approaches of vasoactive intestinal peptide as a pleiotropic immunomodulator. *Curr Pharm Des*, **13**, 1113-1139.

99. Gouin, F, Couillaud, S, Cottrel, M, Godard, A, Passuti, N & Heymann, D. (1999). Presence of leukaemia inhibitory factor (LIF) and LIF-receptor chain (gp190) in osteoclast-like cells cultured from human giant cell tumour of bone. Ultrastructural distribution. *Cytokine*, **11**, 282-289.

100. Graf, N, McLean, M, Capellino, S, Scholmerich, J, Murray, GI, El-Omar, EM & Straub, RH. (2012). Loss of sensory and noradrenergic innervation in benign colorectal adenomatous polyps--a putative role of semaphorins 3F and 3A. *Neurogastroenterol Motil*, **24**, 120-8, e83.

101. Gramoun, A, Goto, T, Nordstrom, T, Rotstein, OD, Grinstein, S, Heersche, JN & Manolson, MF. (2010). Bone matrix proteins and extracellular acidification: potential co-regulators of osteoclast morphology. *J Cell Biochem*, **111**, 350-361.

102. Grant, MP, Francis, NJ & Landis, SC. (1995). The role of acetylcholine in regulating secretory responsiveness in rat sweat glands. *Mol Cell Neurosci*, **6**, 32-42.

103. Grassi, F, Cristino, S, Toneguzzi, S, Piacentini, A, Facchini, A & Lisignoli, G. (2004). CXCL12 chemokine up-regulates bone resorption and MMP-9 release by human osteoclasts: CXCL12 levels are increased in synovial and bone tissue of rheumatoid arthritis patients. *J Cell Physiol*, **199**, 244-251.

104. Groeneveld, TW, Oroszlan, M, Owens, RT, Faber-Krol, MC, Bakker, AC, Arlaud, GJ, McQuillan, DJ, Kishore, U, Daha, MR & Roos, A. (2005). Interactions of the extracellular matrix proteoglycans decorin and biglycan with C1q and collectins. *J Immunol*, **175**, 4715-4723.

105. Guidry, G & Landis, SC. (1998). Target-dependent development of the vesicular acetylcholine transporter in rodent sweat gland innervation. *Dev Biol*, **199**, 175-184.

106. Guidry, G & Landis, SC. (2000). Absence of cholinergic sympathetic innervation from limb muscle vasculature in rats and mice. *Auton Neurosci*, **82**, 97-108.

107. Guidry, G, Willison, BD, Blakely, RD, Landis, SC & Habecker, BA. (2005). Developmental expression of the high affinity choline transporter in cholinergic sympathetic neurons. *Auton Neurosci*, **123**, 54-61.

108. Guihard, P, Boutet, MA, Brounais-Le, RB, Gamblin, AL, Amiaud, J, Renaud, A, Berreur, M, Redini, F, Heymann, D, Layrolle, P & Blanchard, F. (2015). Oncostatin m, an inflammatory cytokine produced by macrophages, supports intramembranous bone healing in a mouse model of tibia injury. *Am J Pathol*, **185**, 765-775.

109. Guyon, A, Skrzydelski, D, De, G, I, Rovere, C, Conductier, G, Trocello, JM, Dauge, V, Kitabgi, P, Rostene, W, Nahon, JL & Melik, PS. (2009). Long term exposure to the chemokine CCL2 activates the nigrostriatal dopamine system: a novel mechanism for the control of dopamine release. *Neuroscience*, **162**, 1072-1080.

110. Ha, J, Choi, HS, Lee, Y, Kwon, HJ, Song, YW & Kim, HH. (2010). CXC chemokine ligand 2 induced by receptor activator of NF-kappa B ligand enhances osteoclastogenesis. *J Immunol*, **184**, 4717-4724.

111. Ha, J, Lee, Y & Kim, HH. (2011). CXCL2 mediates lipopolysaccharide-induced osteoclastogenesis in RANKL-primed precursors. *Cytokine*, **55**, 48-55.

112. Haas, S, Capellino, S, Phan, NQ, Bohm, M, Luger, TA, Straub, RH & Stander, S. (2010). Low density of sympathetic nerve fibers relative to substance P-positive nerve fibers in lesional skin of chronic pruritus and prurigo nodularis. *J Dermatol Sci*, **58**, 193-197.

113. Habecker, BA & Landis, SC. (1994). Noradrenergic regulation of cholinergic differentiation. *Science*, **264**, 1602-1604.

114. Habecker, BA, Pennica, D & Landis, SC. (1995). Cardiotrophin-1 is not the sweat gland-derived differentiation factor. *Neuroreport*, **7**, 41-44.

115. Habecker, BA, Symes, AJ, Stahl, N, Francis, NJ, Economides, A, Fink, JS, Yancopoulos, GD & Landis, SC. (1997). A sweat gland-derived differentiation activity acts through known cytokine signaling pathways. *J Biol Chem*, **272**, 30421-30428.

116. Hanani, M. (2010). Satellite glial cells in sympathetic and parasympathetic ganglia: in search of function. *Brain Res Rev*, **64**, 304-327.

117. Haringman, JJ, Smeets, TJ, Reinders-Blankert, P & Tak, PP. (2006). Chemokine and chemokine receptor expression in paired peripheral blood mononuclear cells and synovial tissue of patients with rheumatoid arthritis, osteoarthritis, and reactive arthritis. *Ann Rheum Dis*, **65**, 294-300.

118. Harle, P, Mobius, D, Carr, DJ, Scholmerich, J & Straub, RH. (2005). An opposing time-dependent immune-modulating effect of the sympathetic nervous system conferred by altering the cytokine profile in the local lymph nodes and spleen of mice with type II collagen-induced arthritis. *Arthritis Rheum*, **52**, 1305-1313.

119. Harle, P, Pongratz, G, Albrecht, J, Tarner, IH & Straub, RH. (2008). An early sympathetic nervous system influence exacerbates collagen-induced arthritis via CD4+CD25+ cells. *Arthritis Rheum*, **58**, 2347-2355.

120. Haynie, DT. (2014). Molecular physiology of the tensin brotherhood of integrin adaptor proteins. *Proteins*, **82**, 1113-1127.

121. Haywood, L & Walsh, DA. (2001). Vasculature of the normal and arthritic synovial joint. *Histol Histopathol*, **16**, 277-284.

122. Hendry, IA, Hill, CE & McLennan, IS. (1987). RU38486 blocks the steroid regulation of transmitter choice in cultured rat sympathetic ganglia. *Brain Res*, **402**, 264-268.

123. Herman, S, Kronke, G & Schett, G. (2008a). Molecular mechanisms of inflammatory bone damage: emerging targets for therapy. *Trends Mol Med*, **14**, 245-253.

124. Herman, S, Muller, RB, Kronke, G, Zwerina, J, Redlich, K, Hueber, AJ, Gelse, H, Neumann, E, Muller-Ladner, U & Schett, G. (2008b). Induction of osteoclast-associated receptor, a key osteoclast costimulation molecule, in rheumatoid arthritis. *Arthritis Rheum*, **58**, 3041-3050.

125. Heymann, D & Rousselle, AV. (2000). gp130 Cytokine family and bone cells. *Cytokine*, **12**, 1455-1468.

126. Hill, EL & Elde, R. (1991). Distribution of CGRP-, VIP-, D beta H-, SP-, and NPY-immunoreactive nerves in the periosteum of the rat. *Cell Tissue Res*, **264**, 469-480.

127. Hill, PA, Murphy, G, Docherty, AJ, Hembry, RM, Millican, TA, Reynolds, JJ & Meikle, MC. (1994). The effects of selective inhibitors of matrix metalloproteinases (MMPs) on bone resorption and the identification of MMPs and TIMP-1 in isolated osteoclasts. *J Cell Sci*, **107**, 3055-3064.

128. Hiltunen, PH & Airaksinen, MS. (2004). Sympathetic cholinergic target innervation requires GDNF family receptor GFR alpha 2. *Mol Cell Neurosci*, **26**, 450-457.

129. Hiura, K, Lim, SS, Little, SP, Lin, S & Sato, M. (1995). Differentiation dependent expression of tensin and cortactin in chicken osteoclasts. *Cell Motil Cytoskeleton*, **30**, 272-284.

130. Hohmann, EL, Elde, RP, Rysavy, JA, Einzig, S & Gebhard, RL. (1986). Innervation of periosteum and bone by sympathetic vasoactive intestinal peptide-containing nerve fibers. *Science*, **232**, 868-871.

131. Hui, W, Bell, M & Carroll, G. (1997). Detection of oncostatin M in synovial fluid from patients with rheumatoid arthritis. *Ann Rheum Dis*, **56**, 184-187.

132. Hui, W, Rowan, AD, Richards, CD & Cawston, TE. (2003). Oncostatin M in combination with tumor necrosis factor alpha induces cartilage damage and matrix metalloproteinase expression in vitro and in vivo. *Arthritis Rheum*, **48**, 3404-3418.

133. Hukkanen, M, Gronblad, M, Rees, R, Kottinen, YT, Gibson, SJ, Hietanen, J, Polak, JM & Brewerton, DA. (1991). Regional distribution of mast cells and peptide containing nerves in normal and adjuvant arthritic rat synovium. *J Rheumatol*, **18**, 177-183.

134. Huston, JP, Weth, K, De Souza, SA, Junghans, U, Muller, HW & Hasenohrl, RU. (2000). Facilitation of learning and long-term ventral pallidal-cortical cholinergic activation by proteoglycan biglycan and chondroitin sulfate C. *Neuroscience*, **100**, 355-361.

135. Imai, S & Matsusue, Y. (2002). Neuronal regulation of bone metabolism and anabolism: calcitonin gene-related peptide-, substance P-, and tyrosine hydroxylase-containing nerves and the bone. *Microsc Res Tech*, **58**, 61-69.

136. Inglis, JJ, Simelyte, E, McCann, FE, Criado, G & Williams, RO. (2008). Protocol for the induction of arthritis in C57BL/6 mice. *Nat Protoc*, **3**, 612-618.

137. Jacobs, JP, Ortiz-Lopez, A, Campbell, JJ, Gerard, CJ, Mathis, D & Benoist, C. (2010). Deficiency of CXCR2, but not other chemokine receptors, attenuates autoantibody-mediated arthritis in a murine model. *Arthritis Rheum*, **62**, 1921-1932.

138. Jenei-Lanzl, Z, Capellino, S, Kees, F, Fleck, M, Lowin, T & Straub, RH. (2015). Anti-inflammatory effects of cell-based therapy with tyrosine hydroxylase-positive catecholaminergic cells in experimental arthritis. *Ann Rheum Dis*, **74**, 444-451.

139. Jessen, KR. (2004). Glial cells. *Int J Biochem Cell Biol*, **36**, 1861-1867.

140. Jimenez-Andrade, JM & Mantyh, PW. (2012). Sensory and sympathetic nerve fibers undergo sprouting and neuroma formation in the painful arthritic joint of geriatric mice. *Arthritis Res Ther*, **14**, R101.

141. Joester, A & Faissner, A. (2001). The structure and function of tenascins in the nervous system. *Matrix Biol*, **20**, 13-22.

142. Jung, H, Toth, PT, White, FA & Miller, RJ. (2008). Monocyte chemoattractant protein-1 functions as a neuromodulator in dorsal root ganglia neurons. *J Neurochem*, **104**, 254-263.

143. Kanazawa, H, Ieda, M, Kimura, K, Arai, T, Kawaguchi-Manabe, H, Matsuhashi, T, Endo, J, Sano, M, Kawakami, T, Kimura, T, Monkawa, T, Hayashi, M, Iwanami, A, Okano, H, Okada, Y,

Ishibashi-Ueda, H, Ogawa, S & Fukuda, K. (2010). Heart failure causes cholinergic transdifferentiation of cardiac sympathetic nerves via gp130-signaling cytokines in rodents. *J Clin Invest*, **120**, 408-421.

144. Kanno, M, Suzuki, S, Fujiwara, T, Yokoyama, A, Sakamoto, A, Takahashi, H, Imai, Y & Tanaka, J. (2005). Functional expression of CCL6 by rat microglia: a possible role of CCL6 in cell-cell communication. *J Neuroimmunol*, **167**, 72-80.

145. Kapoor, M, Martel-Pelletier, J, Lajeunesse, D, Pelletier, JP & Fahmi, H. (2011). Role of proinflammatory cytokines in the pathophysiology of osteoarthritis. *Nat Rev Rheumatol*, **7**, 33-42.

146. Kawanami, A, Matsushita, T, Chan, YY & Murakami, S. (2009). Mice expressing GFP and CreER in osteochondro progenitor cells in the periosteum. *Biochem Biophys Res Commun*, **386**, 477-482.

147. Kawashima, K & Fujii, T. (2000). Extraneuronal cholinergic system in lymphocytes. *Pharmacol Ther*, **86**, 29-48.

148. Kawashima, K & Fujii, T. (2003). The lymphocytic cholinergic system and its biological function. *Life Sci*, **72**, 2101-2109.

149. Kawashima, K & Fujii, T. (2004). Expression of non-neuronal acetylcholine in lymphocytes and its contribution to the regulation of immune function. *Front Biosci*, **9**, 2063-2085.

150. Kawashima, K, Fujii, T, Moriwaki, Y & Misawa, H. (2012). Critical roles of acetylcholine and the muscarinic and nicotinic acetylcholine receptors in the regulation of immune function. *Life Sci*, **91**, 1027-1032.

151. Keyszer, G, Langer, T, Kornhuber, M, Taute, B & Horneff, G. (2004). Neurovascular mechanisms as a possible cause of remission of rheumatoid arthritis in hemiparetic limbs. *Ann Rheum Dis*, **63**, 1349-1351.

152. Kiefer, R, Kieseier, BC, Stoll, G & Hartung, HP. (2001). The role of macrophages in immune-mediated damage to the peripheral nervous system. *Prog Neurobiol*, **64**, 109-127.

153. Kii, I, Nishiyama, T, Li, M, Matsumoto, K, Saito, M, Amizuka, N & Kudo, A. (2010). Incorporation of tenascin-C into the extracellular matrix by periostin underlies an extracellular meshwork architecture. *J Biol Chem*, **285**, 2028-2039.

154. Kim, MH, Park, M, Baek, SH, Kim, HJ & Kim, SH. (2011). Molecules and signaling pathways involved in the expression of OC-STAMP during osteoclastogenesis. *Amino Acids*, **40**, 1447-1459.

155. Kimura, K, Ieda, M & Fukuda, K. (2012). Development, maturation, and transdifferentiation of cardiac sympathetic nerves. *Circ Res*, **110**, 325-336.

156. Kleyer, A & Schett, G. (2014). Arthritis and bone loss: a hen and egg story. *Curr Opin Rheumatol*, **26**, 80-84.

157. Koeck, FX, Bobrik, V, Fassold, A, Grifka, J, Kessler, S & Straub, RH. (2009). Marked loss of sympathetic nerve fibers in chronic Charcot foot of diabetic origin compared to ankle joint osteoarthritis. *J Orthop Res*, **27**, 736-741.

158. Kojima, T, Yamaguchi, M & Kasai, K. (2006). Substance P stimulates release of RANKL via COX-2 expression in human dental pulp cells. *Inflamm Res*, **55**, 78-84.

159. Konttinen, YT, Rees, R, Hukkanen, M, Gronblad, M, Tolvanen, E, Gibson, SJ, Polak, JM & Brewerton, DA. (1990). Nerves in inflammatory synovium: immunohistochemical observations on the adjuvant arthritis rat model. *J Rheumatol*, **17**, 1586-1591.

160. Koopman, FA, Schuurman, PR, Vervoordeldonk, MJ & Tak, PP. (2014). Vagus nerve stimulation: a new bioelectronics approach to treat rheumatoid arthritis? *Best Pract Res Clin Rheumatol*, **28**, 625-635.

161. Koopman, FA, Stoof, SP, Straub, RH, van Maanen, MA, Vervoordeldonk, MJ & Tak, PP. (2011). Restoring the balance of the autonomic nervous system as an innovative approach to the treatment of rheumatoid arthritis. *Mol Med*, **17**, 937-948.

162. Korb-Pap, A, Stratis, A, Muhlenberg, K, Niederreiter, B, Hayer, S, Echtermeyer, F, Stange, R, Zwerina, J, Pap, T, Pavenstadt, H, Schett, G, Smolen, JS & Redlich, K. (2012). Early structural changes in cartilage and bone are required for the attachment and invasion of inflamed synovial tissue during destructive inflammatory arthritis. *Ann Rheum Dis*, **71**, 1004-1011.

163. Kraal, G, van der Laan, LJ, Elomaa, O & Tryggvason, K. (2000). The macrophage receptor MARCO. *Microbes Infect*, **2**, 313-316.

164. Kudo, A. (2011). Periostin in fibrillogenesis for tissue regeneration: periostin actions inside and outside the cell. *Cell Mol Life Sci*, **68**, 3201-3207.

165. Kwan, TS, Padrines, M, Theoleyre, S, Heymann, D & Fortun, Y. (2004). IL-6, RANKL, TNF-alpha/IL-1: interrelations in bone resorption pathophysiology. *Cytokine Growth Factor Rev*, **15**, 49-60.

166. Landis, SC. (1996). The development of cholinergic sympathetic neurons: a role for neuropoietic cytokines? *Perspect Dev Neurobiol*, **4**, 53-63.

167. Landis, SC & Keefe, D. (1983). Evidence for neurotransmitter plasticity in vivo: developmental changes in properties of cholinergic sympathetic neurons. *Dev Biol*, **98**, 349-372.

168. Landis, SC, Siegel, RE & Schwab, M. (1988). Evidence for neurotransmitter plasticity in vivo. II. Immunocytochemical studies of rat sweat gland innervation during development. *Dev Biol*, **126**, 129-140.

169. Langdon, C, Kerr, C, Hassen, M, Hara, T, Arsenault, AL & Richards, CD. (2000). Murine oncostatin M stimulates mouse synovial fibroblasts in vitro and induces inflammation and destruction in mouse joints in vivo. *Am J Pathol*, **157**, 1187-1196.

170. Laurenzi, MA, Persson, MA, Dalsgaard, CJ & Ringden, O. (1989). Stimulation of human B lymphocyte differentiation by the neuropeptides substance P and neurokinin A. *Scand J Immunol*, **30**, 695-701.

171. Lawal, HO & Krantz, DE. (2013). SLC18: Vesicular neurotransmitter transporters for monoamines and acetylcholine. *Mol Aspects Med*, **34**, 360-372.

172. Lebre, MC, Vergunst, CE, Choi, IY, Aarrass, S, Oliveira, AS, Wyant, T, Horuk, R, Reedquist, KA & Tak, PP. (2011). Why CCR2 and CCR5 blockade failed and why CCR1 blockade might still be effective in the treatment of rheumatoid arthritis. *PLoS One*, **6**, e21772.

173. Lee, JE, Shin, HH, Lee, EA, Van, PT & Choi, HS. (2007). Stimulation of osteoclastogenesis by enhanced levels of MIP-1alpha in BALB/c mice in vitro. *Exp Hematol*, **35**, 1100-1108.

174. Lehner, B, Koeck, FX, Capellino, S, Schubert, TE, Hofbauer, R & Straub, RH. (2008). Preponderance of sensory versus sympathetic nerve fibers and increased cellularity in the infrapatellar fat pad in anterior knee pain patients after primary arthroplasty. *J Orthop Res*, **26**, 342-350.

175. Lemons, ML, Barua, S, Abanto, ML, Halfter, W & Condic, ML. (2005). Adaptation of sensory neurons to hyalectin and decorin proteoglycans. *J Neurosci*, **25**, 4964-4973.

176. Lerner, UH & Persson, E. (2008). Osteotropic effects by the neuropeptides calcitonin gene-related peptide, substance P and vasoactive intestinal peptide. *J Musculoskelet Neuronal Interact*, **8**, 154-165.

177. Levi-Montalcini, R. (1952). Effects of mouse tumor transplantation on the nervous system. *Ann N Y Acad Sci*, **55**, 330-344.

178. Levick, JR. (1995). Microvascular architecture and exchange in synovial joints. *Microcirculation*, **2**, 217-233.

179. Levine, JD, Goetzl, EJ & Basbaum, AI. (1987). Contribution of the nervous system to the pathophysiology of rheumatoid arthritis and other polyarthritides. *Rheum Dis Clin North Am*, **13**, 369-383.

180. Levine, YA, Koopman, FA, Faltys, M, Caravaca, A, Bendele, A, Zitnik, R, Vervoordeldonk, MJ & Tak, PP. (2014). Neurostimulation of the cholinergic anti-inflammatory pathway ameliorates disease in rat collagen-induced arthritis. *PLoS One*, **9**, e104530.

181. Levy, S & Shoham, T. (2005a). Protein-protein interactions in the tetraspanin web. *Physiology (Bethesda)*, **20**, 218-224.

182. Levy, S & Shoham, T. (2005b). The tetraspanin web modulates immune-signalling complexes. *Nat Rev Immunol*, **5**, 136-148.

183. Li, X, Udagawa, N, Takami, M, Sato, N, Kobayashi, Y & Takahashi, N. (2003). p38 Mitogen-activated protein kinase is crucially involved in osteoclast differentiation but not in cytokine production, phagocytosis, or dendritic cell differentiation of bone marrow macrophages. *Endocrinology*, **144**, 4999-5005.

184. Lips, KS, Kauschke, V, Hartmann, S, Thormann, U, Ray, S, Schumacher, M, Gelinsky, M, Heinemann, S, Hanke, T, Kautz, AR, Schnabelrauch, M, Szalay, G, Heiss, C, Schnettler, R, Alt, V & Kilian, O. (2014). Cholinergic nerve fibers in bone defects of a rat osteoporosis model and their regulation by implantation of bone substitution materials. *J Musculoskelet Neuronal Interact*, **14**, 173-188.

185. Lipsky, PE. (2009). Are new agents needed to treat RA? *Nat Rev Rheumatol*, **5**, 521-522.

186. Loeser, RF, Olex, AL, McNulty, MA, Carlson, CS, Callahan, MF, Ferguson, CM, Chou, J, Leng, X & Fetrow, JS. (2012). Microarray analysis reveals age-related differences in gene expression during the development of osteoarthritis in mice. *Arthritis Rheum*, **64**, 705-717.

187. Longo, G, Osikowicz, M & Ribeiro-da-Silva, A. (2013). Sympathetic fiber sprouting in inflamed joints and adjacent skin contributes to pain-related behavior in arthritis. *J Neurosci*, **33**, 10066-10074.

188. Longobardi, L, Li, T, Myers, TJ, O'Rear, L, Ozkan, H, Li, Y, Contaldo, C & Spagnoli, A. (2012). TGF-beta type II receptor/MCP-5 axis: at the crossroad between joint and growth plate development. *Dev Cell*, **23**, 71-81.

189. Lorton, D, Lubahn, C, Engan, C, Schaller, J, Felten, DL & Bellinger, DL. (2000). Local application of capsaicin into the draining lymph nodes attenuates expression of adjuvant-induced arthritis. *Neuroimmunomodulation*, **7**, 115-125.

190. Lorton, D, Lubahn, C, Lindquist, CA, Schaller, J, Washington, C & Bellinger, DL. (2005). Changes in the density and distribution of sympathetic nerves in spleens from Lewis rats with adjuvant-induced arthritis suggest that an injury and sprouting response occurs. *J Comp Neurol*, **489**, 260-273.

191. Lorton, D, Lubahn, C, Sweeney, S, Major, A, Lindquist, CA, Schaller, J, Washington, C & Bellinger, DL. (2009). Differences in the injury/sprouting response of splenic noradrenergic nerves in Lewis rats with adjuvant-induced arthritis compared with rats treated with 6-hydroxydopamine. *Brain Behav Immun*, **23**, 276-285.

192. Lotz, M, Moats, T & Villiger, PM. (1992). Leukemia inhibitory factor is expressed in cartilage and synovium and can contribute to the pathogenesis of arthritis. *J Clin Invest*, **90**, 888-896.

193. Lowin, T & Straub, RH. (2011). Integrins and their ligands in rheumatoid arthritis. *Arthritis Res Ther*, **13**, 244.

194. Loy, B, Apostolova, G, Dorn, R, McGuire, VA, Arthur, JS & Dechant, G. (2011). p38alpha and p38beta mitogen-activated protein kinases determine cholinergic transdifferentiation of sympathetic neurons. *J Neurosci*, **31**, 12059-12067.

195. Lukas, RJ, Changeux, JP, Le, NN, Albuquerque, EX, Balfour, DJ, Berg, DK, Bertrand, D, Chiappinelli, VA, Clarke, PB, Collins, AC, Dani, JA, Grady, SR, Kellar, KJ, Lindstrom, JM, Marks, MJ, Quik, M, Taylor, PW & Wonnacott, S. (1999). International Union of Pharmacology. XX. Current status of the nomenclature for nicotinic acetylcholine receptors and their subunits. *Pharmacol Rev*, **51**, 397-401.

196. Lundberg, P, Bostrom, I, Mukohyama, H, Bjurholm, A, Smans, K & Lerner, UH. (1999). Neuro-hormonal control of bone metabolism: vasoactive intestinal peptide stimulates alkaline phosphatase activity and mRNA expression in mouse calvarial osteoblasts as well as calcium accumulation mineralized bone nodules. *Regul Pept*, **85**, 47-58.

197. Ma, CH, Bampton, ET, Evans, MJ & Taylor, JS. (2010). Synergistic effects of osteonectin and brain-derived neurotrophic factor on axotomized retinal ganglion cells neurite outgrowth via the mitogen-activated protein kinase-extracellular signal-regulated kinase 1/2 pathways. *Neuroscience*, **165**, 463-474.

198. Martelli, D, McKinley, MJ & McAllen, RM. (2014a). The cholinergic anti-inflammatory pathway: a critical review. *Auton Neurosci*, **182**, 65-69.

199. Martelli, D, Yao, ST, McKinley, MJ & McAllen, RM. (2014b). Reflex control of inflammation by sympathetic nerves, not the vagus. *J Physiol*, **592**, 1677-1686.

200. Mattey, DL, Nixon, NB & Dawes, PT. (2012). Association of circulating levels of MMP-8 with mortality from respiratory disease in patients with rheumatoid arthritis. *Arthritis Res Ther*, **14**, R204.

201. McCann, FE, Palfreeman, AC, Andrews, M, Perocheau, DP, Inglis, JJ, Schafer, P, Feldmann, M, Williams, RO & Brennan, FM. (2010). Apremilast, a novel PDE4 inhibitor, inhibits spontaneous production of tumour necrosis factor-alpha from human rheumatoid synovial cells and ameliorates experimental arthritis. *Arthritis Res Ther*, **12**, R107.

202. McCurdy, S, Baicu, CF, Heymans, S & Bradshaw, AD. (2010). Cardiac extracellular matrix remodeling: fibrillar collagens and Secreted Protein Acidic and Rich in Cysteine (SPARC). *J Mol Cell Cardiol*, **48**, 544-549.

203. McInnes, IB & O'Dell, JR. (2010). State-of-the-art: rheumatoid arthritis. *Ann Rheum Dis*, **69**, 1898-1906.

204. McInnes, IB & Schett, G. (2007). Cytokines in the pathogenesis of rheumatoid arthritis. *Nat Rev Immunol*, **7**, 429-442.

205. McInnes, IB & Schett, G. (2011). The pathogenesis of rheumatoid arthritis. *N Engl J Med*, **365**, 2205-2219.

206. McLennan, IS, Hill, CE & Hendry, IA. (1980). Glucocorticosteroids modulate transmitter choice in developing superior cervical ganglion. *Nature*, **283**, 206-207.

207. McLennan, IS, Hill, CE & Hendry, IA. (1984). Pharmacology of the steroid regulation of transmitter choice in cultured rat sympathetic ganglia. *Aust J Exp Biol Med Sci*, **62**, 627-639.

208. McQueen, F & Naredo, E. (2011). The 'disconnect' between synovitis and erosion in rheumatoid arthritis: a result of treatment or intrinsic to the disease process itself? *Ann Rheum Dis*, **70**, 241-244.

209. Meek, RL, Eriksen, N & Benditt, EP. (1992). Murine serum amyloid A3 is a high density apolipoprotein and is secreted by macrophages. *Proc Natl Acad Sci U S A*, **89**, 7949-7952.

210. Meheus, LA, Fransen, LM, Raymackers, JG, Blockx, HA, Van Beeumen, JJ, Van Bun, SM & Van, d, V. (1993). Identification by microsequencing of lipopolysaccharide-induced proteins secreted by mouse macrophages. *J Immunol*, **151**, 1535-1547.

211. Mei, Q, Mundinger, TO, Lernmark, A & Taborsky, GJ, Jr. (2002). Early, selective, and marked loss of sympathetic nerves from the islets of BioBreeder diabetic rats. *Diabetes*, **51**, 2997-3002.

212. Melik-Parsadaniantz, S & Rostene, W. (2008). Chemokines and neuromodulation. *J Neuroimmunol*, **198**, 62-68.

213. Merle, B, Bouet, G, Rousseau, JC, Bertholon, C & Garnero, P. (2014). Periostin and transforming growth factor beta-induced protein (TGFbetaIp) are both expressed by osteoblasts and osteoclasts. *Cell Biol Int*, **38**, 398-404.

214. Miller, LE, Grifka, J, Scholmerich, J & Straub, RH. (2002). Norepinephrine from synovial tyrosine hydroxylase positive cells is a strong indicator of synovial inflammation in rheumatoid arthritis. *J Rheumatol*, **29**, 427-435.

215. Miller, LE, Justen, HP, Scholmerich, J & Straub, RH. (2000). The loss of sympathetic nerve fibers in the synovial tissue of patients with rheumatoid arthritis is accompanied by increased norepinephrine release from synovial macrophages. *FASEB J*, **14**, 2097-2107.

216. Miller, LE, Weidler, C, Falk, W, Angele, P, Schaumburger, J, Scholmerich, J & Straub, RH. (2004). Increased prevalence of semaphorin 3C, a repellent of sympathetic nerve fibers, in the synovial tissue of patients with rheumatoid arthritis. *Arthritis Rheum*, **50**, 1156-1163.

217. Milting, H, Ellinghaus, P, Seewald, M, Cakar, H, Bohms, B, Kassner, A, Korfer, R, Klein, M, Krahn, T, Kruska, L, El, BA & Kramer, F. (2008). Plasma biomarkers of myocardial fibrosis and remodeling in terminal heart failure patients supported by mechanical circulatory support devices. *J Heart Lung Transplant*, **27**, 589-596.

218. Miyamoto, H, Suzuki, T, Miyauchi, Y, Iwasaki, R, Kobayashi, T, Sato, Y, Miyamoto, K, Hoshi, H, Hashimoto, K, Yoshida, S, Hao, W, Mori, T, Kanagawa, H, Katsuyama, E, Fujie, A, Morioka, H, Matsumoto, M, Chiba, K, Takeya, M, Toyama, Y & Miyamoto, T. (2012). Osteoclast stimulatory transmembrane protein and dendritic cell-specific transmembrane protein cooperatively modulate cell-cell fusion to form osteoclasts and foreign body giant cells. *J Bone Miner Res*, **27**, 1289-1297.

219. Miyato, H, Kitayama, J, Ishigami, H, Kaisaki, S & Nagawa, H. (2011). Loss of sympathetic nerve fibers around intratumoral arterioles reflects malignant potential of gastric cancer. *Ann Surg Oncol*, **18**, 2281-2288.

220. Mojsilovic-Petrovic, J, Callaghan, D, Cui, H, Dean, C, Stanimirovic, DB & Zhang, W. (2007). Hypoxia-inducible factor-1 (HIF-1) is involved in the regulation of hypoxia-stimulated expression of monocyte chemoattractant protein-1 (MCP-1/CCL2) and MCP-5 (Ccl12) in astrocytes. *J Neuroinflammation*, **4**, 12.

221. Moore, CS & Crocker, SJ. (2012). An alternate perspective on the roles of TIMPs and MMPs in pathology. *Am J Pathol*, **180**, 12-16.

222. Moore, CS, Milner, R, Nishiyama, A, Frausto, RF, Serwanski, DR, Pagarigan, RR, Whitton, JL, Miller, RH & Crocker, SJ. (2011). Astrocytic tissue inhibitor of metalloproteinase-1 (TIMP-1) promotes oligodendrocyte differentiation and enhances CNS myelination. *J Neurosci*, **31**, 6247-6254.

223. Moore, NH, Costa, LG, Shaffer, SA, Goodlett, DR & Guizzetti, M. (2009). Shotgun proteomics implicates extracellular matrix proteins and protease systems in neuronal development induced by astrocyte cholinergic stimulation. *J Neurochem*, **108**, 891-908.

224. Moran, EM, Mullan, R, McCormick, J, Connolly, M, Sullivan, O, Fitzgerald, O, Bresnihan, B, Veale, DJ & Fearon, U. (2009). Human rheumatoid arthritis tissue production of IL-17A drives matrix and cartilage degradation: synergy with tumour necrosis factor-alpha, Oncostatin M and response to biologic therapies. *Arthritis Res Ther*, **11**, R113.

225. Morrison, NA, Day, CJ & Nicholson, GC. (2014). Dominant negative MCP-1 blocks human osteoclast differentiation. *J Cell Biochem*, **115**, 303-312.

226. Nakashima, A. (2012). Proteasomal degradation of tyrosine hydroxylase and neurodegeneration. *J Neurochem*, **120**, 199-201.

227. Nance, DM & Sanders, VM. (2007). Autonomic innervation and regulation of the immune system (1987-2007). *Brain Behav Immun*, **21**, 736-745.

228. Nastase, MV, Young, MF & Schaefer, L. (2012). Biglycan: a multivalent proteoglycan providing structure and signals. *J Histochem Cytochem*, **60**, 963-975.

229. Nemeth, K, Schoppet, M, Al-Fakhri, N, Helas, S, Jessberger, R, Hofbauer, LC & Goettsch, C. (2011). The role of osteoclast-associated receptor in osteoimmunology. *J Immunol*, **186**, 13-18.

230. Nozawa, K, Fujishiro, M, Kawasaki, M, Kaneko, H, Iwabuchi, K, Yanagida, M, Suzuki, F, Miyazawa, K, Takasaki, Y, Ogawa, H, Takamori, K & Sekigawa, I. (2009). Connective tissue growth factor promotes articular damage by increased osteoclastogenesis in patients with rheumatoid arthritis. *Arthritis Res Ther*, **11**, R174.

231. O'Hara, R, Murphy, EP, Whitehead, AS, Fitzgerald, O & Bresnihan, B. (2004). Local expression of the serum amyloid A and formyl peptide receptor-like 1 genes in synovial tissue is associated with matrix metalloproteinase production in patients with inflammatory arthritis. *Arthritis Rheum*, **50**, 1788-1799.

232. Oba, Y, Lee, JW, Ehrlich, LA, Chung, HY, Jelinek, DF, Callander, NS, Horuk, R, Choi, SJ & Roodman, GD. (2005). MIP-1alpha utilizes both CCR1 and CCR5 to induce osteoclast formation and increase adhesion of myeloma cells to marrow stromal cells. *Exp Hematol*, **33**, 272-278.

233. Obata, K, Furuno, T, Nakanishi, M & Togari, A. (2007). Direct neurite-osteoblastic cell communication, as demonstrated by use of an in vitro co-culture system. *FEBS Lett*, **581**, 5917-5922.

234. Orlofsky, A, Lin, EY & Prystowsky, MB. (1994). Selective induction of the beta chemokine C10 by IL-4 in mouse macrophages. *J Immunol*, **152**, 5084-5091.

235. Ota, K, Quint, P, Weivoda, MM, Ruan, M, Pederson, L, Westendorf, JJ, Khosla, S & Oursler, MJ. (2013). Transforming growth factor beta 1 induces CXCL16 and leukemia inhibitory factor expression in osteoclasts to modulate migration of osteoblast progenitors. *Bone*, **57**, 68-75.

236. Page, TH, Charles, PJ, Piccinini, AM, Nicolaidou, V, Taylor, PC & Midwood, KS. (2012). Raised circulating tenascin-C in rheumatoid arthritis. *Arthritis Res Ther*, **14**, R260.

237. Palmqvist, P, Persson, E, Conaway, HH & Lerner, UH. (2002). IL-6, leukemia inhibitory factor, and oncostatin M stimulate bone resorption and regulate the expression of receptor activator of NF-kappa B ligand, osteoprotegerin, and receptor activator of NF-kappa B in mouse calvariae. *J Immunol*, **169**, 3353-3362.

238. Parrish, DC, Alston, EN, Rohrer, H, Nkadi, P, Woodward, WR, Schutz, G & Habecker, BA. (2010). Infarction-induced cytokines cause local depletion of tyrosine hydroxylase in cardiac sympathetic nerves. *Exp Physiol*, **95**, 304-314.

239. Pasterkamp, RJ. (2012). Getting neural circuits into shape with semaphorins. *Nat Rev Neurosci*, **13**, 605-618.

240. Payan, DG, Brewster, DR & Goetzl, EJ. (1983). Specific stimulation of human T lymphocytes by substance P. *J Immunol*, **131**, 1613-1615.

241. Persson, E & Lerner, UH. (2011). The neuropeptide VIP regulates the expression of osteoclastogenic factors in osteoblasts. *J Cell Biochem*, **112**, 3732-3741.

242. Pincus, T, Yazici, Y, Sokka, T, Aletaha, D & Smolen, JS. (2003). Methotrexate as the "anchor drug" for the treatment of early rheumatoid arthritis. *Clin Exp Rheumatol*, **21**, S179-S185.

243. Pongratz, G, Melzer, M & Straub, RH. (2012). The sympathetic nervous system stimulates anti-inflammatory B cells in collagen-type II-induced arthritis. *Ann Rheum Dis*, **71**, 432-439.

244. Pongratz, G & Straub, RH. (2013). Role of peripheral nerve fibres in acute and chronic inflammation in arthritis. *Nat Rev Rheumatol*, **9**, 117-126.

245. Pozo, D & Delgado, M. (2004). The many faces of VIP in neuroimmunology: a cytokine rather a neuropeptide? *FASEB J*, **18**, 1325-1334.

246. Quinones, MP, Ahuja, SK, Jimenez, F, Schaefer, J, Garavito, E, Rao, A, Chenaux, G, Reddick, RL, Kuziel, WA & Ahuja, SS. (2004). Experimental arthritis in CC chemokine receptor 2-null mice closely mimics severe human rheumatoid arthritis. *J Clin Invest*, **113**, 856-866.

247. Rabquer, BJ & Koch, AE. (2014). Rheumatoid arthritis: Microvascular clues to hemiplegia-induced asymmetric RA. *Nat Rev Rheumatol*, **10**, 701-702.

248. Rampersad, RR, Tarrant, TK, Vallanat, CT, Quintero-Matthews, T, Weeks, MF, Esserman, DA, Clark, J, Di, PF, Patel, DD, Fong, AM & Liu, P. (2011). Enhanced Th17-cell responses render CCR2-deficient mice more susceptible for autoimmune arthritis. *PLoS One*, **6**, e25833.

249. Rao, MS & Landis, SC. (1990). Characterization of a target-derived neuronal cholinergic differentiation factor. *Neuron*, **5**, 899-910.

250. Rao, MS, Sun, Y, Escary, JL, Perreau, J, Tresser, S, Patterson, PH, Zigmond, RE, Brulet, P & Landis, SC. (1993). Leukemia inhibitory factor mediates an injury response but not a target-directed developmental transmitter switch in sympathetic neurons. *Neuron*, **11**, 1175-1185.

251. Rao, MS, Symes, A, Malik, N, Shoyab, M, Fink, JS & Landis, SC. (1992). Oncostatin M regulates VIP expression in a human neuroblastoma cell line. *Neuroreport*, **3**, 865-868.

252. Richards, CD. (2013). The enigmatic cytokine oncostatin m and roles in disease. *ISRN Inflamm*, **2013**, 512103.

253. Richards, CD, Langdon, C, Deschamps, P, Pennica, D & Shaughnessy, SG. (2000). Stimulation of osteoclast differentiation in vitro by mouse oncostatin M, leukaemia inhibitory factor, cardiotrophin-1 and interleukin 6: synergy with dexamethasone. *Cytokine*, **12**, 613-621.

254. Ries, C. (2014). Cytokine functions of TIMP-1. *Cell Mol Life Sci*, **71**, 659-672.

255. Rosas-Ballina, M, Olofsson, PS, Ochani, M, Valdes-Ferrer, SI, Levine, YA, Reardon, C, Tusche, MW, Pavlov, VA, Andersson, U, Chavan, S, Mak, TW & Tracey, KJ. (2011). Acetylcholine-synthesizing T cells relay neural signals in a vagus nerve circuit. *Science*, **334**, 98-101.

256. Rowan, AD, Hui, W, Cawston, TE & Richards, CD. (2003). Adenoviral gene transfer of interleukin-1 in combination with oncostatin M induces significant joint damage in a murine model. *Am J Pathol*, **162**, 1975-1984.

257. Sankala, M, Brannstrom, A, Schulthess, T, Bergmann, U, Morgunova, E, Engel, J, Tryggvason, K & Pikkarainen, T. (2002). Characterization of recombinant soluble macrophage scavenger receptor MARCO. *J Biol Chem*, **277**, 33378-33385.

258. Sarafi, MN, Garcia-Zepeda, EA, MacLean, JA, Charo, IF & Luster, AD. (1997). Murine monocyte chemoattractant protein (MCP)-5: a novel CC chemokine that is a structural and functional homologue of human MCP-1. *J Exp Med*, **185**, 99-109.

259. Schafer, MK, Eiden, LE & Weihe, E. (1998). Cholinergic neurons and terminal fields revealed by immunohistochemistry for the vesicular acetylcholine transporter. II. The peripheral nervous system. *Neuroscience*, **84**, 361-376.

260. Schaible, HG & Straub, RH. (2014). Function of the sympathetic supply in acute and chronic experimental joint inflammation. *Auton Neurosci*, **182**, 55-64.

261. Schellings, MW, Pinto, YM & Heymans, S. (2004). Matricellular proteins in the heart: possible role during stress and remodeling. *Cardiovasc Res*, **64**, 24-31.

262. Scherf, U, Ross, DT, Waltham, M, Smith, LH, Lee, JK, Tanabe, L, Kohn, KW, Reinhold, WC, Myers, TG, Andrews, DT, Scudiero, DA, Eisen, MB, Sausville, EA, Pommier, Y, Botstein, D, Brown, PO & Weinstein, JN. (2000). A gene expression database for the molecular pharmacology of cancer. *Nat Genet*, **24**, 236-244.

263. Schett, G. (2011). Effects of inflammatory and anti-inflammatory cytokines on the bone. *Eur J Clin Invest*, **41**, 1361-1366.

264. Schett, G, Elewaut, D, McInnes, IB, Dayer, JM & Neurath, MF. (2013). How cytokine networks fuel inflammation: Toward a cytokine-based disease taxonomy. *Nat Med*, **19**, 822-824.

265. Schett, G & Firestein, GS. (2010). Mr Outside and Mr Inside: classic and alternative views on the pathogenesis of rheumatoid arthritis. *Ann Rheum Dis*, **69**, 787-789.

266. Schreiber, RC, Krivacic, K, Kirby, B, Vaccariello, SA, Wei, T, Ransohoff, RM & Zigmond, RE. (2001). Monocyte chemoattractant protein (MCP)-1 is rapidly expressed by sympathetic ganglion neurons following axonal injury. *Neuroreport*, **12**, 601-606.

267. Schubert, J, Beckmann, J, Hartmann, S, Morhenn, HG, Szalay, G, Heiss, C, Schnettler, R & Lips, KS. (2012). Expression of the non-neuronal cholinergic system in human knee synovial tissue from patients with rheumatoid arthritis and osteoarthritis. *Life Sci*, **91**, 1048-1052.

268. Schütz, B, von, EJ, Gordes, M, Schafer, MK, Eiden, LE, Monyer, H & Weihe, E. (2008). Sweat gland innervation is pioneered by sympathetic neurons expressing a cholinergic/noradrenergic co-phenotype in the mouse. *Neuroscience*, **156**, 310-318.

269. Schwartz, CM, Tavakoli, T, Jamias, C, Park, SS, Maudsley, S, Martin, B, Phillips, TM, Yao, PJ, Itoh, K, Ma, W, Rao, MS, Arenas, E & Mattson, MP. (2012). Stromal factors SDF1alpha, sFRP1, and VEGFD induce dopaminergic neuron differentiation of human pluripotent stem cells. *J Neurosci Res*, **90**, 1367-1381.

270. Semple, BD, Kossmann, T & Morganti-Kossmann, MC. (2010). Role of chemokines in CNS health and pathology: a focus on the CCL2/CCR2 and CXCL8/CXCR2 networks. *J Cereb Blood Flow Metab*, **30**, 459-473.

271. Shi, X & Habecker, BA. (2012). gp130 cytokines stimulate proteasomal degradation of tyrosine hydroxylase via extracellular signal regulated kinases 1 and 2. *J Neurochem*, **120**, 239-247.

272. Shih, CH, Lacagnina, M, Leuer-Bisciotti, K & Proschel, C. (2014). Astroglial-derived periostin promotes axonal regeneration after spinal cord injury. *J Neurosci*, **34**, 2438-2443.

273. Sims, NA & Johnson, RW. (2012). Leukemia inhibitory factor: a paracrine mediator of bone metabolism. *Growth Factors*, **30**, 76-87.

274. Sims, NA & Walsh, NC. (2010). GP130 cytokines and bone remodelling in health and disease. *BMB Rep*, **43**, 513-523.

275. Sisask, G, Bjurholm, A, Ahmed, M & Kreicbergs, A. (1996). The development of autonomic innervation in bone and joints of the rat. *J Auton Nerv Syst*, **59**, 27-33.

276. Sofroniew, MV, Howe, CL & Mobley, WC. (2001). Nerve growth factor signaling, neuroprotection, and neural repair. *Annu Rev Neurosci*, **24**, 1217-1281.

277. Stangenberg, L, Burzyn, D, Binstadt, BA, Weissleder, R, Mahmood, U, Benoist, C & Mathis, D. (2014). Denervation protects limbs from inflammatory arthritis via an impact on the microvasculature. *Proc Natl Acad Sci U S A*, **111**, 11419-11424.

278. Stangl, H, Springorum, HR, Muschter, D, Grassel, S & Straub, RH. (2015). Catecholaminergic-to-cholinergic transition of sympathetic nerve fibers is stimulated under healthy but not under inflammatory arthritic conditions. *Brain Behav Immun*, **46**, 180-191.

279. Stanke, M, Duong, CV, Pape, M, Geissen, M, Burbach, G, Deller, T, Gascan, H, Otto, C, Parlato, R, Schutz, G & Rohrer, H. (2006). Target-dependent specification of the neurotransmitter phenotype: cholinergic differentiation of sympathetic neurons is mediated in vivo by gp 130 signaling. *Development*, **133**, 141-150.

280. Stanke, M, Geissen, M, Gotz, R, Ernsberger, U & Rohrer, H. (2000). The early expression of VAChT and VIP in mouse sympathetic ganglia is not induced by cytokines acting through LIFRbeta or CNTFRalpha. *Mech Dev*, **91**, 91-96.

281. Stock, AT, Smith, JM & Carbone, FR. (2014). Type I IFN suppresses Cxcr2 driven neutrophil recruitment into the sensory ganglia during viral infection. *J Exp Med*, **211**, 751-759.

282. Straub, RH. (2012). Neuronal Regulation of Inflammation & Related Pain Mechanisms.In *Kelley's Textbook of Rheumatology.* Elsevier, Saunders.

283. Straub, RH. (2014). Interaction of the endocrine system with inflammation: a function of energy and volume regulation. *Arthritis Res Ther*, **16**, 203.

284. Straub, RH, Bijlsma, JW, Masi, A & Cutolo, M. (2013). Role of neuroendocrine and neuroimmune mechanisms in chronic inflammatory rheumatic diseases-The 10-year update. *Semin Arthritis Rheum*, **43**, 392-404.

285. Straub, RH, Grum, F, Strauch, U, Capellino, S, Bataille, F, Bleich, A, Falk, W, Scholmerich, J & Obermeier, F. (2008a). Anti-inflammatory role of sympathetic nerves in chronic intestinal inflammation. *Gut*, **57**, 911-921.

286. Straub, RH, Lowin, T, Klatt, S, Wolff, C & Rauch, L. (2011). Increased density of sympathetic nerve fibers in metabolically activated fat tissue surrounding human synovium and mouse lymph nodes in arthritis. *Arthritis Rheum*, **63**, 3234-3242.

287. Straub, RH, Mayer, M, Kreutz, M, Leeb, S, Scholmerich, J & Falk, W. (2000). Neurotransmitters of the sympathetic nerve terminal are powerful chemoattractants for monocytes. *J Leukoc Biol*, **67**, 553-558.

288. Straub, RH, Rauch, L, Fassold, A, Lowin, T & Pongratz, G. (2008b). Neuronally released sympathetic neurotransmitters stimulate splenic interferon-gamma secretion from T cells in early type II collagen-induced arthritis. *Arthritis Rheum*, **58**, 3450-3460.

289. Suga, S, Goto, S & Togari, A. (2010). Demonstration of direct neurite-osteoclastic cell communication in vitro via the adrenergic receptor. *J Pharmacol Sci*, **112**, 184-191.

290. Suzuki, A, Palmer, G, Bonjour, JP & Caverzasio, J. (1998). Catecholamines stimulate the proliferation and alkaline phosphatase activity of MC3T3-E1 osteoblast-like cells. *Bone*, **23**, 197-203.

291. Takeshita, S, Kaji, K & Kudo, A. (2000). Identification and characterization of the new osteoclast progenitor with macrophage phenotypes being able to differentiate into mature osteoclasts. *J Bone Miner Res*, **15**, 1477-1488.

292. Tanaka, S, Toki, T, Akimoto, T & Morishita, K. (2013). Lipopolysaccharide accelerates collagen-induced arthritis in association with rapid and continuous production of inflammatory mediators and anti-type II collagen antibody. *Microbiol Immunol*, **57**, 445-454.

293. Tchetverikov, I, Ronday, HK, Van, EB, Kiers, GH, Verzijl, N, TeKoppele, JM, Huizinga, TW, DeGroot, J & Hanemaaijer, R. (2004). MMP profile in paired serum and synovial fluid samples of patients with rheumatoid arthritis. *Ann Rheum Dis*, **63**, 881-883.

294. Tekin, I, Roskoski, R, Jr., Carkaci-Salli, N & Vrana, KE. (2014). Complex molecular regulation of tyrosine hydroxylase. *J Neural Transm*, **121**, 1451-1481.

295. Thaler, R, Sturmlechner, I, Spitzer, S, Riester, SM, Rumpler, M, Zwerina, J, Klaushofer, K, van Wijnen, AJ & Varga, F. (2014). Acute-phase protein serum amyloid A3 is a novel paracrine coupling factor that controls bone homeostasis. *FASEB J*, **29**, 1344-1359.

296. Tian, H, Habecker, B, Guidry, G, Gurtan, A, Rios, M, Roffler-Tarlov, S & Landis, SC. (2000). Catecholamines are required for the acquisition of secretory responsiveness by sweat glands. *J Neurosci*, **20**, 7362-7369.

297. Togari, A & Arai, M. (2008). Pharmacological topics of bone metabolism: the physiological function of the sympathetic nervous system in modulating bone resorption. *J Pharmacol Sci*, **106**, 542-546.

298. Tsoutsman, T, Wang, X, Garchow, K, Riser, B, Twigg, S & Semsarian, C. (2013). CCN2 plays a key role in extracellular matrix gene expression in severe hypertrophic cardiomyopathy and heart failure. *J Mol Cell Cardiol*, **62**, 164-178.

299. Tsuchida, AI, Beekhuizen, M, 't Hart, MC, Radstake, TR, Dhert, WJ, Saris, DB, van Osch, GJ & Creemers, LB. (2014). Cytokine profiles in the joint depend on pathology, but are different between synovial fluid, cartilage tissue and cultured chondrocytes. *Arthritis Res Ther*, **16**, 441.

300. Udagawa, N, Takahashi, N, Akatsu, T, Tanaka, H, Sasaki, T, Nishihara, T, Koga, T, Martin, TJ & Suda, T. (1990). Origin of osteoclasts: mature monocytes and macrophages are capable of differentiating into osteoclasts under a suitable microenvironment prepared by bone marrow-derived stromal cells. *Proc Natl Acad Sci U S A*, **87**, 7260-7264.

301. Uematsu, T, Sakai, A, Ito, H & Suzuki, H. (2011). Intra-articular administration of tachykinin NK(1) receptor antagonists reduces hyperalgesia and cartilage destruction in the inflammatory joint in rats with adjuvant-induced arthritis. *Eur J Pharmacol*, **668**, 163-168.

302. Van Bezooijen, RL, Farih-Sips, HC, Papapoulos, SE & Lowik, CW. (1998). IL-1alpha, IL-1beta, IL-6, and TNF-alpha steady-state mRNA levels analyzed by reverse transcription-competitive PCR in bone marrow of gonadectomized mice. *J Bone Miner Res*, **13**, 185-194.

303. van Maanen, MA, Lebre, MC, van der Poll, T, Larosa, GJ, Elbaum, D, Vervoordeldonk, MJ & Tak, PP. (2009a). Stimulation of nicotinic acetylcholine receptors attenuates collagen-induced arthritis in mice. *Arthritis Rheum*, **60**, 114-122.

304. van Maanen, MA, Stoof, SP, Larosa, GJ, Vervoordeldonk, MJ & Tak, PP. (2010). Role of the cholinergic nervous system in rheumatoid arthritis: aggravation of arthritis in nicotinic acetylcholine receptor alpha7 subunit gene knockout mice. *Ann Rheum Dis*, **69**, 1717-1723.

305. van Maanen, MA, Stoof, SP, van der Zanden, EP, de Jonge, WJ, Janssen, RA, Fischer, DF, Vandeghinste, N, Brys, R, Vervoordeldonk, MJ & Tak, PP. (2009b). The alpha7 nicotinic acetylcholine receptor on fibroblast-like synoviocytes and in synovial tissue from rheumatoid arthritis patients: a possible role for a key neurotransmitter in synovial inflammation. *Arthritis Rheum*, **60**, 1272-1281.

306. van Maanen, MA, Vervoordeldonk, MJ & Tak, PP. (2009c). The cholinergic anti-inflammatory pathway: towards innovative treatment of rheumatoid arthritis. *Nat Rev Rheumatol*, **5**, 229-232.

307. van Vollenhoven, RF. (2009). Treatment of rheumatoid arthritis: state of the art 2009. *Nat Rev Rheumatol*, **5**, 531-541.

308. van, GN, Torrekens, S, Roberts, SJ, Moermans, K, Schrooten, J, Carmeliet, P, Luttun, A, Luyten, FP & Carmeliet, G. (2012). Engineering vascularized bone: osteogenic and proangiogenic potential of murine periosteal cells. *Stem Cells*, **30**, 2460-2471.

309. Vanhoutte, D & Heymans, S. (2010). TIMPs and cardiac remodeling: 'Embracing the MMP-independent-side of the family'. *J Mol Cell Cardiol*, **48**, 445-453.

310. Veenstra, M & Ransohoff, RM. (2012). Chemokine receptor CXCR2: physiology regulator and neuroinflammation controller? *J Neuroimmunol*, **246**, 1-9.

311. Waldburger, JM, Boyle, DL, Pavlov, VA, Tracey, KJ & Firestein, GS. (2008). Acetylcholine regulation of synoviocyte cytokine expression by the alpha7 nicotinic receptor. *Arthritis Rheum*, **58**, 3439-3449.

312. Walker, EC, McGregor, NE, Poulton, IJ, Solano, M, Pompolo, S, Fernandes, TJ, Constable, MJ, Nicholson, GC, Zhang, JG, Nicola, NA, Gillespie, MT, Martin, TJ & Sims, NA. (2010). Oncostatin M promotes bone formation independently of resorption when signaling through leukemia inhibitory factor receptor in mice. *J Clin Invest*, **120**, 582-592.

313. Wang, H, Yu, M, Ochani, M, Amella, CA, Tanovic, M, Susarla, S, Li, JH, Wang, H, Yang, H, Ulloa, L, Al-Abed, Y, Czura, CJ & Tracey, KJ. (2003). Nicotinic acetylcholine receptor alpha7 subunit is an essential regulator of inflammation. *Nature*, **421**, 384-388.

314. Wang, L, Zhao, R, Shi, X, Wei, T, Halloran, BP, Clark, DJ, Jacobs, CR & Kingery, WS. (2009). Substance P stimulates bone marrow stromal cell osteogenic activity, osteoclast differentiation, and resorption activity in vitro. *Bone*, **45**, 309-320.

315. Webber, C & Zochodne, D. (2010). The nerve regenerative microenvironment: early behavior and partnership of axons and Schwann cells. *Exp Neurol*, **223**, 51-59.

316. Weidler, C, Holzer, C, Harbuz, M, Hofbauer, R, Angele, P, Scholmerich, J & Straub, RH. (2005). Low density of sympathetic nerve fibres and increased density of brain derived neurotrophic factor positive cells in RA synovium. *Ann Rheum Dis*, **64**, 13-20.

317. Weinstein, JN, Myers, TG, O'Connor, PM, Friend, SH, Fornace, AJ, Jr., Kohn, KW, Fojo, T, Bates, SE, Rubinstein, LV, Anderson, NL, Buolamwini, JK, van Osdol, WW, Monks, AP, Scudiero, DA, Sausville, EA, Zaharevitz, DW, Bunow, B, Viswanadhan, VN, Johnson, GS, Wittes, RE & Paull, KD. (1997). An information-intensive approach to the molecular pharmacology of cancer. *Science*, **275**, 343-349.

318. Weiss, TW, Kvakan, H, Kaun, C, Zorn, G, Speidl, WS, Pfaffenberger, S, Maurer, G, Huber, K & Wojta, J. (2005). The gp130 ligand oncostatin M regulates tissue inhibitor of metalloproteinases-1 through ERK1/2 and p38 in human adult cardiac myocytes and in human adult cardiac fibroblasts: a possible role for the gp130/gp130 ligand system in the modulation of extracellular matrix degradation in the human heart. *J Mol Cell Cardiol*, **39**, 545-551.

319. Westacott, CI & Sharif, M. (1996). Cytokines in osteoarthritis: mediators or markers of joint destruction? *Semin Arthritis Rheum*, **25**, 254-272.

320. Westermann, D, Mersmann, J, Melchior, A, Freudenberger, T, Petrik, C, Schaefer, L, Lullmann-Rauch, R, Lettau, O, Jacoby, C, Schrader, J, Brand-Herrmann, SM, Young, MF, Schultheiss, HP, Levkau, B, Baba, HA, Unger, T, Zacharowski, K, Tschope, C & Fischer, JW. (2008). Biglycan is required for adaptive remodeling after myocardial infarction. *Circulation*, **117**, 1269-1276.

321. Westman, M, Engstrom, M, Catrina, AI & Lampa, J. (2009). Cell specific synovial expression of nicotinic alpha 7 acetylcholine receptor in rheumatoid arthritis and psoriatic arthritis. *Scand J Immunol*, **70**, 136-140.

322. Westman, M, Saha, S, Morshed, M & Lampa, J. (2010). Lack of acetylcholine nicotine alpha 7 receptor suppresses development of collagen-induced arthritis and adaptive immunity. *Clin Exp Immunol*, **162**, 62-67.

323. Wolff, C, Krinner, K, Schroeder, JA & Straub, RH. (2014). Inadequate corticosterone levels relative to arthritic inflammation are accompanied by altered mitochondria/cholesterol breakdown in adrenal cortex: a steroid-inhibiting role of IL-1beta in rats. *Ann Rheum Dis*, **0**, 1-8.

324. Yamamori, T, Fukada, K, Aebersold, R, Korsching, S, Fann, MJ & Patterson, PH. (1989). The cholinergic neuronal differentiation factor from heart cells is identical to leukemia inhibitory factor. *Science*, **246**, 1412-1416.

325. Yamamuro, Y & Aizawa, S. (2010). Asymmetric regulation by estrogen at the cholinergic gene locus in differentiated NG108-15 neuronal cells. *Life Sci*, **86**, 839-843.

326. Yoshikawa, H, Kurokawa, M, Ozaki, N, Nara, K, Atou, K, Takada, E, Kamochi, H & Suzuki, N. (2006). Nicotine inhibits the production of proinflammatory mediators in human monocytes by suppression of I-kappaB phosphorylation and nuclear factor-kappaB transcriptional activity through nicotinic acetylcholine receptor alpha7. *Clin Exp Immunol*, **146**, 116-123.

327. You, S, Yoo, SA, Choi, S, Kim, JY, Park, SJ, Ji, JD, Kim, TH, Kim, KJ, Cho, CS, Hwang, D & Kim, WU. (2014). Identification of key regulators for the migration and invasion of rheumatoid synoviocytes through a systems approach. *Proc Natl Acad Sci U S A*, **111**, 550-555.

328. Yu, X, Huang, Y, Collin-Osdoby, P & Osdoby, P. (2004). CCR1 chemokines promote the chemotactic recruitment, RANKL development, and motility of osteoclasts and are induced by inflammatory cytokines in osteoblasts. *J Bone Miner Res*, **19**, 2065-2077.

6.2 List of figures

6.3 Abstract

Objective. Density of sympathetic nerve fibers decreases in inflamed arthritic tissue, which is tested by detection of tyrosine-hydroxylase (TH, key enzyme of catecholamine synthesis). However, under certain circumstances like during the innervation phase of developing sweat glands or in periosteum, sympathetic nerve fibers can change phenotype from catecholaminergic to cholinergic. Therefore, the observed loss of sympathetic nerve fibers in arthritis might be due to undetectable TH. The aim of this study was to investigate a possible catecholaminergic-to-cholinergic transition of sympathetic nerve fibers in synovial tissue of animals with collagen induced arthritis (CIA), and patients with rheumatoid arthritis (RA) and osteoarthritis (OA), and to find a possible factor responsible for the transition.

Methods. Nerve fibers in samples from RA and OA patients as well as in samples from mice were detected by immunofluorescence towards TH (catecholaminergic), vesicular acetylcholine transporter (cholinergic) and vasoactive intestinal peptide (cholinergic). In-vitro co-culture experiments with sympathetic ganglia and lymphocytes or osteoclast progenitors (OCPs) were designed to find stimulators of catecholaminergic-to-cholinergic transition including gene expression and proteome profiling of osteoclast progenitor cells.

Results. In mouse paws, an increased density of cholinergic relative to catecholaminergic nerve fibers appeared towards day 35 post immunization, but most nerve fibers were located in healthy joint-adjacent skin or muscle and almost none in inflamed synovial tissue. In humans, cholinergic fibers were more prevalent in less inflamed OA than in highly inflamed RA synovial tissue. Co-culture of sympathetic ganglia with OCPs obtained from healthy but not from arthritic animals induced catecholaminergic-to-cholinergic transition. OCP mRNA microarray data from healthy animals indicated that leukemia inhibitory factor (LIF) is a candidate transition factor, which was confirmed in ganglia experiments, particularly, in the presence of progesterone. Gene expression and proteome analysis of OCPs furthermore suggested an up-regulation of extracellular matrix related genes and proteins in addition to oncostatin M (OSM) in OCPs from healthy animals and up-regulation of pro-inflammatory chemokines in cells from arthritic mice. Study key results have been recently published (Stangl *et al.*, 2015).

Conclusion. In humans and mice, catecholaminergic-to-cholinergic sympathetic transition happens in less inflamed tissue but not in inflamed arthritic tissue or under inflammatory conditions in-vitro. Under healthy conditions, presence of cholinergic sympathetic nerve fibers may support the cholinergic anti-inflammatory influence recently described.

6.4 Acknowledgements

I hereby want to thank several persons, who helped me designing, performing, interpreting and finally finishing this study:

First, I want to especially thank my supervisor Prof. Rainer H. Straub, who designed the study and guided me through these years by giving regular and very helpful input as well as scientific interpretation and discussion of new ideas and results. Further, I want to thank my supervisor Prof. Jens Schlossmann, and Prof. Frieder Kees and Prof. Susanne Grässel for fruitful discussion and help.

Moreover, I want to thank Dr. Robert H. Springorum and Dr. Florian Weber for evaluation of finger joint samples, and Dr. Klaus Stark for genetic analysis.

Special thanks also go to Dr. Christine Wolff, Dr. Zsuzsa Jenei-Lanzl, Dr. Torsten Lowin and Dominique Muschter for technical and scientific support. I also want to acknowledge technical assistance by Angelika Gräber, Madlen Melzer, Tanja Späth, Luise Rauch, Miriam Schmitt, and Prof. Wegener.

Finally, I have to thank my family, and my friends Jessica Vögeler, Michael Eglmeier, Joachim Mütterlein, Michael Tietze and Maximilian Wackerbauer, who encouraged and supported me through this entire period of time.

Regensburg, June 2015 _____ (Hubert Stangl)